Spring 2018

DEVELOPMENT OF PROTEIN DISPLAY SYSTEMS AND GENETIC TOOLS FOR SPORE-FORMING BACTERIA

Erin Drufva
University of New Hampshire, Durham

DEVELOPMENT OF PROTEIN DISPLAY SYSTEMS AND GENETIC TOOLS FOR SPORE-FORMING BACTERIA

BY

ERIN DRUFVA

B.A. Chemistry, Mount Holyoke College, 2013

DISSERTATION

Submitted to the University of New Hampshire

in Partial Fulfillment

of the Requirements for the Degree of

Doctor of Philosophy

in

Chemical Engineering

May, 2018

This dissertation has been examined and approved in partial fulfillment of the requirements for the degree of Doctor of Philosophy in Chemical Engineering by:

Dissertation Director, Dr. Kang Wu, Assistant Professor of Chemical Engineering

Dr. Russell Carr, Professor and Chair of Chemical Engineering

Dr. Harish Vashisth, Assistant Professor of Chemical Engineering

Dr. Adam St. Jean, Lecturer of Chemical Engineering

Dr. Subhash Minocha, Professor of Biological Sciences and Genetics

On January 18, 2018

Original approval signatures are on file with the University of New Hampshire Graduate School.

DEDICATION

I dedicate this work with love to my parents, Laura and Paul Drufva, who have always encouraged my passion for learning.

ACKNOWLEDGEMENTS

I first must acknowledge like my advisor, Dr. Kang Wu who taught me everything I know about molecular cloning. She was an invaluable source of information regarding synthetic biology and innovative research project ideas. Dr. Wu, thank you for all of your support and your dedication to preserving the environment through your research.

I would also like to acknowledge my other committee members, Dr. Carr, Dr. Vashisth, Dr. St. Jean, and Dr. Minocha. I have taken the laboratory management skills learned from being the Teaching Assistant for Dr. St. Jean's Unit Operations class with me. I would like to thank Dr. Vashisth for teaching me everything I know about thermodynamics. Also, thank you to Dr. Tom Laue and Dr. Clyde Denis for teaching me everything I know about protein structure and folding. And thank you to Dr. Carr for always being willing to help with degree related questions.

I would also like to acknowledge the past and present students of the Wu lab group; Tony Castagnaro, Halie White, Ryan McEachern, Abra Roberts, Sachi Nagada, Brady Camplin, Guo Wu, Lucas Prevost, and Matida Delgado. I could not ask for better lab mates and I wish them the best of luck in their endeavors. Also thanks to my fiancé, Andrew Kraines who believed in my abilities even when I doubted myself. Thank you for always supporting me. Finally, I would like to acknowledge my parents, Paul and Laura Drufva, for unconditionally loving me and encouraging all of my pursuits.

TABLE OF CONTENTS

LIST OF TABLES

LIST OF FIGURES

ABSTRACT

DEVELOPMENT OF PROTEIN DISPLAY SYSTEMS AND GENETIC TOOLS FOR SPORE-FORMING BACTERIA

by

Erin Drufva

University of New Hampshire, May, 2018

One major area of synthetic biology is to engineer microbial cells and subcellular systems for diverse applications including biosynthesis, biocatalysis, therapeutics, drug delivery, and bioremediation. For most applications, robust cellular systems are preferred for longer activity half-life and resistance to harsh environments. Two projects related to robust cellular systems involving Gram-positive bacteria are presented in this work. One is to develop thermostable genetic reporters for *Geobacilli* species and the other is to display an enzyme on the *Bacillus subtilis* spore surface to enhance its robustness and present an alternative to purified enzymes for industrial applications.

Bacillus subtilis and *Geobacillus thermoglucosidans* are gram-positive, spore-forming bacteria. They secrete many proteins used industrially for the production of paper, food, textiles, chemicals, medicine, and cosmetics. Since *G. thermoglucosidans* is thermostable with an optimal growth temperature of 60ºC, its secreted proteins are also thermostable which proves advantageous for a variety of industrial applications. Additionally, a strain of *G. thermoglucosidans* has been used for the production of ethanol from biomass. Unfortunately the inner workings of *G. thermoglucosidans* are still poorly understood and a genetic toolkit is necessary to better discover how to improve them via genetic engineering for industrial use. Important components of this toolkit are genetic reporters which allow for the analysis of gene expression in *G.*

thermoglucosidans. Fluorescent proteins are commonly used reporters for other bacterial species due to their easily observed and readily measured signal, however no thermostable fluorescent proteins have been shown to be functional in *Geobacillus.* Seven different fluorescent proteins including mCherry, Venus, GFP, sfGFP, GFPmut3, mCherry (Gt), and Venus (Gt) were tested for stability and functionality in *Geobacillus thermoglucosidans*. Venus (Gt) and mCherry (Gt) were codon optimized for this bacterium with the goal of increasing expression level and thus improving the fluorescence signal. The fluorescence intensity of each fluorescent protein expressed in *G. thermoglucosidans* was measured after several hours of bacterial growth at 50ºC and 60ºC. Venus, mCherry, Venus (Gt), mCherry (Gt), and sfGFP all had signal when expressed in *G. thermoglucosidans* at 50ºC and sfGFP had signal at 60ºC. Therefore, fluorescent reporter proteins in three different colors were found to be functional in *G. thermoglucosidans*. This will further genetic engineering of the species for thermostable protein production, bioremediation, and biofuel production.

Bacillus subtilis is Generally Regarded as Safe (GRAS) by the FDA and amenable toward genetic manipulation. Thus it has been engineered for the production of many heterologous proteins. Oftentimes, proteins secreted by bacteria are purified for industrial use. However, protein purification is expensive and time-consuming and long-term storage of purified proteins requires extremely low temperatures (-20ºC). *B. subtilis* spores have been used to immobilize a variety of proteins for vaccines, biosensors, and bioremediation applications. Spore surface display eliminates the need for purification and provides a way to easily separate proteins from the final product if necessary. A novel and thermostable laccase, a copper-containing oxidase, was isolated and purified from *G. thermoglucosidans*. It can be used to degrade lignin and a variety of phenolic compounds and thus has applications for the production of paper, textiles, food, and biofuel. This

laccase was isolated, characterized, and immobilized on the surface of *B. subtilis* spores. The purified and spore displayed laccase were tested for heat stability and catalytic function. The purified laccase showed high activity toward 2,6-dimethoxyphenol (2,6-DMP) and moderate activity toward veratryl alcohol and 2,2′-Azino-bis(3-ethylbenzthiazoline-6-sulfonic acid) (ABTS) while the spore displayed laccase showed high activity toward 2,6-DMP. The purified laccase was considerably more heat stable than a commonly used fungal laccase. The spore displayed laccase was also found to be heat stable with a half-life of about 6 hours at 80ºC. The binding affinity of the immobilized laccase for the substrate 2,6-DMP was virtually the same as that of the purified laccase, plus the immobilized laccase showed solid activity. These results show that spore surface display of proteins is a promising, more inexpensive alternative to purifying proteins for industrial use.

CHAPTER 1: INTRODUCTION

1.1 The industrial relevance of proteins

Proteins are ubiquitously used in industry for the production of food, beverages, textiles, paper, cosmetics, biopharmaceuticals, and fuel [1]. The first enzyme found to be useful in 1833 was amylase which converts starch to sugar. It has applications for the production of food, detergents, and biopharmaceuticals [2]. Commercial enzyme production began in Germany in 1914, starting with the isolation of a complex of enzymes called rennet from calf and lamb stomachs for cheese production. Shortly afterward in the early 1930's, pectinases were used to make juice and cellulases were used in the production of detergents [3]. Rennet, pectinase, and cellulase are all still used to this day. Today the most common commercial enzymes include amylases, cellulases, proteases, xylanases, and lipases. These are used for making detergents, starch processing, making animal feed, paper and pulp processing, fruit and vegetable processing, meat processing, baking, and making wine [3, 4]. Microbial enzymes can even be used as therapeutics to treat a variety of diseases and illnesses as shown in Table 1 [4].

Table 1. Biomedical applications of microbial enzymes. [4]

Treatment	Enzyme(s)
Antitumor	L-asparaginase, L-glutaminase, L-tyrosinase, galactosidase
Anti-inflammatory	Superoxide dismutase, serrapeptase
Anticoagulants	Streptokinase, urokinase
Antioxidants	Superoxide dismutase, gluthathione peroxidase, catalase
Skin ulcers	Collagenase
Detoxification	Laccase, rhodanese
Antibiotic resistance	β-Lactamase
Antiviral	Ribonuclease, Serrapeptase
Gout	Uricase
Digestive disorders	α-Amylase, lipase
Cyanide poisoning	Rhodanase

Some commercial enzymes including papain, bromelain, and ficin are plant derived and others including pepsin and rennet are animal derived, however most enzymes are produced by microorganisms [5]. Most of these microorganisms include fungi such as species of *Trichoderma* and *Aspergillus*, along with bacteria including species of *Streptomyces* and *Bacillus*. Enzymes isolated from *Trichoderma*, *Aspergillus*, and *Bacillus* have applications in the food, beverage, animal feed, paper, cleaning product, textile, and biopharmaceutical industries [6]. Additionally, in the biopharmaceutical industry bacteria and yeast are used for recombinant protein production. *E. coli* is used to express large amounts of recombinant proteins. Species of *Bacillus*, *Staphylococcus*, and *Ralstonia* are also used but have lower protein yields. Yeast strains with high recombinant protein yields include *Pichia pastoris, Hansenula polymorpha,* and *Saccharomyces cerevisiae* [7].

1.2 Protein expression systems

A few methods for protein expression have been developed. First, intracellular expression involves the expression of proteins within the cell. The cell must then be broken open to extract the expressed proteins [8]. The most common intracellular protein expression system is *Escherichia coli*, a species of gram-negative bacteria. Using *E. coli* as an intracellular protein expression system provides a number of advantages including very high expression levels, low cost, rapid growth, and scalability. However, there are a number of disadvantages as well including inefficient disulfide bond formation, poor protein folding in the cytoplasm, formation of inclusion bodies, and insufficient post-translational modifications [9].

Second, protein secretion involves the expression of proteins which are then secreted outside the cell. Examples of protein secretion systems include *Bacillus subtilis*, a species of gram-positive bacteria, *Saccharaomyces cerevisiae*, and *Pichia pastoria*, both species of yeast. Protein

secretion systems have a number of advantages such as good expression levels, low cost, scalability, and simple protein purification [10]. On the other hand, some cons to using these systems include poor secretion and folding of heterologous proteins, issues with post-translational modifications such as hyperglycosylation, and specifically for *P. pastoris*, the use of methanol as an expression inducer which poses a potential fire hazard at large scales [10, 11, 12].

Third, cell free protein synthesis (CFPS) involves the expression of proteins without the use of living cells. The necessary cellular components required for protein expression including ribosomes, mRNAs, tRNAs, translation initiation and elongation factors, protein chaperones, metabolic enzymes, etc. are mixed with energy substrates such as adenosine triphosphase (ATP), cofactors, the DNA template, and salts to express the protein of interest [13]. The cellular components required for protein expression are almost always derived from crude cell lysates of microbial, plant, insect, or animal cells. Some benefits to using this system include rapid protein expression (one to two days v. one to two weeks for *in vivo* systems), versatility of cell extract (*E. coli*, wheat germ, insect, and mammalian systems are commercially available), open reaction setup allowing simple manipulation of the protein expression environment, and the ability to use PCR products as templates [14]. However, there are a couple of downsides to using this system including the limited availability of post-translational modifications and the high cost. Cell free expression systems are especially expensive with scale-up [15].

1.3 Protein display systems

In some cases such as vaccine, biocatalyst, and biosensor development, it is advantageous to display proteins on the surface of cellular or other systems. A number of systems for protein display have been developed including bacterial cell surface display, yeast cell surface display, ribosome display, mRNA display, bacteriophage (phage) display, and spore surface display.

Phage, cell, ribosome, and mRNA display systems are protein engineering tools used for *in vitro* protein evolution. In this case, protein libraries are screened via flow cytometry to determine how the gene sequence encoding a protein is connected to its function. In this way, mutations in the genetic code are analyzed to determine how they affect the function of a protein. Phage display is the most widely used display system for this purpose as it is an ideal candidate for high throughput screening to create vast protein libraries. One of the most common industrial applications of this is creating libraries of novel antibodies for pathogenic viruses and bacteria for the medical industry [16]. However, phage displayed antibodies are not suitable for direct industrial use, since bacteriophages are viruses that are toxic to humans. Additionally, the creation of phage display libraries requires many steps to verify the binding affinity of the mutants, and in many cases false positives are identified [17].

Yeast cell surface display has also been used to create protein libraries, in some cases with more variety than phage display. Specifically in the case of the HIV-1 single-chain variable fragment (scFv) which is the fusion protein of the variable regions of the heavy and light chains of antibodies, yeast cell surface display was able to create a chimeric antibody library of 10^7 different mutants. This library contained twice as many novel antibodies as the HIV-1 scFv library created from phage display [18]. Yeast cells can be used to display monomeric, homodimeric, and heterodimeric proteins. Additionally, the binding affinities of mutants for their target molecules can be accurately quantified by flow cytometry. This allows for precise and reproducible measurements for mutant libraries with high binding affinity [19]. In contrast, mutant libraries found using phage, mRNA, and ribosome display cannot be screened in this way which results in more labor to eliminate false positives and mutants with low binding affinity. Finally, because its

protein folding and secretory machineries are similar to those of mammalian cells, yeast cell surface display of mammalian proteins is preferred over other systems [20].

Bacterial cell surface display offers some advantages as well. As with yeast cell surface display, the binding affinities of mutants generated via bacterial cell surface display can be quantified using flow cytometry or fluorescence-activated cell sorting (FACS). Bacterial cell surface display has been used to generate live vaccines, protein libraries, biocatalysts, and tools for bioremediation. In fact, bacterial cell surface display can create larger protein libraries than yeast cell surface display due to higher transformation efficiency [21]. Bacterial cell surface display of antigens for live vaccines presents some advantages. First, foreign bacteria act as adjuvants which boost the body's immune response, whereas with conventional vaccines adjuvants must be added. Additionally, many bacteria are food-grade so the whole bacterial cell can be incorporated into the live vaccine, whereas phage displayed antigens cannot be used directly as vaccines due to the toxicity of the bacteriophage. Finally, oral vaccines can be developed using bacterial cell surface display of antigens, eliminating the need for syringes and needles [22].

Ribosome and mRNA display have been successfully used in the engineering of antibodies and protein therapeutics. They are performed *in vitro* which offers some advantages. When creating protein mutants, the diversity of the library is not limited by the transformation efficiency of cells, only by the number of ribosomes and different mRNA molecules present in the system. They allow a library size as large as 10^{15} members, as opposed to yeast cell surface display and bacterial cell surface display which allow up to 10^{7} and 10^{10} members respectively [23]. Random mutations can also be introduced easily after each selection round which allows for directed evolution of binding proteins over several generations. Furthermore, cell-based systems only allow

for the display of proteins containing natural amino acids, whereas ribosome and mRNA display can display proteins containing non-natural amino acids [24].

Bacterial spore surface display is a newer protein display system that is the focus for part of this work. It has a few advantages over other display methods such as phage display and cell surface display. Bacterial spores are produced as a method of survival and are therefore robust microorganisms that can withstand a variety of harsh environments. They are also stable at room temperature for years [25]. Additionally, spores can display large and multimeric proteins. On the other hand, cell surface display and phage display have size limitations since the size of the protein may affect the structure of a cell-membrane anchoring protein or of a viral capsid. Moreover, cell surface display requires a membrane translocation step to externally expose a protein expressed in the cytoplasm. In contrast, heterologous proteins are expressed in the mother cell and their assembly on the spore surface does not involve membrane translocation. For these reasons, spores can display larger, more complex proteins than cells [26].

1.4 Industrial applications for robust enzymes

Qualifications for enzyme selection include substrate specificity and affinity, enzyme activity, pH and temperature optima for stability, and the effect of inhibitors. Industrially used enzymes must often be tolerant to a variety of heavy metals and have no need for cofactors. They should also be active in the presence of low substrate concentrations [27]. Many industrial processes require or would benefit from using thermostable enzymes. For example, animal feed industry enzymes must be heat tolerant to survive the heat treatment process used to inactivate potential contaminants in animal feed. Using arabinofuranosidases and phytases with increased thermostability in the production of animal feed would enhance the digestibility and nutrition of the feed while combining heat treatment and feed processing in a single step [28]. Additionally,

starch processing would greatly benefit from the use of thermostable amylases for the liquefaction and saccharification of starch. These processes are run at 105ºC and 60ºC respectively, but increasing the saccharification process temperature would present many advantages. Some of these include decreased viscosity and lower pumping costs, decreased risk of bacterial contamination, higher reaction rates, shorter operation time, lower cost of enzyme purification, and longer catalyst half-life [29].

Furthermore, paper and pulp bleaching would greatly benefit from thermostable hemicellulases active at basic conditions since pulping and bleaching are both performed at high temperatures. Pretreatment of pulp with thermostable hemicellulases and xylanases would greatly reduce the amount of chlorine pollutants generated from the process [30]. Thermostable enzymes are also desired for the synthesis of various chemicals. Some of these include hydantoinases for the synthesis of D-amino acids as intermediates in the production of antibiotics, peptide hormones, pyrethroids for pesticides, esterases for transesterification and ester synthesis, aldolases for carbon-carbon bond formation, cytochrome P450 for hydroxylations, and secondary alcohol dehydrogenases for the production of enantiomerically pure chiral alcohols [31]. Finally, since the pretreatment of lignocellulosic biomass is performed at high temperatures, thermostable cellulases, hemicellulases, and lignin degrading enzymes such as laccases are ideal for biomass degradation to produce second generation biofuels [32].

1.5 Problems with fossil fuels; motivation for alternative fuels

According to the US Energy Information Administration, the world produced an average 97.19 million barrels of petroleum and other liquid fuels per day in 2016 and an average of 98.26 million barrels per day in 2017. In 2016 the world consumed an average of 96.91 barrels per day leaving only 0.28 million barrels per day remaining. In 2017 the world consumed a whopping

average of 98.34 million barrels, outnumbering the amount of barrels produced per day. According to the figure below, in 2018 world consumption of fuel is predicted to grow and production of fuel is predicted to barely match consumption. In fact, during a good portion of the next year fuel consumption is predicted to exceed production [33].

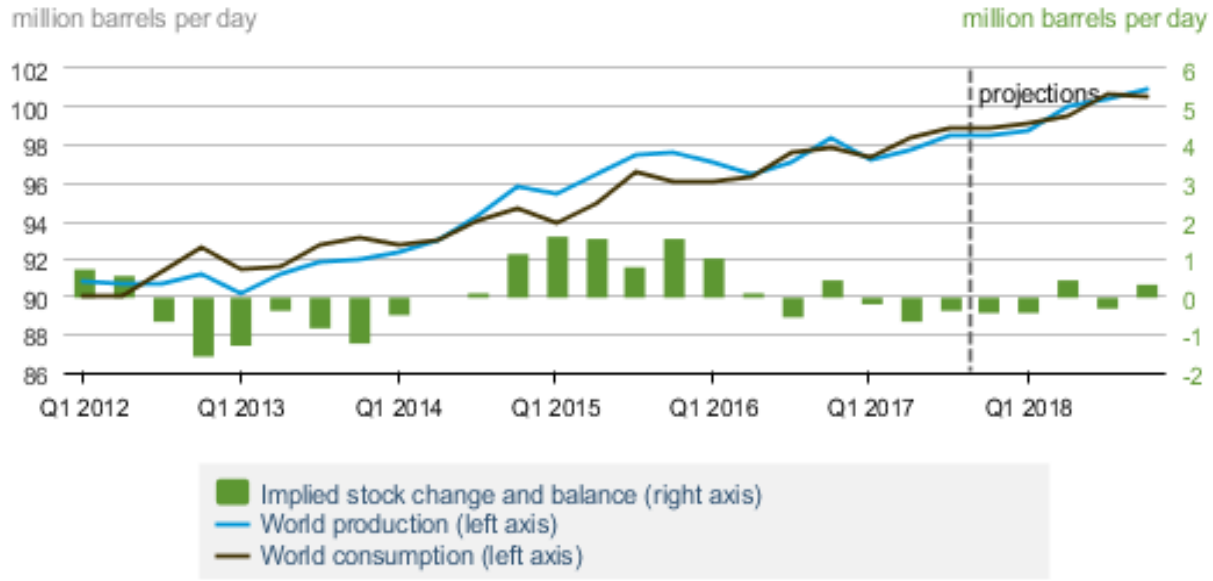

Figure 1. World liquid fuels production and consumption balance [33].

Additionally, the combustion of fossil fuels produces large amounts of CO_2, a harmful greenhouse gas which traps heat in the atmosphere, along with other toxic pollutants like SO_2, NO_x, soot, and mercury. In 2014 approximately 78% of US CO_2 emissions were energy-related. Of these emissions, approximately 42% were from oil and other liquids, 32% were from coal, and 27% were from natural gas [34]. Furthermore, extraction of oil, coal, and natural gas releases toxic emissions and negatively impacts the environment. Coal mining often results in acids and heavy metals leaching into groundwater [35]. Surface mining is less dangerous to workers than underground mining, but the impact on the surrounding land is devastating. Surface mining removal sites are left with poor soil that usually exclusively supports growth of exotic grasses. Surface mining also results in the burial of thousands of miles of headwater streams, eliminating

a huge amount of biodiversity [36]. Oil and gas drilling produce water tainted with heavy metals, hydrocarbons, and radioactive materials. This water which was previously trapped underground is brought to the surface and is difficult to safely dispose [35]. Hydraulic fracturing (fracking) produces even more toxic wastewater, about 3-6 gallons per well, laden with chemicals that cause cancer and a myriad of other health problems [37]. Natural gas and oil transportation and drilling produce a staggering amount of greenhouse gases. Methane, the main component of natural gas is 34 times more effective than CO_2 at trapping heat in the atmosphere over a 100-year timescale. This gas is produced when drilling natural gas and oil and is either released into the atmosphere or flared (burned) to produce CO_2 [38]. The World Bank estimates that 5.3 trillion ft^3 of natural gas is flared annually worldwide generating approximately 400 million tons of CO_2 emissions [39].

1.6 First generation biofuels

Biofuels are derived from contemporary biological processes, such as agricultural and anaerobic digestion, rather than fossil fuels which are derived from prehistoric biological matter. Additionally, fossil fuels contain carbon and hydrogen atoms while biofuels contain carbon, hydrogen, and oxygen [40]. Studies show that biofuels emit less CO_2 than fossil fuels. Combustion of bioethanol emits 18% less greenhouse gases than an energetically equivalent amount of gasoline while biodiesel emits 41% less greenhouse gases than diesel fuel. Additionally, significantly less pollutants are emitted from the extraction of plant matter to produce biofuels than are emitted from oil drilling, natural gas drilling, and fracking [41]. In the process of extracting plant matter, groundwater and soil are not contaminated with cancer causing or radioactive chemicals, and stream ecosystems are not disrupted. Combustion of biofuels also results in fewer emissions of SO_2 and soot. Biodiesel in particular is composed of fewer polycyclic hydrocarbons which have been linked to cancer [42].

Due to the many benefits of using biofuels over fossil fuels, the Energy Independence and Security Act of 2007 was established to set benchmarks for renewable fuel production, assigning a 36 billion gallon target for total biofuels by 2022 which was projected to displace 16-17% of US crude oil in that year [43]. Currently, most gasoline and diesel fuels in North America and Europe are blended with biofuel to improve octane levels and reduce emissions. Blending petroleum based diesel with biodiesel has been found to improve the lifetime of diesel engines. In 2015 the US produced about 14.7 billion gallons of bioethanol and 1.3 billion gallons of biodiesel. About 99.99% of these are first generation biofuels which are derived from food sources such as corn, soybeans, animal fat, and sugarcane. First generation biofuels pose some drawbacks. Much concern has been raised regarding the use of food crops to produce fuel. First generation biofuel production also poses some environmental impacts regarding the amount of land allotted to grow the crops and the amount of water required to grow those crops [44].

1.7 Second generation biofuels

Second generation biofuels are an attractive alternative to first generation biofuels because they are derived from lignocellulosic biomass such as corn stalks, corn stover, wood, switchgrass, and municipal solid waste [44]. In 2015, 144 million tons of biomass, primarily corn stalks, were used within the US to produce biofuels which supplied 5% of domestic transportation fuel needs [45]. However, the amount of available biomass for production is far greater, an estimated 1.1-1.6 billion tons annually. Clearly, the energy potential for second generation biofuels is not even close to being realized [46]. Compared to first generation biofuels, combustion of second generation biofuels results in far greater displacement of fossil fuels with significantly lower greenhouse gas emissions. While first generation bioethanol yields a 28% gain in delivered energy relative to fossil fuel energy output, second generation bioethanol yields a whopping 440-660% gain in delivered

energy relative to fossil fuel energy output [44]. Additionally, while corn ethanol reduces CO_2 emissions by 18%, cellulosic ethanol reduces CO_2 emissions by a whopping 87% [47].

Despite all the advantages of using second generation biofuels, first generation biofuels still occupy the vast majority of the biofuel market. The reason for this is that lignocellulosic biomass has a more complex structure than corn, soybeans, or sugarcane that is very resistant to degradation. It is composed of three polymers; cellulose, hemicellulose, and lignin. Cellulose is a straight chain of D-glucose molecules, hemicellulose is a less structured chain of different sugars including pentose, arabinose, and xylose, and lignin is a very complex, hydrophobic chain of aromatic alcohols [48]. Due to its complex, hardy structure, biomass must undergo many conversion steps to produce fuel. In contrast, converting corn and other food products to fuel merely requires milling or mashing followed by fermentation [49].

1.7.1 Thermochemical conversion of biomass

Currently there are two routes to convert lignocellulosic biomass into fuel. The first is thermochemical conversion which begins with pyrolysis. Pyrolysis uses heat and an inert gas like halogen to convert carbon-based biomass into a number of different products including biochar, bio-oil, methane, hydrogen, carbon monoxide, and carbon dioxide, depending on the temperature used. Biochar is used as a soil additive to improve plant growth, water retention, reduce fertilizer use, and reduce methane and nitrous oxide emissions from soil [50]. Pyrolysis produces mainly biochar at temperatures less than 450ºC with slow heating and mainly a mixture of gases called syngas at temperatures greater than 800ºC with rapid heating. At intermediate temperatures with somewhat rapid heating, the main product is bio-oil [51]. If bio-oil is produced it is converted to syngas through gasification which occurs at high temperatures in the presence of oxygen. The syngas is then converted to diesel, gasoline, or ethanol via a catalyst. Even though bio-oil is not

suitable for direct use in standard internal combustion engines, it can be easily transported to different locations where it can be converted to useful fuel [52].

Thermochemical conversion is a widely used, reliable, and efficient process. However, it is also very energy-intensive, requiring temperatures of 450-800ºC. Even though strategies have been developed to recycle heat from downstream processes, a large amount of energy is still required which is not ideal. Additionally, it requires multiple steps including drying, pyrolysis, gasification, syngas purification to increase hydrogen content and eliminate tar, nitrogen, and sulfur contaminants, and conversion to fuel via a catalyst. All of these processes are energy intensive, requiring high temperatures and a lot of equipment.

1.7.2 Biochemical conversion of biomass

The second method of biomass decomposition is biochemical conversion which contributes to the motivation of this work. This involves the use of microorganisms and enzymes to break down lignocellulosic biomass. Because of its complex, recalcitrant structure, biomass must first be pretreated via heat in combination with an acid or a base. This serves to increase the porosity of the biomass and enhance the solubility of some sugars in the cellulose and hemicellulose. Following this, enzymes are added to the pretreated biomass to break down the cellulose and hemicellulose into their constituent sugar monomers [53]. Finally, microorganisms are added to ferment the sugars and produce bioethanol. Alternatively, the sugars can undergo chemical conversion via catalysis to produce fuels or useful chemicals [53, 54].

Biochemical conversion does not require nearly as much heat energy as thermochemical conversion. However, pretreatment of the biomass and purification of hydrolyzing enzymes is expensive. Additionally, hydrolyzing enzymes cannot be reused for multiple cycles since they are soluble, so new enzymes must be purified for each round of biomass conversion. The lignin content

of biomass is also a challenge since lignin hinders the ability of hydrolyzing enzymes to reach the cellulose and hemicellulose. Research efforts to improve biochemical conversion efficiency involve the identification and engineering of new enzymes to improve the efficiency of hydrolysis, the development of microorganisms that ferment a variety of sugars more effectively, and the identification and engineering of lignin degrading enzymes [55].

This work contributes to biochemical biomass conversion research in two ways. First, fluorescent reporters of multiple colors were found to be functional in *Geobacillus thermoglucosidans* 95A1, a microorganism that has been studied and engineered for fermentation of sugars derived from cellulose and hemicellulose. Second, a novel thermostable laccase, a lignin degrading enzyme, was isolated from *Geobacillus* C56-YS93, characterized, and immobilized on the surface of *Bacillus subtilis* spores. This demonstrated the potential of bacterial spore surface display of enzymes as a more inexpensive alternative to purified enzymes for industrial use. The novel laccase was found to be robust and active when displayed on the surface of bacterial spores.

CHAPTER 2: MATERIALS AND METHODS

2.1 Strains, plasmids and chemicals

All strains used in this work are summarized in Table 2.

Table 2. Bacterial strains and their use(s)

Strain	Source	Use	Growth Media (liquid/solid)
E. coli DH5α	E. coli Genetic Stock Center	Molecular cloning/protein expression and purification	LB/LB agar
G. thermoglucosidans 95A1	Bacillus Genetic Stock Center	Fluorescent protein characterization	TGP/TBAB agar
G. thermoglucosidans C56-YS93		Source of gDNA template for inserts	
B. subtilis 1085		Source of gDNA template for inserts/spore surface display of proteins	LB/LB agar or TBAB agar
B. subtilis 1S101		Spore surface display of laccase	

The pNW33N and pDR111 shuttle vectors were purchased from the Bacillus Genetic Stock Center. Plasmid maps for pNW33N and pDR111 are shown in Figure 2. Note that MCS stands for Multiple Cloning Site which is a collection of enzyme cutting sites used for the incorporation of foreign genes into the shuttle vectors. This process is called molecular cloning.

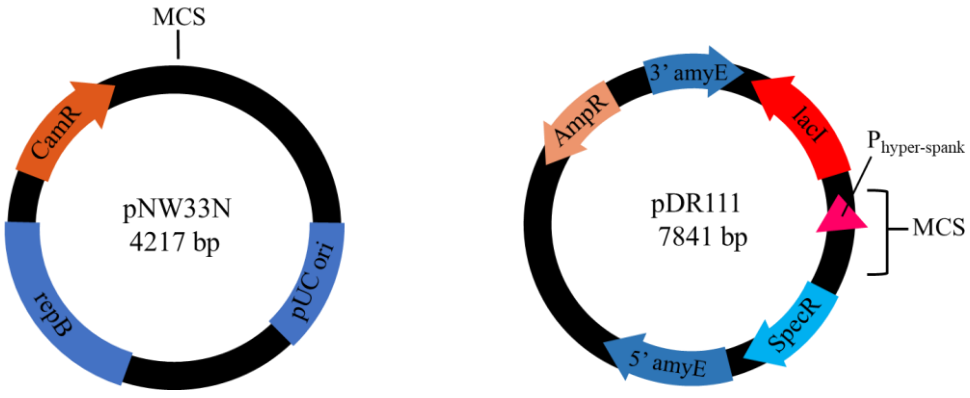

Figure 2. Plasmid maps for pNW33N and pDR111. pNW33N has an antibiotic resistance marker for chloramphenicol in both *E. coli* and *G. thermoglucosidans*. pDR111 has an antibiotic resistance marker for ampicillin in *E. coli* and for spectinomycin in *B. subtilis*.

E. coli and *B. subtilis* strains were primarily grown in Luria-Bertani (LB) media powder from Difco laboratories purchased from VWR. *G. thermoglucosidans* strains were grown in Tryptone Glycerol Pyruvate (TGP) broth which contained 0.5% (w/v) NaCl, 1.7% (w/v) tryptone, 0.3% (w/v) soytone, 0.25% (w/v) K_2HPO_4, 0.4% (w/v) sodium pyruvate and 0.4% (v/v) glycerol. Tryptone, soytone, casamino acids, and nutrient broth were purchased from Difco laboratories, USP grade K_2HPO_4 was purchased from Fisher Scientific, and sodium pyruvate was purchased from Alfa Aesar. Glycerol and NaCl were both purchased from Amresco. 1.5% agar purchased from Difco laboratories was used to solidify LB media for plating *E. coli* strains on petri dishes. Tryptose blood agar base (TBAB), also purchased from Difco laboratories, was used directly for plating *B. subtilis* and *G. thermoglucosidans* strains. USP grade ampicillin from Amresco, tetracycline and spectinomycin from Sigma-Aldrich, and chloramphenicol from Cellgro were used for antibiotic resistance screening of colonies. Isopropyl β-D-1-thiogalactopyranoside (IPTG) purchased from Sigma-Aldrich was used to turn on IPTG inducible promoters.

Trizma (Tris) base, ethylenediaminetetraacetic acid (EDTA), sodium dodecyl sulfate (SDS), proteinase K from Tritirachium album, hexadecyltrimethyl ammonium bromide (CTAB), 24:1 chloroform/isoamyl alcohol, 25:24:1 phenol/chloroform/isoamyl alcohol, isopropanol, KCl, piperazine-N,N'-bis(2-ethanesulfonic acid) (PIPES), sorbitol, copper chloride dihydrate, bromophenol blue, 2-mercaptoethanol, β-mercaptoethanol, glycine, citric acid, 2-(N-morpholine)-ethanesulfonic acid (MES), guaiacol and 2,2'-azine-bis(3-ethylbenzothiazoline-6-sulphonic acid), and a variety of amino acids were all purchased from Sigma-Aldrich.

Ethidium bromide, manganese (II) chloride tetrahydrate, calcium chloride dihydrate, and monosodium phosphate monohydrate were purchased from Amresco. Disodium phosphate was purchased from VWR. Agarose, dimethyl sulfoxide (DMSO), and imidazole were purchased from

Fisher Scientific. Additional chemicals used in this work include ethanol from Macron fine chemicals, acetic acid from Sigma-Aldrich, NaOH, mannitol, and sorbitol from Alfa Aesar. All media, buffers, and solutions used can be found in their appropriate sections below.

2.2 Genomic DNA extraction from *Geobacillus C56-YS93* and *Bacillus subtilis 1085*

The extraction of gDNA from *Geobacillus* C56-YS93 and *Bacillus subtilis* 1085 was completed using the protocol from *Current Protocols in Molecular Biology* [56]. 5 ml of *Geobacillus* C56-YS93 and *Bacillus subtilis* 1085 were incubated overnight at 60°C in TGP media and at 37°C in LB media respectively. Following resuspension of the cell pellets, 1 mg/ml of lysozyme was added to each sample to break the cell wall. The final gDNA pellets were re-suspended in 100 µL of TE buffer (Tris/EDTA buffer), which contains 10 mM TrisCl and 1 mM EDTA. The gDNA of *Geobacillus* was used as a template for PCR amplification of the β-glucanase promoter $P_{\beta\text{-}glu}$ and laccase. The gDNA of *Bacillus* was used as a template for PCR amplification of spore coat proteins such as CotC and CotG.

2.3 DNA amplification by Polymerase Chain Reaction (PCR)

All amplifications were performed using a BioRad T100 Thermal Cycler. GoTaq Green Master Mix purchased from Promega (Ref. # M712C) was used for DNA amplifications of 3 kilobase pairs (kb) and under. Q5 DNA Polymerase purchased from New England Biolabs (NEB) (Cat. No. M0491L) was used for DNA amplifications between 3 kb and 5 kb in length. LongAmp *Taq* DNA Polymerase purchased from NEB (Cat. No. M0323L) was used for DNA amplifications over 5 kb in length. Reactions were set up according to the manufacturers' specifications in PCR tubes from VWR (Cat. No. 82006-606). Specifications for PCR reactions are shown below in Table 3 and the total reaction volumes were 50 µl. Custom oglionucleotide primers were ordered from Integrated DNA Technologies (IDT). Thermocycling conditions for all PCR reactions are

given in Table 4 below according to the manufacturers' instructions. The denaturation, annealing, and extension steps were repeated for 30-35 cycles. All primers were suspended in sterile water upon arrival to a stock concentration of 30 µM and used immediately or stored in the freezer at -20ºC.

Table 3. PCR reaction specifications

	GoTaq Green Master Mix	**Q5 DNA Polymerase**	**LongAmp *Taq* DNA Polymerase**
Water	25 µl	35.5 µl	31.5 µl
Master Mix	22 µl	N/A	N/A
5X Reaction Buffer	N/A	10 µl	10 µl
30 µM Forward Primer	1 µl	1 µl	2 µl
30 µM Reverse Primer	1 µl	1 µl	2 µl
Template	1 µl	1 µl	1 µl
10 mM dNTPs	N/A	1 µl	1.5 µl
Polymerase	N/A	0.5 µl	2 µl

Table 4. Thermal cycler specifications for amplification of DNA via PCR

Polymerase	**Initial Denaturation**	**Denaturation**	**Annealing**	**Extension**	**Final Extension**	**Hold**
GoTaq Green Master Mix	95ºC for 2 minutes	95ºC for 30 seconds	5ºC below the lowest primer T_m for 30 seconds	72ºC for 1 minute/kb of DNA amplified	72ºC for 5 minutes	4ºC
Q5 High-Fidelity	98ºC for 30 seconds	98ºC for 10 seconds	5ºC below the lowest primer T_m for 30 seconds	72ºC for 30 seconds/kb of DNA amplified	72ºC for 2 minutes	4ºC
LongAmp *Taq*	94ºC for 30 seconds	94ºC for 30 seconds	5ºC below the lowest primer T_m for 30 seconds	65ºC for 50 seconds/kb of DNA amplified	65ºC for 10 minutes	4ºC

2.4 PCR Splicing by Overlap Extension (SOEing)

PCR SOEing was used to assemble two insert DNA fragments. The first round of PCR served to amplify the two DNA fragments separately, one with approximately 20 bp of complementary DNA sequence to the other. The second round of PCR served to fuse the two DNA fragments together. This was the same as a typical PCR with the following modification. 1 µl of each DNA template was mixed with 1 µl of the forward primer for the first piece of DNA and 1 µl of the reverse primer for the second piece of DNA. During the reaction, the short overhang of one DNA fragments overlapped with the other DNA fragment, fusing the two DNA fragments together.

2.5 PCR cleanup and DNA concentrator

Following PCR, amplified DNA fragments were purified using the DNA Clean & Concentrator kit from Zymo Research (Cat. No. D4004). This was done to remove unwanted polymerase, primers, nucleotides, and any other impurities from the reaction mixture prior to restriction enzyme digestion or Gibson Assembly. DNA cleaning and concentrating was carried out according to the manufacturer's instructions. Each 50 µl PCR reaction solution was mixed with 450 µl of DNA Binding Buffer in a Zymo-Spin Column which was placed in a Collection Tube. The mixture was centrifuged at 15,000 rpm for 30 seconds using an Eppendorf 5424 Microcentrifuge from Fisher Scientific. Following this, 200 µl of DNA Wash Buffer was added to the column and the column was centrifuged at 15,000 rpm for 30 seconds. This wash step was repeated and following this the column was placed into a sterile 1.5 ml microcentrifuge tube from VWR (Cat. No. 87003-294). Finally, 10-41 µl of sterile water was added to the column which was then centrifuged at 15,000 rpm for 30 seconds. Different volumes of water were used to adjust the

DNA to desired concentrations for digestion with restriction enzymes or Gibson Assembly. DNA solutions were used immediately or stored at -20ºC for future use.

2.6 Gibson Assembly

NEBuilder HiFi DNA Assembly Master Mix purchased from NEB (Cat. No. E2621X) was used for all Gibson Assembly reactions. These reactions were performed to assemble multiple DNA fragments; either multiple insert DNA fragments or vector and insert DNA fragments. Gibson Assembly was used as a faster alternative to molecular cloning of DNA into *E. coli* using restriction enzymes. It was also used to assemble multiple insert DNA fragments together for restriction enzyme digestion. DNA fragments to be assembled were amplified via PCR with approximately 20 bp overhangs of complementary DNA sequences. Total reaction volumes were 10 µl and were performed in PCR tubes. Insert DNA fragments were mixed in equal concentrations with 5 µl of HiFi DNA Assembly Master Mix. Vector and insert DNA fragments were mixed with appropriate volumes to yield a 1:2 DNA concentration ratio of vector to insert and mixed with 5 µl of HiFi DNA Assembly Master Mix. Reactions were performed at 50°C in the thermal cycler or incubator for 2 hours, and were then immediately PCR amplified or stored at -20°C for a maximum of 2 days.

2.7 Measurements of DNA and protein concentrations using the Qubit 3.0 Fluorometer

DNA and protein concentrations in solution were measured in order to optimize Gibson Assembly and ligation reactions. Measurements were taken using the Qubit 3.0 Quantitation starter kit from Thermo Fisher Scientific which includes the Qubit 3.0 Fluorometer (Cat. No. Q33217). DNA and protein concentrations were measured according to the manufacturer's instructions. DNA concentration was measured using either the High Sensitivity (HS) or the Broad Range (BR) settings, though HS settings were preferred for more accurate readings. The three methods used;

DNA HS, DNA BR, or protein, each required unique Qubit buffer, dye, and standards. Standards were read before each set of samples were measured. Two Assay Tubes were used to measure standards for DNA assays and three Assay Tubes were used to measure standards for protein assays. Qubit working solution was prepared by mixing the Qubit dye and buffer in a 1:199 volume ratio and vortexed for a few seconds. 200 µl of working solution was prepared for each standard and sample. To set up each standard, 10 µl of each standard from the kit was added to 190 µl of working solution in a separate Assay Tube. To set up each sample, 1-20 µl of DNA or protein solution to be measured was mixed with working solution to a final volume of 200 µl. Each standard and sample Assay Tube was then vortexed for 3 seconds and incubated at room temperature before readings were taken. All DNA Assay Tubes were incubated for 2 minutes while protein Assay Tubes were incubated for 15 minutes. Standards were read first by inserting the Assay Tubes into the Qubit Fluorometer one at a time and taking readings. Following this, samples were read in the same fashion.

2.8 DNA digest with restriction endonucleases

All restriction endonucleases (enzymes) and their respective buffers were purchased from NEB. All restriction enzymes demonstrated 100% activity in NE Buffer #4, also called Cutsmart Buffer. Total reaction volumes of both single and double enzyme digest reactions were 50 µl. Double enzyme digest reactions contained 41 µl of DNA (varying concentrations), 5 µL of 10x NE Buffer #4, and 2 µl of each appropriate High Fidelity enzyme and were incubated at 37ºC in the thermal cycler or incubator for 4 hours. Single enzyme digest reactions contained 43 µl of plasmid DNA, 5 µL of 10x NE Buffer #4, and 2 µl of the appropriate High Fidelity enzyme. DNA digests were either used immediately, held at 4ºC overnight in the thermal cycler, or stored in the

freezer at -20ºC. DNA digests left overnight at 4ºC in the thermal cycler were first heated to 65ºC for 25 minutes to deactivate the enzyme to eliminate nonspecific digestion.

2.9 Agarose gel electrophoresis

Agarose gel electrophoresis was used to separate DNA molecules based on size. DNA gels were run with 1% (w/v) agarose dissolved in Tris/acetate/EDTA (TAE) buffer, which consisted of 40 mM Tris acetate and 2 mM Na_2EDTA. Gels were stained with 0.5 µg/ml ethidium bromide for DNA band visualization and voltage was applied using the PowerPac Basic unit from BioRad. Gels to be visualized were run for 30 minutes at 120 V while DNA recovery gels were run for 60 minutes at 120 V. DNA solutions were run alongside a 1 kb ladder, purchased from NEB (Cat. No. N3232L), and each sample was mixed with 6x gel loading dye from NEB in a 1:5 volume ratio of dye to sample. DNA to be visualized was run at a total volume of 5-12 µl, and DNA to be recovered was run in deeper wells with a total volume of 50-60 µl. Image visualization was performed with a UVP Benchtop 2UV BioDoc-It Imaging System at 302 or 365 nm.

2.10 DNA recovery from agarose gels

DNA was recovered and purified from agarose gels following electrophoresis using the Zymoclean Gel DNA Recovery Kit (Cat. No. D4002). First, the visualized DNA band was cut out of the gel using a clean razor and placed into a sterile 1.5 µl microcentrifuge tube. Approximately 3 volumes of Agarose Dissolving Buffer was added to the tube for each volume of gel and the sample was incubated at 45-55ºC in a water bath until the gel was completely dissolved. Next, the solution was loaded into a Zymo-Spin Column in a Collection Tube and centrifuged at 15,000 rpm for 30 seconds. Following this, 200 µl of DNA Wash Buffer was added to the column which was then centrifuged at 15,000 rpm for 30 seconds. This wash step was repeated and the column was then placed in a new sterile 1.5 µl microcentrifuge tube. Finally, 10-50 µl of sterile water was

added to the column which was then centrifuged at 15,000 rpm for 30 seconds. Different volumes of water were used to adjust the DNA to desired concentrations for Gibson Assembly, DNA ligation, or transformation into *B. subtilis*. Recovered DNA samples were either used immediately or stored at -20ºC.

2.11 Ligation

Vectors and inserts were ligated using materials from NEB and reactions were performed in sterile 1.5 µl microcentrifuge tubes. Ligation reaction mixtures contained 2 µl of 10x T4 DNA Ligase Reaction Buffer (Cat. No. B0202S) and 1 µl of T4 DNA Ligase (Cat. No. M0202L). The volumes of vector and insert DNA were adjusted to achieve a 1:3 molar ratio of vector to insert and water was added to a total reaction mixture of 20 µl. The ligation mixture was incubated at 25°C for 30 minutes and was then used immediately for transformation. Any remaining ligation mixture was then stored at -20ºC and could be used for subsequent transformations for up to one week.

2.12 Preparation of chemically competent *E. coli* cells

Chemical competence was induced in wild-type DH5α *E. coli* using the Inoue method found in *Molecular Cloning* with a few modifications [57]. Chemically competent *E. coli* could then uptake extracellular DNA from the environment via extreme temperature changes. Inoue Transformation Buffer (ITB) was prepared with 55 mM $MnCl_2$, 15 mM $CaCl_2$, 250 mM KCl, and 10 mM PIPES in water. Aliquots were used immediately or stored at -20ºC. *E. coli* DH5α cells were grown overnight on an LB plate at 37ºC. Following this, a few colonies were mixed with 2 ml of LB in a sterile test tube and grown for 6-8 hours via shaking at 37ºC. 0.5-1 ml of this culture was added to 50 ml of LB and grown overnight via shaking at 25ºC. Cells were grown to an OD_{600} of approximately 0.6 and OD_{600} was measured using an Ultraspec 10 cell density meter from

Amersham Biosciences. The culture was then centrifuged at 4,000 rpm and 4ºC in an Eppendorf 5804 R Centrifuge. The supernatant was discarded and the remaining liquid was drained onto a paper towel for 5 minutes. Cells were then re-suspended in 15-20 ml of cold ITB via inversion and centrifuged for 15 minutes at 4,000 rpm and 4ºC. The wash steps (discarding the supernatant, draining, re-suspending, and centrifuging) were repeated twice more to thoroughly wash the cells. Cells were finally re-suspended in 4 ml cold ITB and DMSO was added to a final concentration of 7.5% (v/v). Competent cells were flash frozen for 10 minutes using 100% ethanol poured over dry ice. They were either used immediately or stored in aliquots at -80ºC for up to one year.

2.13 Heat shock transformation of *E. coli*

Transformation of chemically competent *E. coli* was performed using the protocol found in *Molecular Cloning* [57]. In a sterile 1.5 µl microcentrifuge tube 50 µl of competent cells were mixed with 5 µl of ligation mixture, 5 µl of Gibson assembly mixture, or 2 µl of purified plasmid DNA. The mixture was placed on ice for 30 minutes, transferred to a 42ºC water bath for 2 minutes, and then placed back on ice for 5 minutes. The competent cells and DNA were transferred to 1 ml of LB in a sterile test tube, and the cells were recovered via shaking for 1 hour at 37ºC. The cells and LB were spun down at room temperature for ten minutes in a new sterile 1.5 µl microcentrifuge tube and 800 µl of the supernatant was removed via pipette. The cell pellet was mixed thoroughly with the remaining liquid via gentle pipetting, then spread on an LB plate containing the appropriate antibiotic. Transformation plates were incubated overnight and were examined for colonies the following day.

2.14 DNA verification via colony PCR

Colonies from transformation plates were checked for desired DNA using colony PCR. All amplifications were performed using a BioRad T100 Thermal Cycler. GoTaq Green MasterMix

purchased from Promega was used. Colony PCR reactions contained 12.5 µl of GoTaq Green MasterMix, 10.5 µl of autoclaved water, and 1 µl each of forward and reverse primers in a PCR tube for a total reaction volume of 25 µl. One colony from the transformation plate was used as the DNA template. After mixing the colony into the PCR reaction mixture with a toothpick, the same toothpick was used to streak the colony on a new LB plate containing the appropriate antibiotic. This plate was incubated overnight at 37ºC. Plating of colonies was done to save *E. coli* containing the desired DNA for future use. These plates were stored in the refrigerator at 4ºC for up to 3 months and were used to make freezer stocks for long term storage.

2.15 Plasmid DNA isolation from liquid culture

Transformed colonies containing the desired DNA were mixed into a 5 ml liquid culture with the appropriate antibiotic concentration, shown in Table 5. A process called miniprep was used to extract and purify plasmid DNA from the 5 ml *E. coli* cell culture. The Plasmid DNA Miniprep- Classic kit from Zymo Research (Cat. No. D4016) was used for this purpose.

Table 5. Working antibiotic concentrations for different vectors and strains

Strain	Parent Vector	Antibiotic(s)	Working Concentration (µg/ml)
E. Coli DH5α	pNW33N	chloramphenicol	20-30
E. Coli DH5α	pDR111	ampicillin	100
G. thermoglucosidans 95A1	pNW33N	chloramphenicol	5-7
B. subtilis 1085	pDR111	spectinomycin	100
B. subtilis 1S101	None	chloramphenicol	5
B. subtilis 1S101	pDR111	spectinomycin & chloramphenicol	100 & 5

First, the liquid culture was poured into a sterile 15 ml centrifuge tube and centrifuged at 4ºC for 12 minutes. The supernatant was then discarded and the remaining liquid was drained onto a paper towel for 5 minutes. After this, the cell pellet was suspended in 200 µl of P1 Buffer via

pipetting and the mixture was transferred to a sterile 1.5 ml microcentrifuge tube. Next, P2 Buffer was added to the tube and mixed via inverting 5 times. The mixture was incubated for 1-3 minutes after which time P3 Buffer was added to the tube. The tube was then inverted gently until the mixture was completely yellow/white. The tube was then centrifuged at 15,000 rpm for 3 minutes. Following this the supernatant was loaded into a Zymo-spin column in a Collection Tube. The mixture was then centrifuged for 30 seconds at 15,000 rpm. The flow-through was discarded and 200 µl of Endo-Wash Buffer was added to the column which was then centrifuged for 30 seconds at 15,000 rpm. Next, 400 µl of Plasmid Wash Buffer was added to the column which was then centrifuged for 30 seconds at 15,000 rpm. Following this, the column was placed into a new 1.5 µl microcentrifuge tube and the DNA was eluted by adding 50 µl of sterile water and centrifuging the tube for 30 seconds at 15,000 rpm. This eluted DNA was either used immediately or stored at -20ºC for future use. DNA was stored this way for up to two years.

2.16 Preparation of electrocompetent *G. thermoglucosidans* 95A1

Electrocompetence was induced in the wild type *Geobacillus thermoglucosidans* 95A1 strain for introduction of foreign plasmids. Electrocompetent *Geobacillus thermoglucosidans* could then uptake extracellular DNA from the environment via the application of an electric charge. In a sterile 250 ml Erlenmeyer flask 1 ml of *G. thermoglucosidans* cells from freezer stock were added to 50 ml of TGP media. The culture was grown at 52ºC via shaking until the OD_{600} reached 2.0. The cells were centrifuged at 4,000 rpm and 4ºC for 15 minutes. The supernatant was discarded and the remaining liquid was drained onto a paper towel for 5 minutes. Cells were then re-suspended in cold electroporation buffer which contained 0.5 M mannitol, 0.5 M sorbitol, and 10% glycerol via inversion and centrifuged for 15 minutes at 4,000 rpm and 4ºC. The wash steps (discarding the supernatant, draining, re-suspending, and centrifuging) were repeated twice more

to thoroughly wash the cells. The cells were then re-suspended in 2 ml of electroporation buffer and were used immediately or stored at -80ºC for up to 6 months.

2.17 Electroporation of *G. thermoglucosidans* 95A1

To transform foreign plasmid DNA into *G. thermoglucosidans* 95A1 electroporation was used. Electroporation was performed using a BioRad Gene Pulser Xcell and BioRad PC Module. 1 mm, sterile cuvettes were purchased from VWR and were chilled at -20ºC prior to use (Cat. No. 89047-206). 60 µl of electrocompetent cells were mixed with 2 µl of purified plasmid DNA in a PCR tube. The mixture was then transferred to an electroporation cuvette and pulsed. Electroporation settings were 2.5 kV, 10 µF, and 600 Ω with an exponentially decaying pulse. Cells were immediately suspended in 1 ml TGP pre-warmed to 52ºC and were recovered via shaking at 52ºC for one hour. 200 µl of recovered cells were plated on TBAB with appropriate antibiotic. Plates were incubated overnight at 52ºC and were examined the following day for colonies.

Colonies were checked for desired DNA using colony PCR as described above with one adjustment. *G. thermoglucosidans* 95A1 cells cannot be stored at 4ºC because they will form spores. Therefore, after the colonies were streaked out and grown overnight on a new plate, positive colonies were selected to make freezer stocks immediately, after which the plates were discarded.

2.18 Cell line freezer stocks

A library of all transformed strains was created and stored at -80ºC for future use. *E. coli* and *B. subtilis* strains were grown for 5-6 hours in LB with appropriate antibiotic. Freezer stocks consisted of 50% (v/v) liquid cell culture and 25% (v/v) glycerol in sterile water. In a freezer stock tube from VWR (Cat. No. 66008-754) 600 µl of cell culture was mixed with 400 µl of sterile 50

(v/v) glycerol. For *Geobacillus* strains, cells were grown on TBAB plates with appropriate antibiotic overnight. A large amount of colonies were extracted from the plates with a sterile wooden stick and suspended in sterile 10% (v/v) glycerol. *E. coli* freezer stocks were stored for up to 4 years, *B. subtilis* freezer stocks were stored for up to 2 years, and *Geobacillus* freezer stocks were stored for up to 1 year.

2.19 *In vitro* protein fluorescence measurements

In vitro fluorescent protein fluorescence measurements were taken using crude protein extracts from *E. coli* with extract from empty *E. coli* cells as a negative control. Colonies of *E. coli* strains expressing fluorescent proteins were grown on plates overnight at 37ºC with the appropriate antibiotic. A few colonies were inoculated into 10 ml of LB media with the appropriate antibiotic and grown overnight at 37ºC with shaking in sterile test tubes. In the morning, cultures were centrifuged at 4,000 rpm and 4ºC for 15 minutes in 15 ml centrifuge tubes. All of the supernatant was discarded and cells were re-suspended in 10 ml of TE buffer which contained 10 mM Tris-Cl, pH 8 and 1 mM EDTA. Lysozyme was added to a final concentration of 1 µg/ml and the mixture was left on the bench for 10 minutes. The mixture was aliquoted into 15 ml centrifuge tubes which were frozen at -80ºC and then thawed to break the cells. This freeze/thaw process was repeated 3 times. The mixture was then centrifuged at 4,000 rpm and 4 ºC for 10 minutes and the supernatant was collected and used as the crude protein extract. The heat stability of the fluorescent proteins was tested by incubating the protein extracts in the 80ºC water bath for 14-100 minutes in 2-20 minute increments. 50 µl of protein extracts were transferred to 96-well microplates to take readings. Fluorescence Intensity measurements were taken using the Microplate Reader and all experiments were done in triplicate. The Fluorescence Intensity of the negative control was

subtracted from the Fluorescence Intensity of each sample to obtain the Fluorescence Intensity resulting from each fluorescent protein.

2.20 *In vivo* protein fluorescence measurements

Fluorescence readings were taken for *E. coli* and *G. thermoglucosidans* strains expressing fluorescent proteins with empty cells as a negative control. *E. coli* and *G. thermoglucosidans* strains expressing fluorescent proteins were grown on plates overnight at 37ºC and 52ºC respectively with the appropriate antibiotic. Colonies were taken from the plates and inoculated into 5 ml of LB or TGP media with the appropriate antibiotic. *E. coli* cultures were grown at 37ºC for 5 hours before readings were taken. *G. thermoglucosidans* cultures were grown at 50ºC for 20 hours and 60ºC for 6 hours before readings were taken. 50 µl of liquid culture was transferred to 96-well microplates from Thermo Fisher Scientific (Cat. No. 07-200-567) to take readings. OD_{600} and Fluorescence Intensity measurements were taken using a Synergy H1 Hybrid Multi-Mode Microplate Reader from BioTek. All experiments were done in triplicate. First, protein expression level was calculated by dividing the Fluorescence Intensity reading of the sample or negative control by the OD_{600} reading. Next, expression level was calculated by dividing each fluorescence intensity reading by the fluorescence intensity of the negative control. Expression level data were plotted in Microsoft Excel for each *E. coli* and *G. thermoglucosidans* sample grown at their respective temperatures.

2.21 Laccase extraction from transformed cell lines

Intracellular laccase was extracted from transformed cell lines via sonication. The general protocol was adapted from *Molecular Cloning* [57]. 0.5 L of *E. coli* producing laccase were grown overnight with the appropriate antibiotic and 0.5 mM $CuSO_4$. Cultures were centrifuged at 4ºC for 15 minutes at 4,000 rpm. Cell pellets were re-suspended in buffer which contained 50 mM Tris-Cl, 500 mM NaCl, and 15% (v/v) glycerol, after which lysozyme was added to a concentration of

1 mg/ml and phenylmethylsulfonyl fluoride (PMSF) was added to a concentration of 1 mM. The mixture was incubated on ice for 30 minutes before sonication. Samples were kept on ice and NaCl during sonication to prevent overheating. Cells were sonicated for 10 minutes with a sonicator and microtip purchased from Qsonica Sonicators (Pt. No. Q700 and 4420). The process of sonication consisted of 30 second intervals followed by 45 second cooling intervals. Sonicated cells were then spun down for 30 minutes at 15,000 rpm to precipitate cell debris. The laccase was purified from the resulting supernatant which is the protein extract.

2.22 Laccase purification

Laccase was purified from cell extract using immobilized metal ion chromatography. 3 ml HisPur Ni-NTA columns were purchased from Thermo Fisher Scientific (Prod. No. 88229). The manufacturer's suggested protocol was followed. Phosphate Buffered Saline (PBS) contained 137 mM NaCl, 2.7 mM KCl, 10 mM Na_2HPO_4, and 1.8 mM KH_2PO_4. 10 mM imidazole in PBS was used for equilibration buffer, 25 mM imidazole in PBS was used for wash buffer, and 250 mM imidazole in PBS was used for elution buffer. The sample was prepared by mixing the protein extract with an equal volume of equilibration buffer in a 50 ml centrifuge tube. Additionally, the HisPur Ni-NTA column was equilibrated to room temperature. Following this the bottom tab was removed from the column which was then placed in a 50 ml centrifuge tube. The column was then centrifuged at 700 rcf for 2 minutes to remove the storage buffer. Next, 6 ml of equilibration buffer was added to the column. The buffer was allowed to enter the resin bed and the column was then centrifuged at 700 rcf for 2 minutes. A stopper was used to plug the bottom of the column and the prepared sample was added and allowed to enter the resin bed. If the volume exceeded the volume of one column, the sample was divided equally between two columns. The sample was then shaken gently at room temperature for 30 minutes to allow for maximum binding. The sample was then

centrifuged at 700 rcf for 3 minutes and the flow-through was discarded. Next, 6 ml of wash buffer was added to the column which was then centrifuged for 3 minutes. The wash step was then repeated two more times. Following this the column was placed into a new 50 ml centrifuge tube and 3 ml of elution buffer was added to the column. The column was then centrifuged for 3 minutes at 700 rcf. The elution step was then repeated 5 more times with each elution stored in a new 50 ml centrifuge tube. Typically the 4^{th}, 5^{th}, and 6^{th} tubes contained the most laccase. Eluted laccase was transferred to 1.5 ml microcentrifuge tubes and stored at 4ºC for short-term use and -20ºC for long-term use. Columns were regenerated using filtered 20 mM 2-(N-morpholino)ethanesulfonic acid (MES) buffer, pH 5.0 with 0.1 M NaCl. First, the column was filled with the buffer containing 20 mM MES buffer and 0.1 M NaCl and centrifuged at 800 rcf for 4 minutes. Next, the column was filled with sterile water and centrifuged at 800 rcf for 5 minutes. The column was then stored at 4ºC in 12 ml of sterile 20% (v/v) ethanol.

2.23 SDS-PAGE, Native PAGE, and gel staining

BioRad Mini-PROTEAN TGX precast gels (Cat. No. 456-1094) were purchased for running Sodium Dodecyl Sulfate Polyacrylamide Gel Electrophoresis (SDS-PAGE) and Native PAGE gels. 2x Laemmli sample buffer was used for SDS-PAGE gels and contained 65.8 mM Tris-Cl (pH 6.8), 2.1% (w/v) SDS, 26.3% (v/v) glycerol and 0.1% (w/v) bromophenol blue. Total sample volume was 50 µl and contained 25 µl of purified protein, 23 µl of 2x Laemmli sample buffer, and 2 µl of 2-mercaptoethanol. The mixture was heated to 95ºC for 5 minutes to denature the protein. SDS-PAGE gel running buffer contained 2.5 mM Tris base, 19.2 mM glycine, and 0.1% (w/v) SDS, pH 8.3. Samples were run for 60 minutes alongside Benchmark His-tagged Protein Standard (Ref. No. LC5606) at a constant voltage of 200 V in a BioRad Mini-PROTEAN Tetra System (Cat. No. 1658005). Native PAGE gel sample buffer contained 62.5 mM Tris (pH

6.8), 25% glycerol, and 0.1% bromophenol blue. Total sample volume was 50 µl and contained 25 µl of purified protein and 25 µl of Native PAGE gel sample buffer. Native PAGE gel running buffer contained 25 mM Tris base and 192 mM glycine. Samples were run for 100 minutes alongside Benchmark His-tagged Protein Standard at a constant voltage of 80 V in a BioRad Mini-PROTEAN Tetra System on ice.

SDS-PAGE and Native PAGE gels were removed and stained using SimplyBlue SafeStain from Themo Fisher Scientific (Cat. No. LC6060). Three 5-minute washes were performed on the gels with sterile water followed by 1 hour of staining. While staining the gels were gently shaken in a plastic container at room temperature. Following staining, Native PAGE gels were washed with sterile water for 2 hours and SDS-PAGE gels were washed with sterile water overnight. Clear bands were then visualized and captured.

2.24 *Bacillus subtilis* competent cell preparation and transformation

The protocol for *B. subtilis* competent cell preparation and transformation was taken from the *Bacillus* Genetic Stock Center with a few modifications to enhance transformation efficiency [58]. 10x Medium A base contained 1% (w/v) yeast extract, 0.2% (w/v) casamino acids, and 5% (v/v) glucose in sterile water. 10x Bacillus salts contained 2% (w/v) $(NH_4)SO_4$, 1.2% (w/v) KH_2PO_4, 0.04% (w/v) $MgSO_4*7H_2O$, 27.94% (w/v) K_2HPO_4, and 1% (w/v) sodium citrate in sterile water. Medium A contained 10% (v/v) 10x Medium A base and 9% (v/v) 10x Bacillus salts in sterile water. Medium B contained 5 mM $CaCl_2 \cdot 2H_2O$ and 25 mM $MgCl_2 \cdot 6H_2O$ in Medium A. A few colonies of *B. subtilis* 1085 or *B. subtilis* 1S101 from a fresh plate were inoculated into 1 ml of Medium A in a sterile test tube to an OD_{600} of 0.1-0.2. The cell culture was incubated at 37ºC with vigorous shaking for 4 hours. 100 µl of the culture was then transferred to 800 µl of pre-warmed Medium B in a new test tube. One test tube was set up for each transformation performed,

plus one extra for a DNA-less control. 20 µl of digest DNA fragments were added to the test tubes which were shaken slowly for 3-4 hours at 37ºC. Following this each cell culture was transferred into a 1.5 ml microcentrifuge tube and centrifuged for ten minutes at 3,000 rpm. 700 µL of the supernatant was discarded and the cells were re-suspended in the remaining liquid. The cells and liquid were then spread onto LB or TBAB plates with the appropriate antibiotic and incubated overnight at 37ºC.

2.25 Sporulation of *B. subtilis*

The protocol for *B. subtilis* sporulation was found in *Molecular Biological Methods for Bacillus* [59]. 2xSG medium contained 1.6% (w/v) nutrient broth, 0.05% (w/v) $MgSO_4 \cdot 7H_2O$, 0.2% (w/v) KCl, 1 mM $Ca(NO_3)_2$, 0.1 mM $MnCl_2 \cdot 4H_2O$, 1 µM $FeSO_4$, and 0.1% (w/v) glucose. Cells from a *B. subtilis* strain of interest were taken from freezer stock and streaked on an LB or TBAB plate with the appropriate antibiotic which was incubated overnight at 37ºC. A colony was taken from the plate and inoculated into 10-50 ml of LB or 2xSG medium with the appropriate antibiotic. The culture was grown with shaking at 37ºC for 6-8 hours. This culture was then diluted 1/200 into 50-10,000 ml of 2xSG medium with the appropriate antibiotic and grown with shaking at 37ºC for 3-7 days. The spore culture was transferred to 50 ml centrifuge tubes and centrifuged at 4,000 rpm for 45-60 minutes at 4ºC. The supernatant was carefully discarded. Spores were then washed 5-8 times with sterile water to remove residual medium and lyse the remaining vegetative cells. This was done by re-suspending the spores in sterile water, centrifuging for 60 minutes, and carefully removing the supernatant. Spores were stored in a small amount of sterile water at room temperature or 4ºC for short term use or -80ºC for long term use.

2.26 Laccase activity assays

The activity of purified laccase was tested using 5 different substrates; guaiacol, ABTS, 2,6-dimethoxyphenol, 4-methoxybenzyl alcohol, and veratryl alcohol. The reaction mixture

contained 800 µl of 150 mM citrate-phosphate buffer (varying pH) which contained 0.2 M Na_2HPO_4 and 0.1 M citric acid, 100 µl of 10x substrate for a final concentration of 5 mM, and 100 µl of purified laccase. The reaction activity was tested from pH 3.0 to 7.0 and at temperatures ranging from 50ºC to 80ºC. Absorbances were measured spectrophotometrically using a Genesys 10uv spectrophotometer by Thermo Scientific in 1 cm cuvettes supplied by VWR (Ref. No. 97000-586). Substrates along with their accompanying wavelengths and molar absorptivities are shown in Table 6. 1 unit (U) of enzyme activity was defined as the amount of enzyme required to oxidize 1 µmol of substrate in 5 minutes.

Table 6. Wavelengths and molar absorptivities for laccase substrates

Substrate	Wavelength (nm)	Molar Absorptivity ($M^{-1}cm^{-1}$)
guaiacol	465	48,000
ABTS	436	29,300
2,6-dimethoxyphenol	468	14,800
veratryl alcohol	310	9,000
4-methoxybenzyl alcohol	500	38,000

Due to the results of the studies on purified laccase, spore displayed laccase activity was tested using 2,6-dimethoxyphenol as the substrate. ABTS was also considered, but the substrate reacted with the spores to create a cloudy solution which was unable to be measured with the spectrophotometer. The reaction mixture consisted of 800 µl of 150 mM citrate-phosphate buffer, 100 µl of 10x substrate for a final concentration of 5 mM, and 100 µl of spores with displayed laccase. Activity assays were performed at pH 7.0 and 80ºC for 5 minutes. The half-lives of spore displayed laccase were found by incubation of the spore displayed laccase at 80ºC for 0-9 hours in 1 hour increments prior to setting up reactions. All experiments were done in triplicate.

2.27 Laccase enzyme kinetics measurement

For this system it was assumed that the laccase reaction followed Michaelis-Menten kinetics. The Michaelis-Menten model assumes that the rate of reaction, or the amount of substrate consumed with time, varies with the amount of substrate present in the reaction according to the curve shown below in Figure 3.

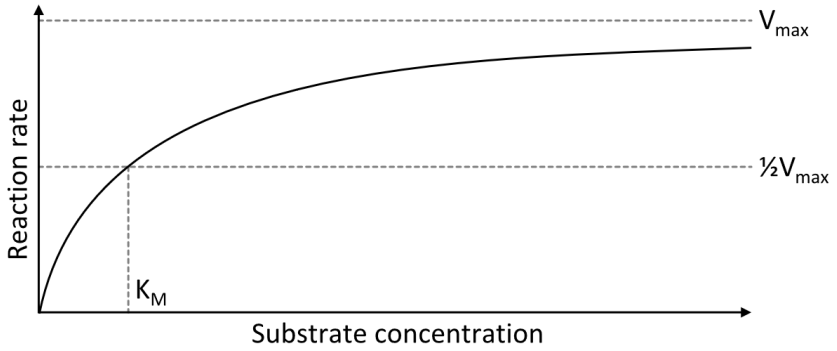

Figure 3. The Michaelis-Menten saturation curve for an enzyme reaction [60].

The Michaelis-Menten curve shows that the enzyme reaction rate increases with increasing substrate concentration. The increase in reaction rate is rapid and linear at first and then tapers off until a maximum ration rate is reached, labelled V_{max}. Another important parameter, K_M, is the substrate concentration at which half of the maximum reaction rate, $0.5V_{max}$, is reached. When enzyme concentration is much less than the substrate concentration, the rate of reaction is given by Equation 1. Rearrangement of Equation 1 gives Equation 2 which is linear and allows for the determination of the Michaelis-Menten parameters experimentally. Determining the Michaelis-Menten parameters gives a quantitative measurement of enzyme efficiency [61].

$$V = Vmax\frac{[S]}{Km + [S]} = kcat[Eo]\frac{[S]}{Km + [S]} \quad (1)$$

$$\frac{1}{V} = \frac{1}{Vmax} + \frac{Km}{Vmax}\frac{1}{[S]} \quad (2)$$

To determine the Michaelis-Menten parameters, K_M, V_{max}, and k_{cat} initial reaction rate was measured at a variety of different substrate concentrations. 2,6-DMP was used as the substrate for these experiments and the reaction was carried out in Sørensen's phosphate buffer at pH 8 which contained 94.7 ml of 0.2 M Na_2HPO_4, 5.3 ml of 0.2 M NaH_2PO_4, and 100 ml of water. Reactions were carried out in cuvettes as described previously with 100 µl of enzyme, 800 µl of buffer, and 100 µl of substrate. 100 mM 2,6-DMP was used as a stock solution and dilutions were performed to vary the concentration. Absorbance readings were taken every 5 seconds for 60 seconds as described previously with the same reaction conditions, except this time reactions were carried out at room temperature. This was because readings could not be taken with the spectrophotometer in the incubator. It should be noted that prior to the start of the reactions the laccase was heated at 80ºC for 30 minutes to improve the efficiency of the enzyme. The inverse of the initial reaction rate verses the inverse of the substrate concentration was plotted in Microsoft Excel and the Michaelis-Menten parameters were calculated.

CHAPTER 3: FLUORESCENT PROTEINS AS GENETIC TOOLS FOR *GEOBACILLUS THERMOGLUCOSIDANS*

3.1 Introduction

3.1.1 The Discovery of *Geobacillus*

When thermophilic *Geobacillus* species were first discovered in 1949 they were classified by Nathan R. Smith and Ruth E. Gordon as thermophilic *Bacillus* species, either *B. stearothermophilus* or *B. coagulans*. These were described as any spore-former capable of growing at 65ºC, especially if they hydrolyzed starch and gelatin and showed a growth sensitivity to lysozyme and 7% NaCl [62]. Over the next 30 years a myriad of evidence showed that thermophilic *Bacilli* are a diverse group. In 1993, White et al. analyzed 234 strains located worldwide, looking into nearly 100 phenotypic characteristics including growth, carbohydrate usage, toleration of inhibitors, degradation of substrates, and chromosomal DNA melting temperature among others [63]. These studies revealed enormous diversity which led to further investigations. Ash et al. analyzed 51 species of *Bacillus* using 16S rRNA sequencing and found that they spanned five separate groups which they believed represented different genera [64].

The work by Ash and colleagues started a reorganizational period for the genus *Bacillus* which is ongoing. Several new genera have been created for organisms previously known as *Bacillus* and other genera have been created for novel organisms that would have been previously assigned to *Bacillus*. Three species including *B. stearothermophilus*, *B. kaustophilus*, and *B. thermoglucosidans* were termed “group 5” by Ash and colleagues because they were phylogenetically distinct from the other four groups [64]. After 10 years a group of Moscow scientists led by N. A. Nazina at the Russian Academy discovered many different thermophilic *Bacilli* in high temperature oil fields in Kazakhstan [65]. Later studies resulted in the discovery of similar bacteria from oil fields in western Siberia and China [66, 67]. Physiologic and genetic

analysis revealed that these organisms fell into two groups, some of which were very similar to the Ash et al. “group 5” isolates. Upon further examination of the “group 5” organisms, a new physiologically and morphologically consistent genera was classified and given the name *Geobacillus*. All of the “group 5” species along with the species discovered in Kazakhstan, Siberia, and China were then reclassified as *Geobacillus* species [68].

3.1.2 *Geobacillus* characteristics and industrial applications

Geobacillus was given the prefix “geo” meaning earth because they were found deep in the earth, particularly in geothermal environments like hot oil fields. Their vegetative cells are rod-shaped and are flagellated for cell motility. They are gram-positive and their colonies vary in shape and size depending on the species. Their cells produce endospores when under stress; one ellipsoidal or cylindrical endospore is produced per cell. They are aerobic or facultatively anaerobic and thermophilic. Their growth temperatures range from 37-75ºC with an optimum growth temperature ranging from 55-65ºC. Additionally, growth occurs at a pH range of 6.0-8.5 with the optimum pH ranging from 6.2-7.5 [68].

Geobacillus species have many industrial applications. They have been found to produce many thermostable enzymes such as α-amylase which is used to process sweeteners from starch, xylanase which is used in the pulp and paper industry to degrade hemicellulose in wood pulp, and catalase which is used in the food and textile industries to convert hydrogen peroxide in milk and fabrics to water and oxygen [69, 70, 71]. In many cases, industrially used enzymes must be able to withstand high processing temperatures and consequently, the enzymes must be thermostable. Because of this, the isolation of thermostable enzymes from thermophiles such as *Geobacillus* is imperative. A list of patented thermostable enzymes from *Geobacillus* species is given in Table 7 [72]. Additionally, *Geobacillus* spores are often used as Biological Indicators (BIs) to test the

lethality of autoclaves and other sterilization equipment. Furthermore, *Geobacillus* species are used industrially for cellobiose fermentation and ethanol production [73]. *Geobacillus* also have great potential for bioremediation since certain species can degrade pollutants such as arsenate, phenols, aliphatic hydrocarbons, and azo dyes [74, 75].

Table 7. U.S. patents for thermostable enzymes from *Geobacillus*

Enzyme	Use	Patent No.
α-arabinofuranosidase	degradation of hemicellulose	US05434071
acetate kinase	glycolysis/metabolism	US05610045
α-amylase	hydrolysis of starch	US05824532, US05849549
BsrFI restriction endonuclease	molecular cloning	US06066487
catalase	decomposition of hydrogen peroxide	US06022721
DNA polymerase	DNA replication and construction	US05747298, US05830714, US05834253, US05874282, US06013451, US06066483, US06100078, US06238905
glucose-6-phosphate dehydrogenase	glycolysis/metabolism	US04331762
malate dehydrogenase	glycolysis/metabolism	US04331762
neutral proteases	protein degradation	US06103512
polynucleotide phosphorylase	RNA degradation	US04331762
pyruvate kinase	glycolysis/metabolism	US04331762
superoxide dismutase	conversion of O_2- free radical into O_2	US05772996
xylanase	degradation of hemicellulose	US05434071
xylosidase	degradation of cellulose and hemicellulose	US05489526

*Adapted from the Bacillus Genetic Stock Center Catalog, *The Genus Geobacillus* [72]

3.1.3 *G. thermoglucosidans* characteristics and industrial applications

The *Geobacillus* species of interest in this work is *Geobacillus thermoglucosidans*. The species name is a combination of “therme” meaning “heat” and “glucosidans” meaning “glucosidase producing”. Thus the bacteria are thermophilic and they produce the enzyme glucosidase which hydrolyzes starch. The species was first isolated from high temperature soil in Japan. It grows at temperatures ranging from 37-68ºC and pH 6.0-8.0 with an optimum growth

temperature range of 50-60ºC [72]. *G. thermoglucosidans* produces many thermostable enzymes with industrial applications including xylosidases, xylanases, glucuronidases, aldolases, xylose isomerases, laccases, and nitrile hydratases. These can be used industrially for xylan and lignin degradation along with the production of acrylamide and acrylonitrile [76].

G. thermoglucosidans is of industrial interest for a variety of purposes. A genetically engineered strain, *G. thermoglucosidans* TM242 was able to convert a palm kernel cake hydolysate into ethanol with high yields, approximately 92% of the theoretical yield based on the total fermentable sugars in palm kernel cake [77]. Another genetically engineered strain, *G. thermoglucosidans* DSM 2542T was able to produce 3.3 g/L of isobutanol from glucose and 0.6 g/L of isobutanol from cellobiose [78]. Using *G. thermoglucosidans* for the fermentation of sugars into alcohols for fuel provides a few advantages over other organisms such as yeast; yeast is the most commonly used organism for the production of bioethanol. First, the high growth temperature of *G. thermoglucosidans* improves the rate of feed conversion and reduces the cooling costs during fermentation. Second, using these thermophiles reduces the risk of contamination by other organisms, particularly mesophiles which cannot survive at high temperatures. Third, they have advantageous growth properties such as reduced viscosity in the growth media, reduced energy requirements for mixing, higher diffusion rates, and increased substrate solubility [79].

Additionally, *G. thermoglucosidans* has been shown to catalyze the formation of 100-µm hexagonal fluorescent magnesium-calcite crystals at 60ºC in a hydrogel containing sodium acetate, calcium chloride, and magnesium sulfate. These calcite crystals have unusually large excitation and emission wavelength intervals, 260-400 nm and 350-600 nm respectively, and have a variety of applications. Some potential applications include being used as novel phosphors in fluorescent lamps and cathode ray tubes which can be prepared without rare earth metals, fillers for rubbers

and plastics, fluorescent particles in stationary ink, fluorescent markers for biochemistry applications, and indicators for dosimetry and dating [80].

3.1.4 Genetic studies and tools for *Geobacillus*

Many genome-sequencing studies for *Geobacillus* species have been completed and more are in progress. As of this year the complete genome sequences are known for over 30 *Geobacillus* strains, including some strains of *G. thermoglucosidans*, *G. thermoleovorans*, *G. kaustophilus*, *G. thermocatenulatus*, *G. thermodentrificans*, *G. stearothermophilus*, and *G. caloxylosilyticus* in addition to several strains that have not been assigned to named species. A list of 16 of these genome-sequenced *Geobacillus* strains along with their industrial applications is shown in Table 5. These genome sequences provide a basis for understanding the regulatory mechanisms resulting in various phenotypes of these bacteria such as thermostability, tolerance to heavy metals and organic compounds, and tolerance to denitrification. Understanding these regulatory mechanisms also aids in the genetic modification of these bacteria for improved industrial use [81].

Additionally, some genetic tools have been developed for *Geobacillus* species. A library of synthetic ribosome binding sites, many constitutive promoters, and a few inducible promoters have been discovered or developed for strains of *G. thermoglucosidans*, although the inducible promoters are activated in the presence of sugars which interfere with the metabolic status in the cell. They also have a high basal level of expression, meaning even in the absence of the inducer some protein expression is observed [82]. Additionally, genetic transformation methods have been developed for *G. thermoglucosidans*, but the efficiency by which the bacteria can uptake extracellular DNA is low [82, 83]. The investigation and development of *Geobacillus* species such as *G. thermoglucosidans* is impeded due to a lack of genetic tools such as efficient and robust genetic transformation, tightly regulated inducible promoters, and thermostable expression

reporters. For this reason, a more robust genetic toolkit is required to further physiological studies of *Geobacillus* species in order to genetically modify them for improved industrial use.

Table 8. Genome-sequenced *Geobacillus* strains and their industrial applications.

Species and strain	Application	Accession number
G. caldoxylosilyticus CIC9	Unknown	NZ_AMRO01000000.1
G. kaustophilus GBlys	Lysogenic, containing an integrated prophage	NZ_BASG01000001.1
G. kaustophilus HTA426	Source of 6-phospho-β-glycosidase and β-fucosidase	NC_006510.1
G. sp. CAMR5420	Hemicellulose degradation	JHUS01000001.1
G. sp. FW23	Bioremediation of oil spills	JGCJ01000001.1
G. sp. GHH01	Source of a thermostable lipase	NC_020210.1
G. sp. JF8	Degrades biphenyl and polychlorinated biphenyls	NC_011080.4
G. sp. MAS1	Source of enzyme-encoding genes	NZ_AYSF01000001.1
G. sp. WSUCF1	Grows on lignocellulosic substrates	NZ_ATCO01000001.1
G. stearothermophilus NUB3621	Genetically susceptible host for metabolic engineering	AOTZ01000001.1
G. thermocatenulatus GS-1	Unknown	JFHZ01000001.1
G. thermodenitrificans NG80-2	Degradation of long-chain alkanes, oil recovery	NC_009328.1
G. thermodenitrificans T12	Hemicellulose degradation	Unknown
G. thermoglucosidans TNO-09.020	Used for studies to avoid contamination of dairy products (the strain is a dairy contaminant)	NZ_CM001483.1
G. thermoglucosidans C56-YS93	Hemicellulose and lignin degradation	NC_015660.1
G. thermoleovorans B23 DNA	Degradation of alkanes, secretes an unidentified alkane monooxygenase	BATY01000001.1

*Adapted from "Some (bacilli) like it hot: genomics of *Geobacillus* species" [81]

Genetic reporters are used to connect a specific molecular event with a phenomenon that can be measured, for example, connecting gene expression to chemiluminescence, fluorescence, or enzymatic activity. They are necessary for studying the regulation of gene expression and

engineering strains overexpressing genes. [84]. There are three types of commonly used reporters; enzymatic assays, luminescence, and fluorescence. Luminescence and fluorescence are more convenient than enzymatic assays because no enzymes or substrates are required. Additionally, results from enzymatic assays are often semi-quantitative at best while luminescence and fluorescence can be accurately quantified using microscopy or a microplate reader. Localized fluorescence and luminescence can even be quantified using flow cytometry [85].

3.1.5 Fluorescent proteins

The focus of this work is on fluorescent proteins which are the most widely used reporter proteins in all areas of biology. The wild-type green fluorescent protein (wtGFP or GFP) is the first fluorescent protein to be isolated and studied. Osamu Shimomura and his colleagues isolated GFP in the early 1960s from the jellyfish *Aequorea victoria*. They published a paper in 1962 detailing the properties of GFP, but its application for use in molecular biology was not recognized until 1994 when Martin Chalfie and his colleagues expressed GFP in *E. coli* cells [86, 87]. The protein was able to fold and fluoresce at room temperature but had several drawbacks such as dual peaked excitation spectra, chloride sensitivity, poor photostability and poor folding at 37ºC. These flaws led to the genetic engineering of GFP, specifically two point mutations (S65T and F64L). The former mutation increased the protein's fluorescence, photostability, and resulted in a single peak excitation spectra while the latter mutation increased the protein's folding stability and fluorescence at 37ºC. The final mutant is called Enhanced GFP (EGFP) and is suitable for use in *E. coli*, the model organism of gram-negative bacteria, and eukaryotes [88]. Additionally, "Cycle-3" mutations, F99S, M153T, and V163A were introduced to GFP to create the variant GFPuv which has greatly reduced aggregation and is also suitable for *E. coli* expression [89]. The "cycle-3" mutations plus six additional mutations; S30R, Y39N, N105T, Y145F, I171V, and A206V,

have been made to EGFP to create superfolder GFP (sfGFP). This new GFP variant has improved folding kinetics compared to EGFP and GFPuv, has increased thermal stability, resistance to chemical denaturants, and folds correctly when fused to other proteins or polypeptides [90].

Although mutants like EGFP and sfGFP are suitable for *E. coli*, they are not expressed well in other bacteria, specifically gram-positive bacteria, the model organism of which is *Bacillus subtilis*. This may be due to differing intracellular environments influencing gene expression and protein function including codon usage, absence of chaperones aiding in protein folding, transcription rate, translation initiation, and mRNA stability. Despite reduced signal, EGFP has been widely used for expression in *B. subtilis*, although it was revealed later that other mutants including GFPmut3 and GFP+ have stronger signal when expressed in *B. subtilis* [91]. Two amino acid substitutions, S65G and S72A, were performed on GFP to create GFPmut3 while GFP+ has the "cycle-3" mutations of GFPuv and the two point mutations (S65T and F64L) of EGFP. [92, 93] Additionally, a variant of sfGFP was engineered for the International Genetically Engineered Machine (iGEM) Competition in 2008 for expression in both *E. coli* and *B. subtilis*. Its codon usage is a compromise for optimum expression in *E. coli* and *B. subtilis* and it carries two additional mutations, S2R and S72A. Its expression in *B. subtilis* is comparable to GFP+. Curiously, it was found that a GFP variant codon optimized for expression in the bacteria *Streptococcus pneumoniae* had much stronger fluorescence over a GFP variant codon optimized for *B. subtilis*. It has chromophore and folding mutations similar to those in GFPmut2 and has stronger fluorescence than GFP+, sfGFP, and EGFP [91].

Furthermore, fluorescent proteins in different colors have been engineered from GFP including BFP (blue), CFP (cyan), and YFP (yellow). However, YFP was found to have a slow maturation time along with sensitivities to acidic environments and chloride ions [94, 95]. A novel

mutation, F46L, was introduced to YFP. This mutation was found to speed up oxidation to the chromophore at 37ºC which resulted in faster maturation. Four additional mutations were then introduced; F64L, M153T, V163A, and S175G. The resulting fluorescent protein is called Venus which has improved folding along with increased tolerance to low pH environments and chloride ions. Furthermore, at 37ºC Venus has 30-fold higher fluorescence signal than EYFP, a widely used YFP variant with S65G, S72A, and T203Y amino acid substitutions. Venus was successfully fused to the dense-core granules of PC12 cells. This allowed for early detection of fluorescence resonance energy transfer (FRET) signals for calcium ion measurements in brain slices. EGFP was also tested for this purpose. It gave detectable fluorescence, but the intensity was approximately 10-fold lower than that of Venus [95].

Fluorescent proteins have also been engineered from other sources including mRFP1 (monomeric Red Fluorescent Protein 1) and the mFruit variants which were engineered from DsRed, a red dimeric fluorescent protein found in a species of coral called *Discosoma*. First, mRFP1 was engineered via directed evolution to increase the speed of maturation and separate the subunits while maintaining fluorescence. This required a total of 33 amino acid substitutions [96]. The mRFP1 fluorescent protein was then subjected to more mutations since it was lacking in fluorescence quantum yield and photostability. Ultimately the end result was mCherry which contains the mutations Q66M, V7I, M182K, M163Q, N6aD, R17H, K194N, T195V, and D196N. These resulted in improved folding, photostability, brightness, and faster maturation time compared to mRFP1. Additionally, since EGFP can fold and function properly when fused with other proteins, the first seven amino acids of mCherry were replaced with the corresponding residues of EGFP (MVSKGEE) followed by a spacer sequence (NNMA). Because of this, mCherry has the same high level of fluorescence when fused to other proteins at the N-terminus.

The other mFruits including mHoneydew (yellow/green), mBanana (yellow), mOrange (orange), mTangerine (orange/red), and mStrawberry (red/orange) were derived from various point mutations of mRFP1. The most promising of the mFruits are mCherry, mOrange, and mStrawberry. mCherry is by far the most photostable and has the fastest maturation rate while mOrange is the brightest and mStrawberry has the highest extinction coefficient. However, a disadvantage of mOrange is its significant acid sensitivity [97].

A few GFP variants have been shown to be functional in *Bacillus* species. Additionally, sfGFP was found to be thermostable *in vitro*. However, no fluorescent reporters have been found to fluoresce strongly in *Geobacillus* species. This work hopes to uncover some fluorescent proteins that can be used as reporters for *G. thermoglucosidans*. This species of *Geobacillus* is of particular interest to this work due to its efficient conversion of sugars into alcohols for biofuel production. This work will further investigation and engineering of *Geobacilli* for enzyme secretion, bioremediation, biosensing, and biofuel production.

3.2 Experimental Section

The goal of this work was to examine fluorescent protein reporters suitable for use in *G. thermoglucosidans* 95A1. Two green fluorescent proteins commonly used for expression in gram-positive bacteria including *Bacillus* species, EGFP and GFPmut3, were tested since *Geobacillus* are gram-positive and related to *Bacillus*. Due to its thermostability and the fact that its codon usage is a compromise for optimum expression in *E. coli* and *B. subtilis*, the sfGFP variant engineered for the iGEM competition was also tested. In this work it will be referred to as sfGFP although it should be noted that it is one of many sfGFP variants. Additionally, two of the most stable red and yellow fluorescent proteins, mCherry and Venus respectively, were tested. Finally, since mCherry and Venus were codon optimized for expression in *E. coli*, versions of Venus and

mCherry codon optimized for expression in *G. thermoglucosidans* were tested as well. Venus and mCherry were codon optimized by Integrated DNA Technologies (IDT) and the resulting gBlock DNA strands synthesized by IDT encoded the new proteins Venus (Gt) and mCherry (Gt). It should be noted that even though the codon usage of sfGFP was a compromise for *E. coli* and *B. subtilis*, it also happened to be codon optimized for *G. thermoglucosidans*. The fluorescent proteins had to be expressed in *E. coli* first, followed by expression in *G. thermoglucosidans* 95A1.

The first plasmid vector constructed for expression of fluorescent proteins in *G. thermoglucosidans* 95A1 was pED08. pNW33N was the parent plasmid used for the base of construction which was first performed in *E. coli* DH5α. The β-glucanase gene encodes for $P_{\beta\text{-}glu}$, a promoter induced in the presence of cellobiose. In *G. thermoglucosidans* C56-YS93, this promoter turns on the expression of β-glucanase which degrades cellobiose into its constituent glucose monomers. Glucose is then metabolized by the cell. Although the promoter is technically inducible, it is not tightly regulated due to the fact that sugars like glucose and cellobiose are used as a carbon source when growing *Geobacillus*. $P_{\beta\text{-}glu}$ was PCR amplified using gDNA from *G. thermoglucosidans* C56-YS93 as a template. The primers for this are shown in Table 9. Following PCR amplification, double digestions were performed on the vector and amplified insert gene with Cutsmart buffer and two enzymes, EcoRI-HF and XbaI. Following this, ligation and heat shock transformation were done as described previously. Insertion of $P_{\beta\text{-}glu}$ into pNW33N yielded pED08. Colony PCR and double digestion of DNA miniprep confirmed the successful transformations. Freezer stocks were made of successful transformants as described previously.

The genes encoding each fluorescent protein were inserted after the $P_{\beta\text{-}glu}$ promoter. The first fluorescent protein amplified from pKW1035 was GFPmut3 using primers shown in Table 9. Following PCR, double digestions were performed on the vector and amplified insert gene with

Cutsmart buffer and two enzymes, XbaI and SphI-HF. Next, ligation and heat shock transformation resulted in the insertion of the gene encoding for GFPmut3 into pED08 immediately following the $P_{\beta\text{-glu}}$ promoter to create pED09. The genes encoding EGFP, sfGFP, Venus, mCherry, Venus (Gt), and mCherry (Gt) were amplified and inserted into pED08 immediately following $P_{\beta\text{-glu}}$ to create pED11, pED12, pED13, pED14, pED27, and pED28 respectively. The genes encoding EGFP, sfGFP, Venus, and mCherry were amplified from pKW02, psfGFP, pKW576, and pKW597 respectively. Venus (Gt) and mCherry (Gt) were amplified from gBlock DNA from IDT. Next, double digestion, ligation, and heat shock transformation in *E. coli* DH5α resulted in the final constructed plasmids shown in Figure 4.

Table 9. Primers used for Polymerase Chain Reaction (Ch. 3)

Insert	**Sequence (5' to 3')**	**Enzyme**	**T_m (ºC)** ǂǂ
$P_{\beta\text{-glu}}$	ATAGAATTCCGATAAACGCGAAGAAGGTG	EcoRI-HF	58.6
$P_{\beta\text{-glu}}$	ATATCTAGAATGCAACCTCCTTTATGTTCG	XbaI	56.6
GFPmut3	ATATCTAGAATGCGTAAAGGAGAAGAACTTTTC	XbaI	56.7
GFPmut3	ATAGCATGCTTATTATTTGTATAGTTCATCC	SphI-HF	53.9
EGFP or Venus	ATATCTAGAATGAGTAAAGGAGAAGAACTTTTC	XbaI	54.8
EGFP or Venus	AGCATGCTTATTTGTATAGTTCATCCATG	SphI-HF	55.6
Venus (Gt)	ATATCTAGAATGAGCAAAGGCGAAGAACTTTTC	XbaI	58.6
Venus (Gt)	ATAGCATGCTTATTTGTAAAGTTCATCCATG	SphI-HF	56.2
sfGFP	ATATCTAGAATGCGTAAAGGCGAAGAGCTG	XbaI	59.7
sfGFP	ATAGCATGCTTATTTGTACAGTTCATCCATACC	SphI-HF	58.5
mCherry or mCherry (Gt)	ATATCTAGAATGGTGAGCAAGGGCGAAGAAG	XbaI	61.0
mCherry or mCherry (Gt)	ATAGCATGCTTACTTGTACAGCTCGTCCATG	SphI-HF	61.4

ǂǂMelting temperature calculated by Integrated DNA Technologies (IDT)

The pNW33N based plasmids containing the promoter from *Geobacillus* followed by the genes encoding for each fluorescent protein were then transformed into *G. thermoglucosidans* 95A1 via electroporation. Colony PCR and PCR of DNA miniprep confirmed the successful transformations. Freezer stocks were made of successful transformants as described previously. Following this, liquid cultures of *E. coli* and *G. thermoglucosidans* expressing GFPmut3, EGFP,

sfGFP, Venus, and mCherry under the control of $P_{\beta\text{-glu}}$ were grown along with negative controls to quantify the signal of the fluorescent proteins as described previously. *E. coli* cultures were grown at 37ºC for 5 hours and *G. thermoglucosidans* cultures were grown at 50ºC for 20 hours and 60ºC for 6 hours before OD_{600} and fluorescence readings were taken. Fluorescence intensity measurements were calculated and plotted in Microsoft Excel as described previously.

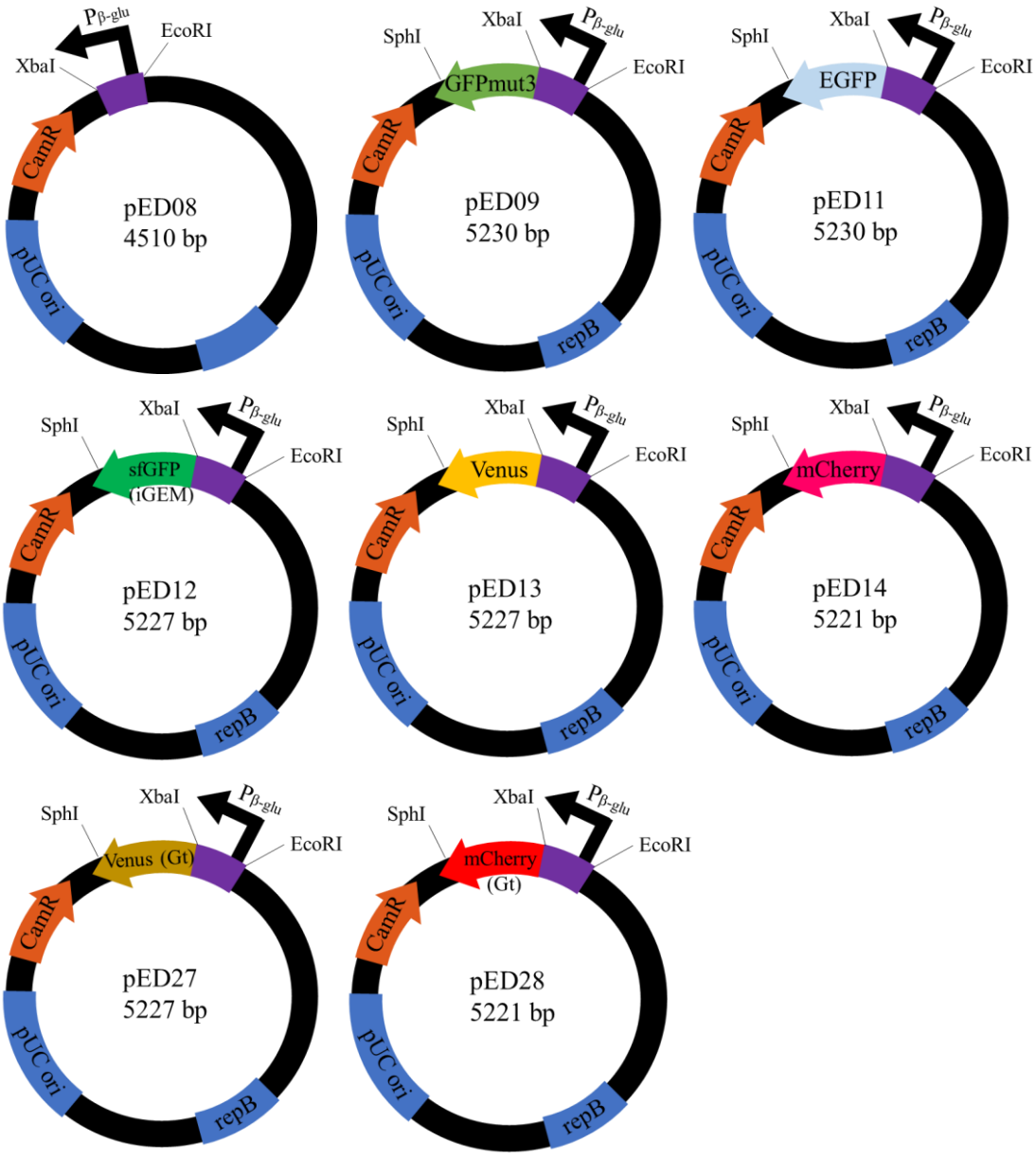

Figure 4. pNW33N based plasmids constructed for the expression of fluorescent proteins under the control of $P_{\beta\text{-glu}}$.

Since thermal stability is required for fluorescent proteins to function in *Geobacillus* species, thermal stability measurements were measured *in vitro* as described previously. The thermal stability of the fluorescent proteins was tested by incubating the protein extracts in the 80ºC water bath. Crude protein extract samples of EGFP and GFPmut3 were incubated at 80ºC for 14 minutes with fluorescence intensity readings taken every 2 minutes. Crude protein extract samples of sfGFP, Venus, mCherry, Venus (Gt) and mCherry (Gt) were incubated at 80ºC for 100 minutes with fluorescence intensity readings taken every 20 minutes. Readings were plotted and analyzed in Microsoft Excel.

3.3 Results

Colonies of pED9, pED11, pED12, pED13, pED14, pED27, and pED28 were checked immediately following transformation using colony PCR. After colony PCR, DNA from positive transformants were isolated using miniprep and cut via double digestion as described previously. The enzymes EcoRI-HF and SphI-HF were used for the double digestion to verify that the DNA

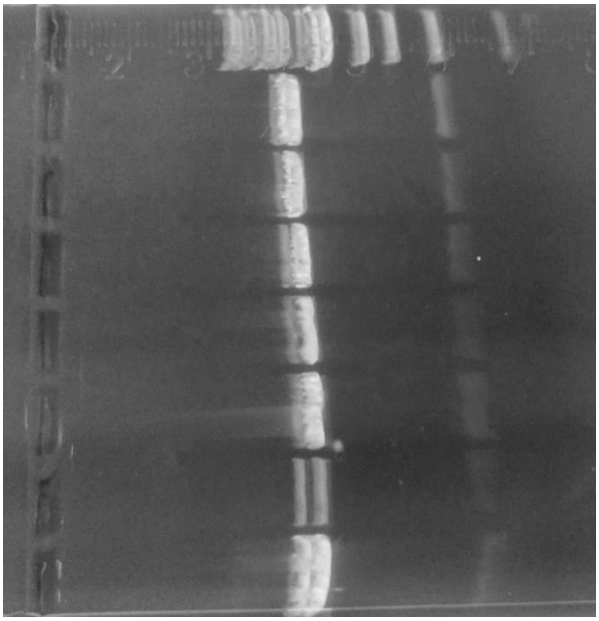

Figure 5. Double digest gel image of pED9, pED11, pED12, pED13, pED14, pED27, and pED28 cut with EcoRI-HF and SphI-HF.

encoding for $P_{\beta\text{-glu}}$ and the fluorescent proteins were inserted into the correct cutting sites. The results are shown in Figure 5. It should be noted that additional bands showing partially cut plasmid are also visible which are slightly longer than the cut plasmid.

Fluorescence intensity measurements for fluorescent proteins expressed in *E. coli* and *G. thermoglucosidans* 95A1 were calculated and recorded in Excel. The results for *E. coli* are shown below in Figure 6. Cultures were grown in LB media with chloramphenicol and in the absence of cellobiose. It was first observed that $P_{\beta\text{-glu}}$ was turned on in the absence of cellobiose when successful transformants were fluorescent on the transformation plates. Therefore, when the colonies were proliferated in liquid culture, the fluorescence was clearly observed and measured

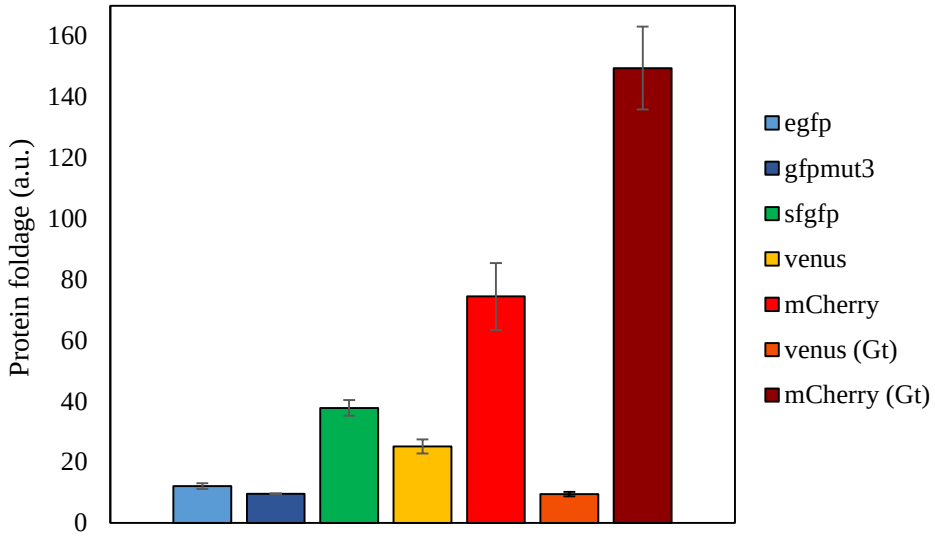

Figure 6. Fluorescence signal of fluorescent proteins expressed in *E. coli* DH5α.

with the microplate reader. The reason for the promoter being activated in the absence of cellobiose is unclear although some component of the LB media may have activated the promoter. LB media is a complex, somewhat undefined mixture of tryptone and yeast extract. Yeast extract is made by allowing yeast cells to die which causes their endogenous digestive enzymes to break down their proteins into simpler compounds. Therefore, yeast extract is composed of many amino acids, undefined peptides, and carbohydrates and may contain cellobiose or a carbohydrate similar in

structure to cellobiose. It is also possible that LB media contains a carbohydrate that, when enzymatically degraded by the cell for consumption, is similar in structure to cellobiose, thus activating the promoter. Alternatively, the promoter may have a high basal level of expression even in the absence of inducer.

Fluorescence intensity readings were taken using excitation and emission wavelengths of 485 and 528 nm respectively for all GFP and Venus variants. Excitation and emission wavelengths of 585 and 628 nm respectively were used for the mCherry variants. While the GFP and Venus variants were all comparable in signal, the mCherry variants appeared to have much greater fluorescence than the rest. The reason for this was that the negative control, *E. coli* DH5α, had a much greater signal at 485 nm compared to 585 nm, about 45-fold greater to be exact. Therefore, when calculating the fluorescence signal values, the mCherry variants had a much lower baseline than the GFP and Venus variants. The important point to note from this data is that all fluorescent proteins are functional *E. coli* DH5α with fluorescence at least 9.5-fold of the negative control. Of the GFP variants, sfGFP and Venus had the strongest signal. It is interesting to note that while mCherry (Gt) had roughly 2-fold higher signal than mCherry, Venus had roughly 2.5-fold higher signal than Venus (Gt).

The fluorescence intensity results for fluorescent proteins expressed in *G. thermoglucosidans* 95A1 are displayed below in Figure 7. Data were recorded at two different temperatures, 50ºC, the optimal growth temperature for performing plasmid transformations and 60ºC, the optimal growth temperature for the strain. The bacteria were grown in TGP media with no cellobiose added. Again, the $P_{\beta\text{-glu}}$ promoter was activated and fluorescence was observed in the absence of cellobiose. TGP media contains soy peptone which, similar to yeast extract, is made via enzymatic digestion of soybeans. It is composed of undefined peptides, amino acids, and

carbohydrates. Among the carbohydrates may be cellobiose or a compound similar in structure to cellobiose. It is also possible that soy peptone contains carbohydrates that, when enzymatically degraded by the cell for consumption, are similar in structure to cellobiose. Alternatively, the promoter may have a high basal level of expression even in the absence of inducer.

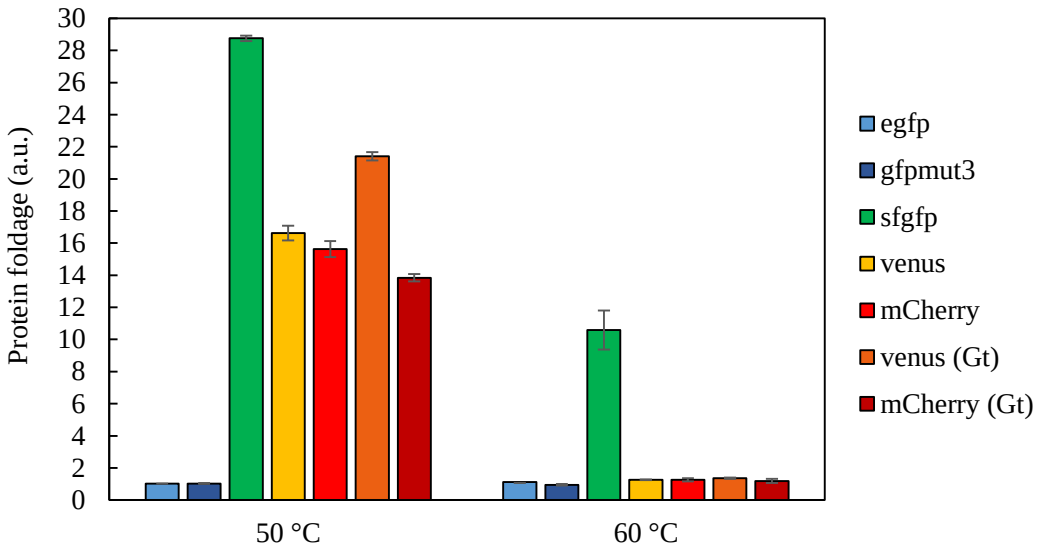

Figure 7. Fluorescence signal of fluorescent proteins expressed in *G. thermoglucosidans*

Venus and mCherry were found to be functional in *G. thermoglucosidans* at 50ºC despite being engineered for expression in *E. coli*. Codon optimization of Venus and mCherry for *G. thermoglucosidans* did not result in brighter fluorescence, thus in the case of Venus and mCherry, codon usage did not hinder their expression and fluorescence. All of the Venus and mCherry variants were found to lose fluorescence at 60ºC. Again, this was not a result of codon usage, but was due to some change in the intracellular environment with increased temperature.

Neither EGFP nor GFPmut3 were fluorescent in *G. thermoglucosidans* at either temperature. Both of these are commonly used for expression in *Bacillus* species, and *Bacillus* and *Geobacillus* are closely related. However, the intracellular environment of *G. thermoglucosidans* must be more dissimilar to that of *Bacillus* species than originally anticipated. The only fluorescent protein found to function at both temperatures was sfGFP. It had the brightest fluorescence at both

temperatures and maintained 37% of its fluorescence with a 10ºC increase in temperature. In contrast, the Venus and mCherry variants lost over 90% of their fluorescence after a 10ºC temperature increase. Because sfGFP was previously found to be thermostable while Venus and mCherry were not tested for heat stability, the most obvious explanation for the difference in fluorescence at 60ºC is that sfGFP is more heat stable than Venus and mCherry. Additionally,

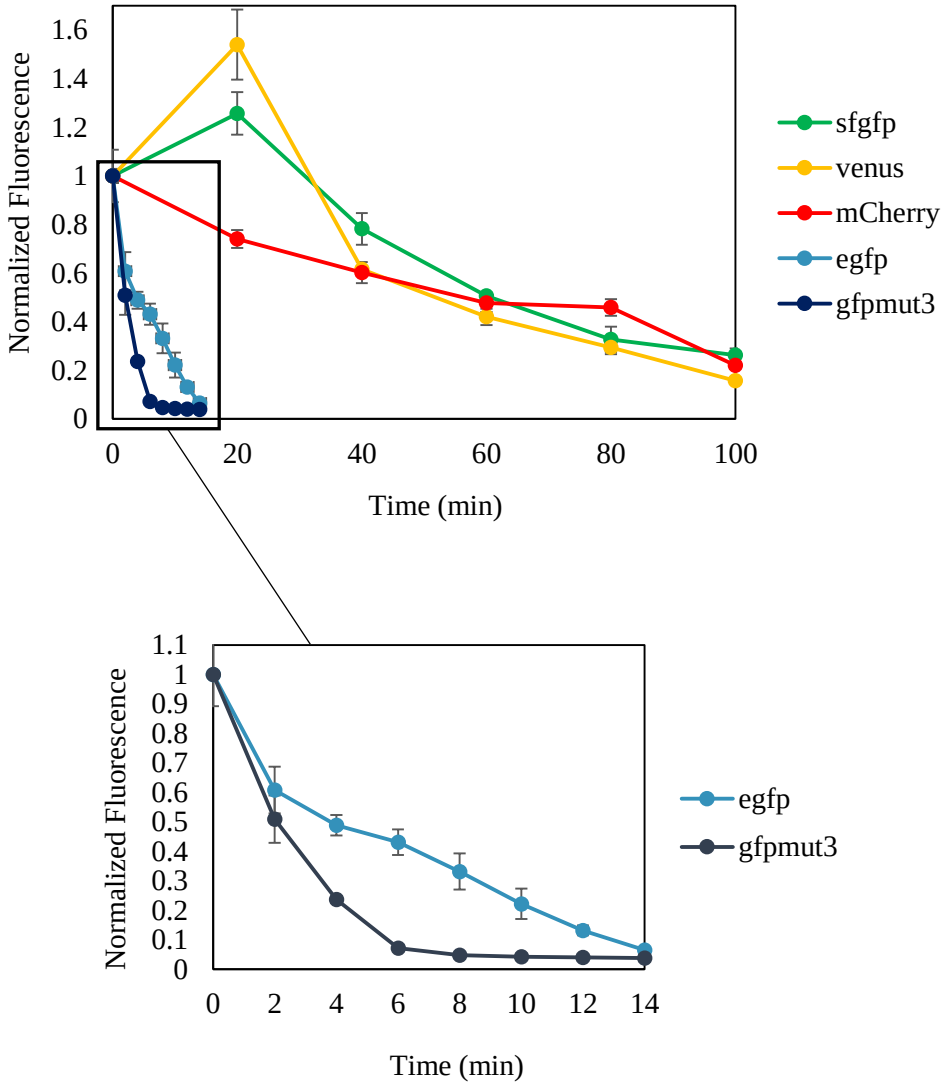

Figure 8. Protein fluorescence *in vitro* at 80ºC monitored over time.

EGFP and GFPmut3 were not tested for thermal stability before this study. Because of this, heat stability tests were performed on all fluorescent proteins *in vitro* to assess how extreme

temperatures affected their functioning and fluorescence. The results for this are shown in Figure 8.

Both EGFP and GFPmut3 were found to be unstable at 80ºC *in vitro*. Both had half-lives of less than 4 minutes at this temperature, meaning they are not suitable for use in thermophiles such as *Geobacillus* species. On the other hand, sfGFP, Venus, and mCherry were all stable at 80ºC and had similar half-lives. Venus had a half-life of approximately 55 minutes. Following a very similar trajectory to Venus (Gt), sfGFP had the longest half-life of approximately 60 minutes at 80ºC. Finally, the trajectory for mCherry had less fluctuations compared to sfGFP and Venus yet it had a similar half-life of approximately 59 minutes.

3.4 Discussion

In this study five different fluorescent proteins were expressed and characterized for fluorescence signal in the thermophilic, Gram-positive bacterium *G. thermoglucosidans*. As a result, three fluorescent reporter proteins; sfGFP, Venus, and mCherry, were found to be stable and fluorescent when expressed in the thermophile under the control of the $P_{\beta\text{-glu}}$ promoter. These reporter proteins will greatly simplify future studies involving protein expression level in *G. thermoglucosidans* and bring us one step closer to fluorescence live cell imaging of the bacteria. Fluorescence live cell imaging allows for the investigation of virtually any cellular process under the microscope and requires an array of fluorescent proteins in different colors to tag the different cellular components.

When selecting fluorescent proteins for testing, factors taken into account were expression level in gram-positive bacteria, signal strength, and stability in the presence of extreme heat, extreme pH, and the ability to fold and function when fused to other proteins. EGFP and GFPmut3 have both been used for a variety of protein expression level studies in gram-positive bacteria

which require the fusion of the fluorescent proteins to proteins of interest. In addition to being used for similar studies in gram-positive bacteria, sfGFP was found to be thermostable *in vitro*. Finally, Venus and mCherry were shown to be the most stable, fastest maturing variants in their respective colors for *E. coli* expression. Since sfGFP was successfully used in gram-positive bacteria and shown to be stable in the presence of extreme heat, it was the most promising candidate for expression in *Geobacillus*.

From this study it is clear that thermal stability of the fluorescent proteins was integral to their functioning in *G. thermoglucosidans*. EGFP and GFPmut3, the only two fluorescent proteins that were not stable *in vitro* at 80ºC were also not fluorescent in *G. thermoglucosidans* 95A1. However, thermal stability was not the only factor determining whether or not a fluorescent protein would express strongly in *G. thermoglucosidans*. Although sfGFP, Venus, and mCherry showed similar thermostability *in vitro*, only one protein, sfGFP fluoresced when expressed in *G. thermoglucosidans* at 60ºC. The remaining fluorescent proteins, although functional when expressed at 50ºC, lost virtually all fluorescence at 60ºC. Codon optimization of Venus and mCherry for *G. thermoglucosidans* resulted in improved thermostability *in vitro* for Venus but did not result in brighter fluorescence in *G. thermoglucosidans* for either fluorescent protein. Therefore, other factors must be contributing to how well the proteins fluoresce in *G. thermoglucosidans* with increased temperature such as absence of chaperones aiding in protein folding, transcription rate, translation initiation, and mRNA stability.

Although only one of the tested fluorescent proteins, sfGFP was fluorescent in *G. thermoglucosidans* at the optimal growth temperature of 60ºC, Venus and mCherry showed fluorescence when expressed in the thermophile at a growth temperature of 50ºC. For practical purposes, including protein expression level studies in *G. thermoglucosidans* or using the

fluorescent proteins as tags within the bacterial cells, sfGFP, Venus, and mCherry can all be used. However, for optimal fluorescence the bacteria must be grown at 50ºC. Future work could involve genetic engineering of sfGFP, Venus, and mCherry to attempt to improve their fluorescence in *G. thermoglucosidans* at 60ºC. Additionally, while expression levels of 15-fold to 28-fold of the negative control are a great start, higher expression levels are ideal for testing a wide variety of protein expression levels, for example, in order to engineer inducible promoters for the species. Therefore, genetic engineering could also be used to improve the overall expression level of sfGFP, Venus, and mCherry. One possible method of genetic engineering is directed evolution which involves applying error-prone PCR to the genes encoding the fluorescent proteins in order to create a library of fluorescent proteins with random mutations. This library can then be screened for improved expression level in *G. thermoglucosidans*.

3.5 Conclusions and Future Work

Through this work thermostable fluorescent reporters in three different colors were revealed to be suitable for expression in *G. thermoglucosidans*; sfGFP, Venus, and mCherry. Thermal stability was found to be necessary for fluorescent proteins to function in *G. thermoglucosidans*. However, codon optimization of fluorescent proteins for *G. thermoglucosidans*, as shown by Venus and mCherry, did not result in improved functioning. Although all three fluorescent proteins were satisfactory reporters for *G. thermoglucosidans*, sfGFP was the most stable of the three fluorescent proteins, showing fluorescence at the optimal growth temperature of the species, 60ºC. This will further fundamental investigation and metabolic engineering of *Geobacillus* strains for metabolite production, bioremediation, and the production of green fuel. Additionally, the ability to use fluorescent proteins in three different colors allows for monitoring the expression of multiple enzymes simultaneously and brings us one step closer

to multi-color live cell imaging of *G. thermoglucosidans*. Future work will involve genetic engineering to increase the fluorescence level of sfGFP, Venus, and mCherry in *G. thermoglucosidans* and improve the functioning of Venus and mCherry at 60ºC. One method of genetic engineering is directed evolution which involves introducing random amino acid mutations to the fluorescent proteins to create a massive protein library. These fluorescent proteins would then be tested for improved functioning in *G. thermoglucosidans* and the brighter mutants would be isolated, characterized, and analyzed to obtain their genetic sequences.

Since *G. thermoglucosidans* is also lacking in tightly controlled, thermostable inducible promoters, future work in developing a robust genetic toolkit for the species will involve the development of a thermostable inducible promoter. Inducible promoters are a very powerful tool in genetic engineering because the expression of genes linked to them can be tightly controlled. This allows for the activation or deactivation of gene expression at certain stages of development of a bacteria. Additionally, expression level of genes can be controlled to understand their function, for example in studying the toxicity of a gene to a particular organism. Furthermore, many proteins expressed from genes participate in specific equilibria characteristics for a physiological or developmental state [98]. In this case an inducible promoter is required to vary the concentration of an expressed protein around a specific value to determine its role *in vivo*. A few inducible promoters exist for strains of *Geobacillus* species, although they are induced in the presence of sugars such as glucose, cellobiose, and xylose, and are not tightly regulated. They have a high basal level of expression, meaning even in the absence of the inducer some protein expression is observed. Therefore, these cannot be used experimentally as tightly controlled inducible promoters [82, 99].

One commonly used inducible expression system in mesophilic organisms such as *E. coli* and *Bacillus* species is the lac regulatory system. This system is regulated by the lac repressor (LacI), a protein which inhibits the expression of genes coding for proteins involved in the metabolism of lactose. When lactose is present, it is converted into allolactose, which binds to LacI. This results in conformational changes to the protein that inhibit its DNA binding ability. Once this occurs, the proteins involved in the metabolism of allolactose can be expressed and lactose is metabolized by the cell. Typically, a non-hydrolyzable analog of allolactose, isopropyl β-D-1-thiogalactopyranoside (IPTG) is used in molecular biology to induce the lac expression system [100]. The lac repressor has been used ubiquitously in microbiology and is therefore an ideal candidate for a tightly controlled inducible expression in *Geobacillus* species. However, the LacI protein denatures completely at 53ºC rendering it useless for inducible expression in thermophiles such as *Geobacillus.* So, another future project will involve engineering LacI *in vivo* to enhance its thermostability and in turn enhance its stability in *G. thermoglucosidans* 95A1. A thermostable LacI that is also stable in *Geobacillus* would be an integral part of a robust genetic toolkit for the species. This would facilitate investigation and engineering of *Geobacillus* strains for metabolite production, bioremediation, and the production of green fuel.

CHAPTER 4: CHARACTERIZATION AND SPORE SURFACE DISPLAY OF A LACCASE FROM *GEOBACILLUS THERMOGLUCOSIDANS*

4.1 Introduction

4.1.1 Laccases and their functions

Laccases are copper-containing (multicopper) polyphenol oxidases that use the redox ability of copper ions to catalyze oxidation reactions. They are ubiquitous in nature, occurring in some plants, fungi, insects, and bacteria. They received the name "laccase" because they were first discovered in latex obtained from the Japanese lacquer tree *Rhus vernicifera* in 1883. In this species the laccase contributed to the sap's dark color. Since then laccases have been discovered in nearly all wood-rotting fungi. Fungal laccases serve a variety of functions including the degradation of lignin [102]. Laccases have also been found in the wood and cellular walls of plants. In contrast to fungal laccases, these aid in lignin biosynthesis and in the stiffness of the plant cell wall. Bacterial laccases contribute to the bacterial morphology and to copper homeostasis since free copper is toxic to the cell. For spore-forming bacteria, laccase has a role in the brown pigment of the spore and in shielding the spore from UV light and hydrogen peroxide [103].

Fungal laccases are the most widely studied due to their high catalytic activity. Most fungal laccases are extracellular monomeric globular enzymes approximately 55-85 kDa in size with isoelectric points typically ranging from pH 3.5-7.0, although multimeric fungal laccases have also been identified. They are generally 10-25% glycosylated and only in a few cases higher than 30%. Fungal laccases have a variety of industrial applications and are currently being used for textile dyeing and finishing, wine cork bleaching, and teeth whitening [104].

Bacterial laccases are both the most recently discovered and the least studied. In the last decade there have been reports indicating laccase-type activity in different bacterial species. At least some of these have advantages over fungal laccases [105]. For example, the laccase CotA

from *Bacillus subtilis* has much higher thermostability than fungal laccases. Research regarding bacterial laccases is still on the rise and relatively few have been studied. [106] However, rapid progress in genome analysis suggests that laccases are frequently occurring in bacteria. They are widespread within certain genera of gram-positive bacteria such as *Azospirillum*, *Bacillus*, *Streptomyces*, and *Geobacillus*. [107, 108] There are also occurrences in certain species of gram-negative bacteria such as *Pseudomonas maltophila*, *Pseudomonas syringae*, and *Escherichia coli* [105].

Bacterial laccases are typically 50-120 kDa in size and along with fungal laccases, are typically 10-25% glycosylated. However, they have higher isoelectric points than fungal laccases, slightly alkaline in some cases [109]. The most well-known bacterial laccase is CotA from *B. subtilis*, a 65-kDa protein present in the outer layer of the bacterial endospore coat. It is a thermostable protein with a half-life of about 2 hours at 80ºC and an optimum temperature of 75ºC. CotA protects the spore from heat, UV light, and hydrogen peroxide. It is also responsible for the brown pigment of the spore and contributes to endospore morphology [110, 111]. Bacterial and fungal laccases are similar overall in secondary structure. However, few or even single amino acid substitutions result in differences in structure and function between the two [109].

4.1.2 Structure and reaction mechanisms of laccases

Although significant differences exist between laccases from different organisms, all laccases maintain the same overall structure. All laccases contain at least three copper ions arranged in a trinuclear cluster in the catalytic center of the enzyme. Most contain four copper ions and among these four are three different types named T1, T2, and T3 which are distinguished by their spectroscopic properties. Most laccases contain the T1 copper which absorbs strongly at 600 nm and gives the laccase its blue color. Some authors hesitate to call enzymes that lack the T1

copper laccases while others refer to them as yellow laccases since they lack the corresponding blue color. All laccases contain at least one T2 copper which exhibits weak absorption in the visible region and is electron paramagnetic (EPR)-active. Additionally, all laccases contain a diamagnetic spin-coupled copper-copper pair, the T3 coppers, which absorb at 330 nm. Typically, substrates are oxidized by the T1 copper and the electrons are transferred to the T2/T3 trinuclear cluster where molecular oxygen is reduced to water [112].

The copper atoms in the catalytic center of all laccases are surrounded by four histidine-rich copper ligands, L1-L4. These regions contain 12 amino acid residues, 8 of which are histidines surrounding the trinuclear cluster, occurring in a highly conserved pattern of four HxH motifs. In one of these motifs, X is the histidine bound to the T1 copper while each of the histidines is bound to a T3 copper [113]. Laccases with mutations where histidines were substituted by other amino acids showed significant reduction in activity. This suggests that the histidine-rich amino acid residues are crucial to the function of the coppers in the catalytic center of the enzyme.

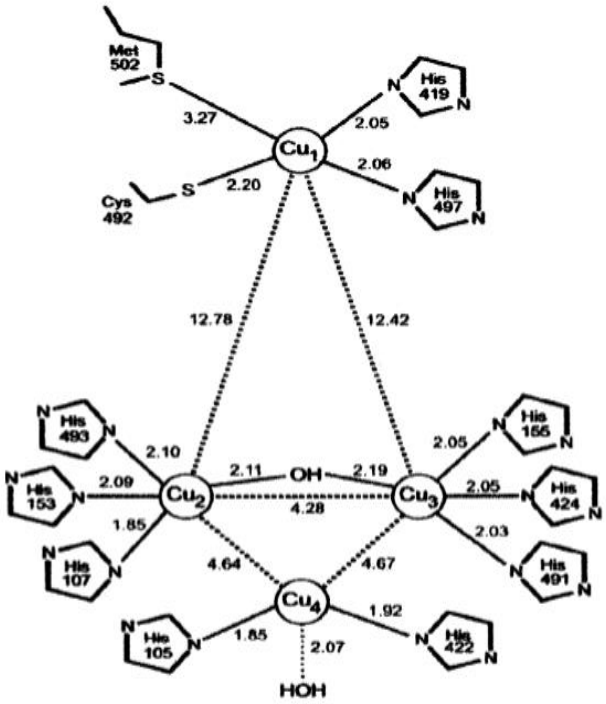

Figure 9. Copper centers and surrounding ligands of the laccase CotA from *B. subtilis* [113].

Additionally, both fungal and bacterial laccases are 10-25% glycosylated. Glycosylation in laccase contributes to secretion, enzyme activity, copper retention, vulnerability to proteolysis, and thermal stability [114].

Fungal and bacterial laccases usually contain three domains, each of which folds into a β-barrel structure. The first domain is an 8-stranded β-barrel and a coiled subdomain connecting it to the second domain via hydrogen bonding. This subdomain only appears in bacterial laccases, giving them a more compact structure and possibly contributing to their thermal stability. The second domain is a 12-stranded β-barrel. For bacterial laccases, this has an extended loop connecting it to the third domain whereas for fungal laccases, the second and third domains are linked via an internal connection. The third domain contains the T1 copper and the substrate binding site located at the surface of the protein. For bacterial laccases, the third domain also contains an α-helix extending outward from the catalytic center. This feature is absent in fungal laccases [114].

a. 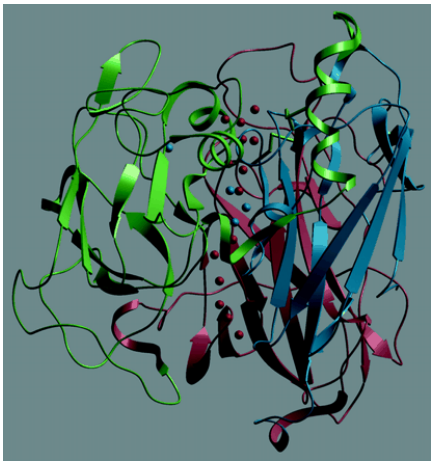 b. 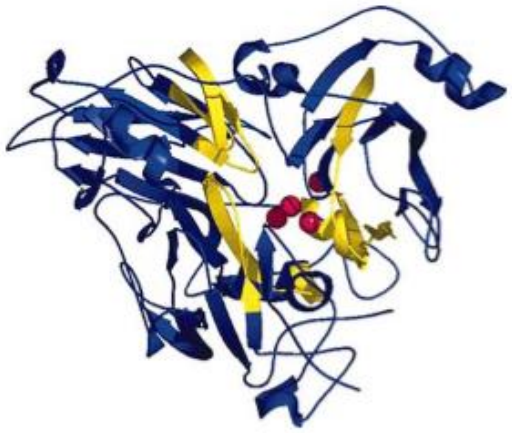

Figure 10. Ribbon diagrams for a fungal and a bacterial laccase. a.) TvL, a laccase from the fungus, *Trametes versicolor*. Water molecules are depicted as purple spheres and coppers are depicted as blue spheres [115]. b.) CotA from *B. subtilis* is shown on the right. Copper molecules are depicted as pink spheres [109].

Laccases typically use phenolic compounds as substrates because their redox potentials are low enough to allow the extraction of electrons by Cu(I) [114]. They can catalyze reactions that join monomers, cleave aromatic rings, and degrade polymers. Their substrate range is quite broad and varies depending on the type of laccase. Laccase also has an overlapping range of substrates with another enzyme, tyrosinase. Monophenols like 2,6-dimethoxyphenol (2,6-DMP) are often better substrates than diphenols, however laccases are able to catalyze oxidation of diphenols along with aminophenols, polyphenols, polyamines, aryl diamines, 1-napthol, 2,2'-azino-bis(3-ethylbenzthiazoline-6-sulphonic acid (ABTS), and some inorganic compounds such as potassium ferrocyanide [116].

Laccase oxidizes phenolic compounds and non-phenolic compounds via two different pathways. The former pathway involves the loss of a single electron and the formation of a free radical. First, the electron is transferred from the substrate to the T1 copper and the free radical may be further oxidized by laccase or it may undergo a different non-enzymatic reaction such as hydration. Next, the single electron travels through the interior of the enzyme to the T2 and T3 coppers. Finally, the electron is transferred to O_2 which is reduced to water [111]. The latter pathway requires a redox mediator compound such as ABTS and proceeds as follows. First, oxygen activates laccase and the mediator is oxidized by the enzyme and becomes a free radical. Next, the mediator radical diffuses to the substrate and oxidizes it. The reaction then proceeds exactly as described previously. It should be mentioned that access of oxidizing agents other than O_2 to the T2/T3 trinuclear cluster is restricted because O_2 is the only substrate molecule small enough to diffuse through the enzyme to reach this site. Because of this, the T2 and T3 coppers do not participate in electron transfer of the substrate which is too large to access this site [111, 117].

4.1.3 Industrial applications of laccase

Laccases are currently being used industrially for a variety of purposes. At this time nearly all of these laccases are fungal in origin. In the industrial production of paper, up to 90% of lignin is solubilized and removed during the pulping process. The remaining 10% leaves the pulp with a residual brown color and must be removed. Using laccase with ABTS as a mediator for this purpose over chlorine or oxygen based chemical oxidants provides a few advantages. First, using laccase results in brighter pulp with low lignin content. Second, using laccase improves the chemical and physical properties of pulp fiber products. Finally, using laccase as opposed to chlorine based oxidants eliminates the formation of toxic chlorinated byproducts [118].

Contamination of industrial wastewater and soil by phenolic compounds such as aromatic xenobiotics is of great concern. Laccase has been used as a method for industrial wastewater decontamination. The polyphenolic derivatives that are produced from laccase-catalyzed oxidation are usually soluble and can be easily removed via adsorption or sedimentation [119]. Additionally, laccase along with ABTS can activate wool fabrics for an anti-shrink treatment [120]. Laccase has also been used to degrade dye in fabrics for textile bleaching with the use of ABTS as a mediator. The total world production of dyes is approximately 800,000 tons per year and at least 10% of the used dyestuff is discarded into the environment as waste. These industrial effluents are resistant to light, temperature, and microbes along with being toxic to the environment. Laccase has been reported to degrade azo, heterocyclic, reactive, and polymeric dye effluents. It is more efficient and cost-effective than alternative methods of dye degradation such as adsorption, coagulation-flocculation, oxidation, filtration, and electrochemical methods [121].

Laccase also has applications for the food industry. It can be used to remove phenol derivatives for the stabilization of fruit juices, wine, and beer. In this case the enzyme would have

to be immobilized and separated from the final product because laccase has not been approved as a food additive [122]. A laccase has also been commercialized for bleaching cork stoppers for wine bottles [123]. Additionally, the presence of polyphenols in wine causes the color and flavor of the wine to change over time. Typically polyphenols are removed with polyvinylpyrrolidone (PVP). However, treatment of wine by laccase was shown to successfully oxidize and polymerize the polyphenols in Reisling wine which were then removed by clarification. Therefore, laccase is a viable alternative to chemical methods for the elimination of polyphenols from wine [124].

Finally, laccase has the potential to pretreat lignocellulosic biomass for conversion to second generation biofuels. According to the US Energy Information Administration, worldwide production of petroleum and other liquid fuels is barely able to match up with worldwide consumption of these fuels. The process of obtaining crude oil is often a dangerous endeavor involving drilling into the earth. Additionally, the burning of these fuels results in the release of greenhouse gases and other toxic chemicals like carbon monoxide, sulfur dioxide, nitrogen dioxide, and lead. Converting lignocellulosic biomass such as corn husks, woodchips, and switchgrass to ethanol offers a safer alternative to fossil fuels, but the pretreatment of the lignocellulose is expensive and difficult. Laccase has the potential to be used to break down the lignin in lignocellulose and remove phenolic inhibitors of subsequent enzyme reactions for the production of ethanol [125]. However, the purification and storage of laccase is costly and fungal laccases lack high temperature and pH stability. Fortunately, bacterial laccases have been found to have decent reactivity and much higher stability at high temperatures and pH values [114, 125].

4.1.4. Comparison of fungal and bacterial laccases

Even though most laccases being investigated experimentally and used in industry are fungal in origin, there are some important advantages to using bacterial laccases. Under ambient

conditions and acidic to neutral pHs, fungal laccases generally show higher activity than bacterial laccases. Additionally, in the process of purifying these enzymes the yield is often low. However, despite their lower redox potential, bacterial laccases are more stable than fungal laccases in the presence of high temperatures, a wider range of pHs, chloride, and metals [126, 127]. Additionally, the catalytic properties and stability of bacterial laccases can be expressed in *E. coli* and improved via directed evolution. This process is considerably more difficult for fungal laccases since they are genetically dissimilar to bacteria and therefore more difficult to express and manipulate in *E. coli*. Finally, the more compact structure of bacterial laccases may allow for improved diffusion into lignocellulosic biomass for catalytic deconstruction [128].

4.1.5. Laccase isolated from *Geobacillus*

Many US patents exist for enzymes isolated from *Geobacillus* species. These enzymes are thermostable and maintain activity at high temperatures. The complete genome is known for over 30 *Geobacillus* strains, one of which, *Geobacillus thermoglucosidans* C56-YS93, was predicted by the National Center of Biotechnology Information (NCBI) to contain the DNA encoding for a laccase. The NCBI predicted a multi-copper polyphenol oxidoreductase with a protein ID of AEH 48673.1 [129]. Additionally, the Basic Alignment Search Tool (BLAST) provided by the NCBI was used to predict the existence of laccases in other *Geobacillus* strains via alignment of the DNA sequence of the laccase from *G. thermoglucosidans* C56-YS93 with the DNA sequences of other *Geobacillus* strains. The identity is a measure of how similar the sequence of interest is to the sequence encoding for the laccase from *G. thermoglucosidans* C56-YS93. The results of the BLAST query revealed the presence of genes similar to that encoding for the *G. thermoglucosidans* C56-YS93 laccase and are shown in Table 10. From the data it can be deduced that laccase may be a common enzyme across the *Geobacillus* genus [130]. Further BLAST analyses revealed that

six additional *Geobacillus* strains all possess this type of laccase including *G. stearothermophilus*, *G. kaustophilus*, *G. thermodentrificans*, *G. thermoleovorans*, *G. vulcani*, and an unclassified *G.* spp.

Table 10. Genes encoding for laccase-like enzymes predicted in *Geobacillus* strains using BLAST

Strain	Length (Amino Acids)	Identity	Accession No.
G. thermoglucosidans C56-YS93	272	N/A*	WP 003251898.1
G. sp. Y4.1MC1	272	99%	WP 013401304.1
G. sp. WCH70	272	81%	WP 015863368.1
G. caldoxylosilyticus	274	77%	WP 017434715.1
G. thermocatenulatus	274	61%	WP 025949772.1
G. thermodenitrificans	274	61%	WP 029760424.1
G. sp. C56-T3	274	60%	WP 013145836.1
G. sp. G11MC16	274	60%	WP 008878671.1

*The laccase sequence from *G. thermoglucosidans* C56-YS93 was used as the query for BLAST.

The laccase isolated from *G. thermoglucosidans* C56-YS93 is suspected to be a member of a recently discovered family of laccases harboring the "domain of unknown function" DUF152. It showed some similarities in amino acid sequence to RL5, a laccase of this family discovered from the metagenome expression of bovine rumen [131]. This laccase had strong polyphenol oxidase activity and four copper ions per monomer [132]. RL5 and other laccases in this family including BT4389 from *Bacteriodes thetaiotaomicron* and YiFH from *E. coli* have no sequence similarity with fungal or other bacterial laccases [133, 134]. They are also much smaller than other fungal or bacterial laccases, ranging from 241-270 amino acids while CotA from *B. subtilis* has 511 amino acids [109]. At this time only five proteins in the DUF152 family have been confirmed experimentally, however DUF152 proteins are conserved in bacteria and match over 500 entries in the protein database of NCBI [131].

It is known that thermophiles like *Geobacillus* contain thermostable proteins. Therefore, it is hypothesized that this novel laccase will also be thermostable. Heat stable laccases are

advantageous for a variety of industrial applications including paper/pulp bleaching and biofuel production. Additionally, this laccase is thought to be a member of the DUF152 family, a group of laccases unlike any others isolated from fungi or bacteria. Further characterization of DUF152 proteins in the future will provide insight into their structures and functions, new information about the evolution of laccases, and novel laccases for industrial applications.

4.1.6. *B. subtilis* spore surface display

Using *Bacillus subtilis* as a host organism has a few advantages. First, it is generally regarded as safe (GRAS) by the FDA. Second, it is a model organism for laboratory research directed at discovering the fundamental characteristics and mechanisms of gram-positive spore-forming bacteria. It is easily genetically modified and is very closely related to *E. coli* which has many industrial applications and has been extensively studied for useful genetic modifications. In fact, *Bacillus subtilis* is often described as the gram-positive equivalent of *E. coli* which is gram-negative [144]. Finally, *Bacillus* is one of two genera that generate endospores under unfavorable conditions as a method of survival, the other being *Clostridium*. *B. subtilis* in particular is the model organism used to study endospore formation. *B. subtilis* endospores are approximately 1 μm in diameter and can survive in a variety of harsh conditions including extreme temperature, extreme pH, desiccation, and exposure to toxic chemicals and lytic enzymes [145]. Proteins displayed on the surface of these spores have been shown to have improved stability and longer shelf-life [146]. Additionally, because the proteins are immobilized on the spore surface they can be isolated and reused for multiple cycles. Proteins can also be immobilized on the cell surface. However, cells do not possess the advantages of robustness and reusability. Spores remain stable at room temperature for years while cells die off in one or two days.

Endospore formation takes several hours and begins after the cell enters a vegetative state. First, the cell divides asymmetrically resulting in the creation of two entities, the mother cell and what is called the "forespore". These two entities can communicate intercellularly with each other. Next, the peptidoglycan in the septum degrades and the mother cell surrounds the forespore. After this the structure of the endospore begins to form followed by the dehydration and maturation of the endospore. Finally, the mother cell dies in a programmed apoptosis and the endospore is released. The spore will be in a dormant state until it senses conditions suitable for germination and cell growth [147]. The *B. subtilis* spore is composed of five layers and is shown in Figure 11. The core, the center of the spore, contains DNA, ribosomes, dipicolinic acid, and small acid-soluble proteins (SASPs). The dipicolinic acid aids in the spore remaining dormant while and SASPs tightly compress the DNA which protects them from harmful chemicals. Small acid-soluble proteins also aid in the spore's resistance to UV light. The core is encompassed by four protein layers; the cortex, the inner coat, the outer coat, and the crust. The cortex is made of a special peptidoglycan layer and is required for dehydration of the core which contributes to the spore's thermal stability. The inner, outer coat, and crust are composed of many proteins which protect the spore from toxic chemicals. Many of these proteins can serve as anchors to attach a foreign protein to the spore surface [147].

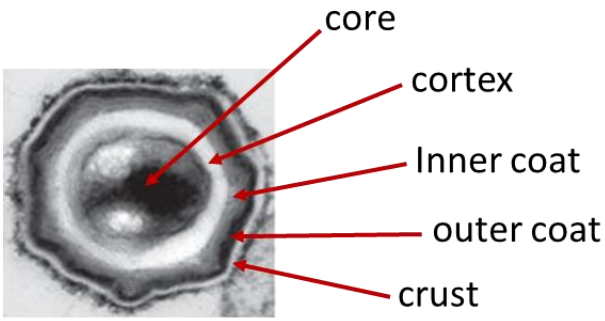

Figure 11. SEM image of the *B. subtilis* endospore adapted from McKenney, Peter et al [148].

B. subtilis spore surface display has a few advantages over other display methods such as phage display and cell surface display. First, spores remain stable at room temperature for years and can withstand a variety of harsh environments [149]. Second, spores have the possibility to display large and multimeric proteins. In contrast, cells and phages have a size limit when it comes to protein display since the size of the protein may affect the structure of a cell-membrane anchoring protein or of a viral capsid. Furthermore, cell surface display requires a membrane translocation step to externally expose a protein expressed in the cytoplasm. On the other hand, with spore surface display, heterologous proteins are expressed in the mother cell and their assembly on the surface does not involve membrane translocation [150]. Third, *B. subtilis* spores in particular are GRAS by the FDA. This is necessary if the spore is to be used as a drug delivery vehicle [151]. Finally, certain proteins can only be displayed as multimers on the spore surface. Therefore, for proteins that are only functional in their multimeric form, spore surface display is the obvious choice [152].

The most commonly used anchor proteins to display foreign proteins are CotB, CotC, and CotG although other proteins such as OxdD and CotZ have been studied as well. These anchor proteins have been used to immobilize proteins for applications in pharmaceuticals, bioremediation, and biocatalysis. A list of proteins displayed on the *B. subtilis* spore surface via different anchor proteins is shown in Table 11. Almost all have biomedical applications and the majority were developed for mucosal vaccine delivery systems [147].

This work involves the investigation of *B. subtilis* spores as a way to immobilize and maintain the robustness of useful proteins using a laccase from *G. thermoglucosidans* as an example. These spores displaying laccase are not only stable in the presence of extreme heat, pH, and toxic solvents, but they can also be isolated and reused for multiple cycles for the conversion

of laccase substrates, including the decomposition of lignin from biomass for the production of second generation biofuels. Therefore, spore surface displayed laccase presents a more inexpensive alternative to purified laccase for industrial use, and the same can be said for other industrially used proteins.

Table 11. List of anchors used for *B. subtilis* spore surface display of different proteins.

Anchor	Displayed protein	Potential application
CotB, CotC	TTFC from *C. tetani*	Vaccine
CotB, CotC	LTB from *E. coli*	Vaccine
CotB, CotC	PA from *B. anthracis*	Vaccine
CotB, CotC, CotG, CotZ	UreA from *H. acinonychis*	Vaccine
CotB, CotC	TcdA-TcdB from *C. difficile*	Vaccine
CotB	VP28 from WSSV	Vaccine
CotB	CPA from *C. perfringens*	Vaccine
CotB	18xHis	Bioremediation
CotC	Pep23 from HIV	Vaccine
CotC	TP22.3 from *C. sinensis*	Vaccine
CotC	GP64 from *B. mori*	Antiviral
CotC	HAS	Clinical use
CotC	ADH from *B. mori*	Biocatalysis
CotG	Streptavidin	Diagnostic tool
CotG	GFP_{uv}	Display system
CotG	ω-Transaminase	Biocatalysis
CotG	β-Galactosidase	Biocatalysis
CotG	Neu5Ac aldolase	Biocatalysis
CotG, OxdD	Phytase	Animal probiotic
OxdD	β-Glu	Animal probiotic
SpsC	Plll coat protein from M13	Display system
CotZ	FiliD from *C. difficile*	Vaccine
CotZ	CagA from *H. pylori*	Vaccine

*Adapted from “Spore Surface Display” [147].

4.2 Experimental Section

The goal of this work was to isolate, characterize, and immobilize a laccase from *G. thermoglucosidans* C56-YS93 on the surface of *B. subtilis* 1S101 spores. The wild-type *B. subtilis* 1085 naturally contains a laccase, CotA, on the spore surface. To eliminate interference of the native laccase with the laccase isolated from *G. thermoglucosidans* C56-YS93, *Bacillus subtilis* 1S101 which has the gene encoding for CotA deleted, was used. The isolation and characterization work involved the construction of the plasmid pTC13 which is a pNW33N plasmid containing GFPmut3 immediately following laccase under the control of the $P_{\beta\text{-glu}}$ promoter. The construction of pTC13 was done previously by Anthony Castagnaro. GFPmut3 was used as a fluorescent reporter to observe laccase expression in *E. coli*. The spore surface display work involved construction of the plasmids pED31, pED32, pED34, and pED35 to test the stability of the laccase on the spore surface when immobilized using a variety of linker peptides and anchor proteins. All primers used for PCR amplification are described in Table 12.

Two spore coat proteins, CotC and CotG, and two linker peptides were used to immobilize laccase on surface of *B. subtilis* 1S101 spores. The anchor proteins CotC and CotG have been used to successfully immobilize a variety of other proteins on the *B. subtilis* spore surface as shown in Table 11. Linker peptides are used to separate the target protein, in this case laccase, from the anchor protein. This prevents misfolding of the resulting fusion protein on the spore surface. A short, flexible peptide linker with the amino acid sequence GGGGS and a longer, α-helical linker with the amino acid sequence GGGEAAAKGGG were both tested to display laccase on the spore surface. Two anchor proteins and two linker peptides resulted in a total of four fusion proteins in total to display on the spore surface. These fusion proteins were first expressed in *E. coli* DH5α via the four plasmids pED31, pED32, pED34, and pED35. These plasmids were then integrated

into the *B. subtilis* 1S101 chromosome. Following this the new strains of *B. subtilis* were sporulated and the spores were characterized.

Table 12. Primers used for Polymerase Chain Reaction (Ch. 4)

Insert	**Sequence (5' to 3')**	**Enzyme**	**T_m (°C) ǂ**
CotC (short linker)	ATAGAATTCTGTAGGATAAATCGTTTGGGCC	EcoRI	58.3
CotC (short linker)	TGAACCTCCGCCTCCGTAGTGTTTTTTATGCTTTTTATAC	None*	63.2
laccaseǂ	CACTACGGAGGCGGAGGTTCAATGTTAGACATTTTTCAACAAG	None*	65.0
laccaseǂ	ATAGCATGCTCAATGATGATGATGATGATGTTCCCCCTTCCTGCCG ATAAACG	SphI	68.2
CotC (long linker)	TAGAATTCTGTAGGATAAATCGTTTGGGCC	EcoRI	58.3
CotC (long linker)	TCCTCCACCTTTCGCTGCTGCTGCTTCTCCTCCACC	None*	68.8
laccaseǂ	GCAGCAGCGAAAGGTGGAGGAATGTTAGACATTTTTCAACAAG	None*	65.7
laccaseǂ	ATAGCATGCTCAATGATGATGATGATGATGTTCCCCCTTCCTGCCG ATAAACG	SphI	68.2
CotG (short linker)	ATAGAATTCAGTGTCCCTAGCTCCGAGAAAAAATCC	EcoRI	61.8
CotG (short linker)*	TGAACCTCCGCCTCCTTTGTATTTCTTTTTGACTAC	None*	62.3
laccaseǂ	TACAAAGGAGGCGGAGGTTCAATGTTAGACATTTTTCAACAAG	None*	64.1
laccaseǂ	ATAGCATGCTCAATGATGATGATGATGATGTTCCCCCTTCCTGCCG ATAAACG	SphI	68.2
CotG (long linker)	ATAGAATTCAGTGTCCCTAGCTCCGAGAAAAAATCC	EcoRI	61.8
CotG (long linker)	TCCTCCACCTTTCGCTGCTGCTTCTCCTCCACCTTTGTATTTCTTTTT GACTAC	None*	68.7
laccaseǂ	GCAGCAGCGAAAGGTGGAGGAATGTAAGACATTTTTCAACAAG	None*	65.7
laccaseǂ	ATAGCATGCTCAATGATGATGATGATGATGTTCCCCCTTCCTGCCG ATAAACG	SphI	68.2

*Primers with no restriction enzyme sites were used for PCR SOEing. The entire fused DNA sequence was cloned into the vector using EcoRI and SphI.
ǂ Indicates that laccase has a C-terminal 6xHistidine (6xHis) tag.

The *B. subtilis* integration vector pDR111 was the parent plasmid for the construction of pED31, pED32, pED34, and pED35. The gene encoding laccase was PCR amplified from *G. thermoglucosidans* C56-YS93 gDNA for the construction of all plasmids. The genes encoding the spore coat proteins CotC and CotG were PCR amplified from *B. subtilis* 1085 gDNA. PCR SOEing was used to fuse the genes encoding spore coat proteins, linker peptides, and laccase as described

previously. For the construction of pED31, CotC and the short linker were fused to laccase via PCR SOEing. Following this, double digestion was performed on pDR111 and the fusion protein with the enzymes EcoRI-HF and SphI-HF. Ligation and heat shock transformation into *E. coli* DH5α resulted in the final construct, pED31. Similarly, CotC and the long linker were fused to laccase via PCR SOEing. Double digestion of pDR111 and the fusion protein with EcoRI-HF and SphI-HF, ligation, and heat shock transformation resulted in the final constructed plasmid, pED32. Fusion of CotG and the short linker to laccase with PCR SOEing, double digestion with EcoRI-HF and SphI-HF, and heat shock transformation resulted in the final constructed plasmid, pED34. Finally, fusion of CotG and the long linker to laccase, double digestion with EcoRI-HF and SphI-HF, and heat shock transformation gave the final construct, pED35. Diagrams of the constructed

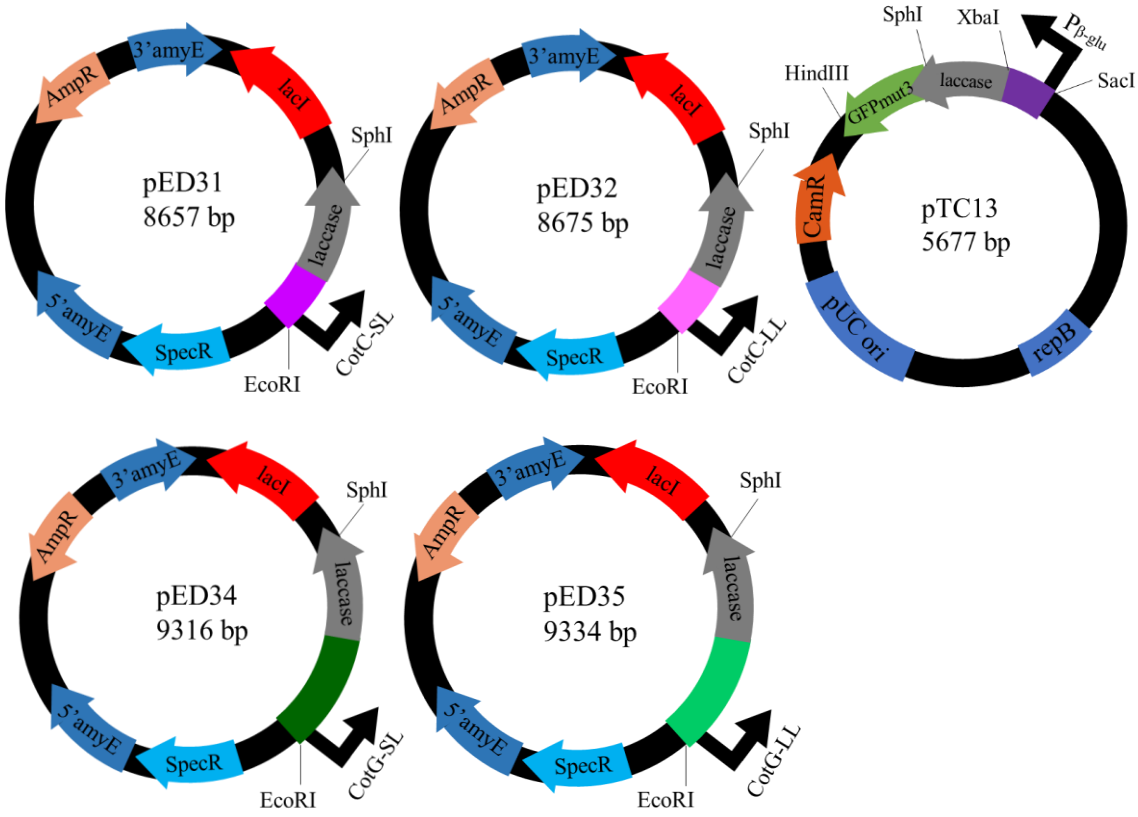

Figure 12. pNW33N and pDR111 based plasmids constructed for the characterization and spore surface display of laccase.

plasmids are shown in Figure 12. Freezer stocks were made of all successful transformants of pED31, pED32, pED34, and pED35.

Laccase was purified from *E. coli* DH5α transformed with pTC13 (DH5α/pTC13) as described previously. The purified laccase was run on an SDS-PAGE gel as described previously to verify the presence of laccase and its size which was determined to be 29.8 kDa via BLAST. Protein bands were visualized at 302 nm. Once the purification of laccase was confirmed, the purified laccase was characterized by measuring its ability to oxidize 4 different phenolic substrates (guaiacol, 2,6-DMP, veratryl alcohol, and 4-methoxybenzyl alcohol) and 1 non-phenolic substrate (ABTS). Laccase activity was tested at pHs ranging from 3.0 to 7.0 and temperatures ranging from 50ºC to 80ºC. Reactions were performed as described previously. Laccase was added last, upon which spectrophotometric readings were taken immediately. The initial rate of reaction was calculated by converting the change in absorbance to the change in concentration in 5 minutes using the Beer-Lambert law shown here in Equation 3.

$$A = \varepsilon c l \quad (3)$$

In Equation 3, A is the absorbance of the sample, ε is the molar absorptivity of the substrate given in Table X, and l is the path length which is 1 cm for our cuvettes. 1 unit (U) of enzyme activity was defined as the amount of enzyme required to oxidize 1 μmol of substrate in 5 minutes. It is conventional to express activity not in U, but in U/L which was obtained by dividing the units of enzyme activity (U) by the total reaction volume, 1 ml.

Activities of the *G. thermoglucosidans* C56-YS93 laccase and a fungal laccase from *T. versicolor* were measured at two different temperatures, the optimal temperature for the fungal laccase, 35ºC, and 80ºC. This was done to determine the thermostability of the *G. thermoglucosidans* 95A1 laccase along with comparing its activity and stability to that of the

fungal laccase. The substrate ABTS was used for these experiments and the laccases were incubated in 30 minute increments for 3 hours at both temperatures. The activities of both laccases were measured after each incubation period by reacting with ABTS at 80ºC for 5 minutes. From the data the half-life of the *G. thermoglucosidans* C56-YS93 laccase was found at 80ºC. The concentrations of the purified laccase from *G. thermoglucosidans* C56-YS93 and the laccase from *T. versicolor* were 0.09 mg/ml. The concentration of the *G. thermoglucosidans* laccase was estimated by comparing the band intensity of laccase and the ladder on the SDS-PAGE gel and a stock solution of *T. versicolor* laccase was made from powdered protein.

Enzyme kinetic studies were also done for the purified *G. thermoglucosidans* laccase as described previously. The Michaelis-Menten model was used for this. Absorbance readings were converted to product concentration readings using the Beer-Lambert law. These were plotted against time for the first 15-20 seconds to determine the initial reaction rates for different initial substrate concentrations. Once reaction rates were determined for a few different substrate concentrations, the inverse of the substrate concentration was plotted against the inverse of the reaction rate to obtain a Lineweaver-Burke plot. This plot was used to calculate the Michaelis-Menten parameters and determine the catalytic efficiency of the laccase.

For the spore surface display of the novel laccase, plasmids pED31, pED32, pED33, and pED34 were transformed into *B. subtilis* 1S101 as described previously to create 4 new strains of *B. subtilis*; 1S101::pED31, 1S101::pED32, 1S101::pED34, and 1S101::pED35. Each new strain of *B. subtilis* has either the short or the long peptide linker and laccase integrated into the *B. subtilis* 1S101 chromosome immediately following the gene encoding either CotC or CotG. For example, 1S101::pED31 has the short linker and laccase integrated into the *B. subtilis* chromosome immediately following the gene encoding CotC.

Once all 4 strains were developed, they were grown and sporulated as described previously. The wild-type *B. subtilis* 1S101 was also grown and sporulated. The spores were then washed, collected, and characterized. Substrates were chosen for the spore displayed laccase based on results from the characterization experiments of purified laccase. These were tested with buffers at the optimal pHs for purified laccase. Once product formation from the substrates was observed, the half-life measurements of the spore displayed laccase were obtained as described previously. Kinetic studies were also performed for the spore displayed laccase. These were the same as the kinetic studies for the purified laccase. A Lineweaver-Burke plot was generated and the Michaelis-Menten parameters were calculated.

4.3 Results

Colonies of pED31, pED32, PED34, and pED35 were checked immediately following transformation using colony PCR. After colony PCR, DNA from positive transformants were isolated using miniprep and cut via double digestion as described previously. The enzymes EcoRI-HF and SphI-HF were used for the double digestions of pED31, pED32, pED34, and pED35 to verify that the DNA encoding for the spore coat proteins and laccase were inserted into the correct

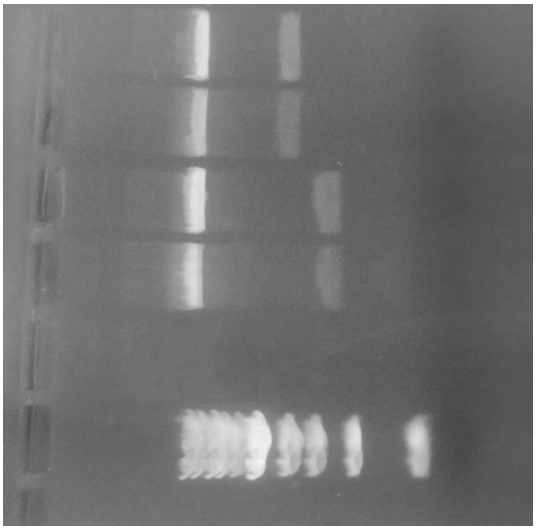

Figure 13. Double digest gel image of pED31, pED32, pED34, and pED35 (bottom to top).

cutting sites. The results are shown in Figure 13. From the gel it is clear that the vector bands for pED31, pED32, pED34, and pED35 are all approximately 8 kb. The insert bands for pED31 and pED32 are approximately 1.1 kb while the insert bands for pED34 and pED35 are approximately 1.8 kb.

The SDS-PAGE gel image of the purified laccase is shown in Figure 14. In the image the 29.8 kDa band, the band for the *G. thermoglucosidans* laccase, is circled. The appearance of this band confirms that the laccase was successfully purified from *E. coli* DH5α/pTC13. In addition to laccase, bands representing proteins of other sizes can be visualized from the gel. Theoretically, only proteins containing 6xHis tags would be purified from the Ni-NTA column. However, DH5α contains many proteins, some of which contain multiple histidine residues. These have also bound to the column and are contained in our sample. Fortunately, these extraneous proteins did not interfere with subsequent characterization experiments. They only appear as noise on the SDS-PAGE gel. Since it was confirmed that our laccase was successfully purified, characterization experiments followed.

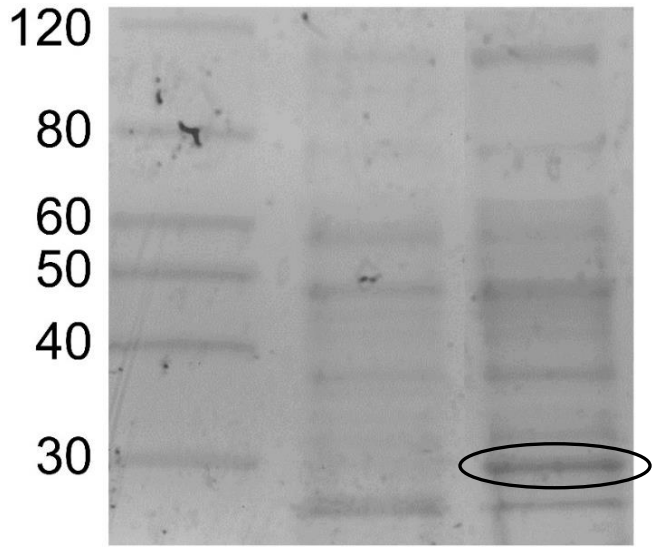

Figure 14. SDS-PAGE gel of histidine rich proteins purified from DH5α (middle) and DH5α/pTC13 (right), 6xHis tagged laccase is circled in black.

For this work, guaiacol, 2,6-DMP, veratryl alcohol, 4-methoxybenzyl alcohol, and ABTS were tested for the characterization of laccase. The substrate preference of this laccase is as follows from highest to lowest activity: DMP >> veratryl alcohol > ABTS >> 4-methoxybenzyl alcohol > guaiacol. The activity of the laccase in oxidizing 4-methoxybenzyl alcohol and guaiacol was negligible and the data are not shown. The activity of the laccase for the other three substrates varied considerably depending on pH.

The results for laccase activity as a function of temperature and pH for 2,6-DMP are shown in Figure 15. The activity for 2,6-DMP was much higher than the activity for guaiacol or ABTS. There were observable trends in the data; laccase activity was strongly dependent on pH, showing much greater activity at the highest pH which was 7.0. Because of the dramatic increase in laccase activity from pH 6.5 to pH 7.0, activity was compared at pH 7.0, 8.0, and 9.0. The data are not shown, but at 80ºC laccase activity increased under basic conditions. This is consistent with another DUF152 laccase, Tfu1114 from *T. fusca*, which was determined to have the highest activity toward 2,6-DMP under neutral to mildly basic conditions. The maximum measured activity was 149.7 U/L at 80ºC and pH 7.0.

The trends in laccase activity for ABTS are shown in Figure 16. Laccase activity toward ABTS was overall about 50-fold lower than laccase activity toward 2,6-DMP. As with 2,6-DMP, there were observable trends in the data. The highest activities at all temperatures were observed at acidic pHs, between 3.0 and 4.5 and activity dropped off significantly at pH 5.0 and higher. This is in agreement with other laccases which have maximum activity toward ABTS at around pH 4.0. The maximum activity was approximately 3.0 U/L at 50ºC. At 50°C, the laccase displayed activity toward ABTS at pHs ranging 3.0-5.0, but no activity from 5.5 to 7.0. Upon an increase in

temperature to 80°C the activity slightly decreased at lower pHs from 3.0 to 5.0, but interestingly it demonstrated some activity at pHs from 5.5 to 7.0, about 10-20% of the highest activity.

The trends in laccase activity for veratryl alcohol are shown below in Figure 17. As with

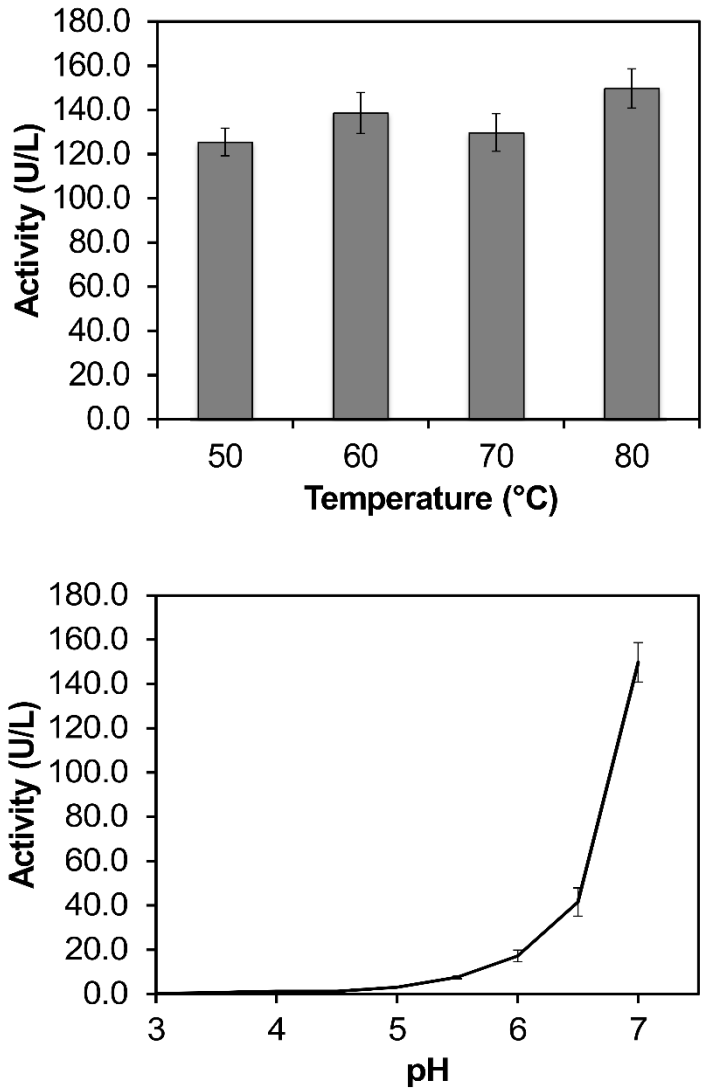

Figure 15. Activity of laccase as a function of temperature and pH with 2,6-DMP as the substrate

the previous two tested substrates, there were observable trends in the data. Activity appeared to be somewhat dependent on temperature since it dropped off considerably at 80ºC. At temperatures between 50ºC and 70ºC activity seemed to be dependent on pH as well, although laccase could

oxidize the substrate at pHs ranging 3.0-7.0. The highest activities were observed at pHs between 3.5 and 5.5. The highest activity was approximately 6.60 U/L, observed at 60ºC and pH 4.5. This was about twice the maximum activity of ABTS.

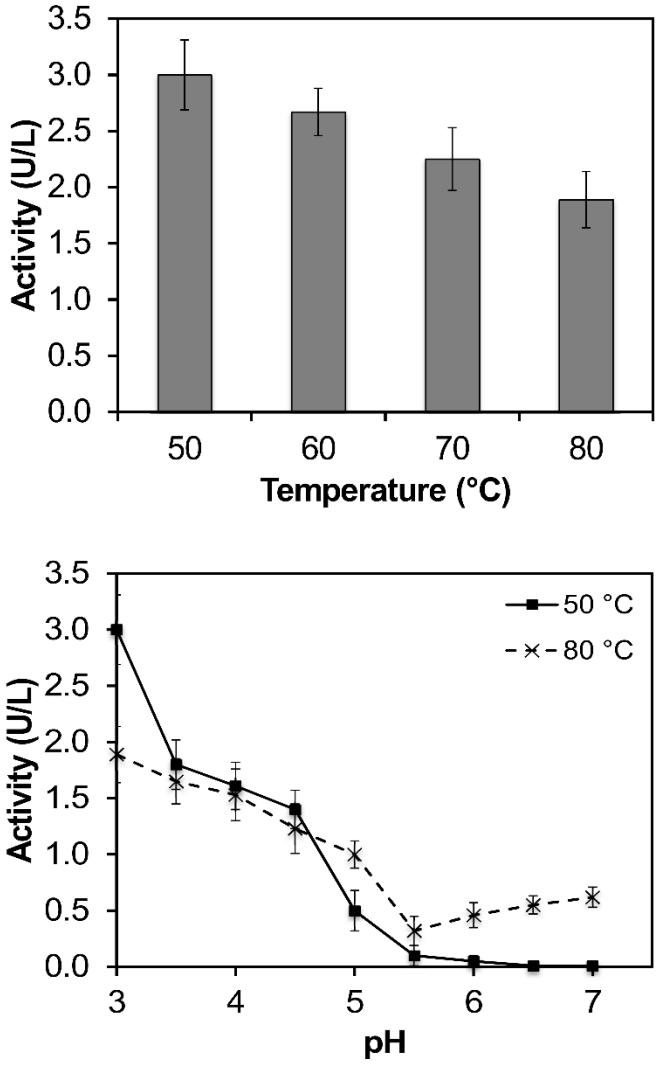

Figure 16. Activity of laccase as a function of temperature and pH with ABTS as the substrate

Overall, laccase activity varied greatly with pH but was fairly independent of temperature. This remained consistent with all substrates tested. The fact that laccase activity was fairly independent of temperature pointed to the fact that this laccase is thermostable. This was clearly shown in the data for 2,6-DMP, since activity remained consistent from 50ºC-80ºC. From the data

it can be concluded that 2,6-DMP is the most ideal substrate for this laccase followed by ABTS and veratryl alcohol. For the remaining studies, ABTS and 2,6-DMP were used as substrates.

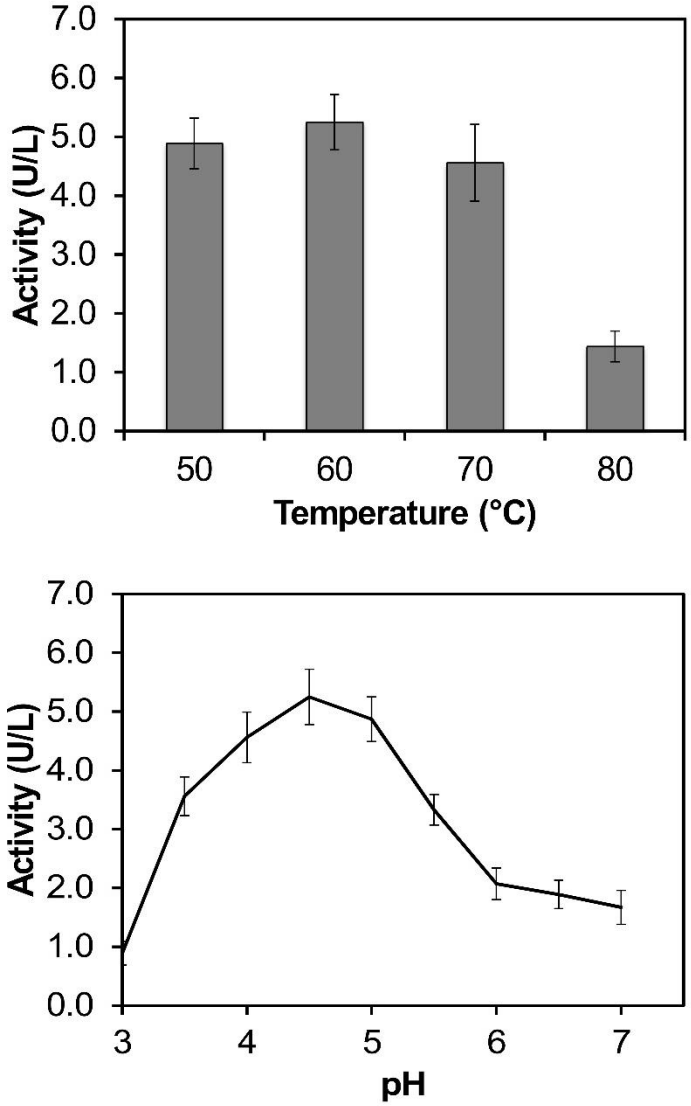

Figure 17. Activity of laccase as a function of temperature and pH with veratryl alcohol as the substrate

The results of the *T. versicolor* and *G. thermoglucosidans* laccase activity measurements are shown in Figure 18. Since the laccase activity data pointed to the thermal stability of the *G. thermoglucosidans* laccase its thermal stability was tested further and its half-life was determined

at 80ºC. Since optimum temperatures for the *T. versicolor* laccase range from 20ºC to 50ºC, 35ºC was chosen as a low temperature in order to compare the two laccases. To prevent evaporation of samples and for safe handling of reaction mixtures, 80ºC was chosen as the higher temperature to test the thermal stability of the *G. thermoglucosidans* laccase. pH was held constant at 4.0 and 5 replicates were taken.

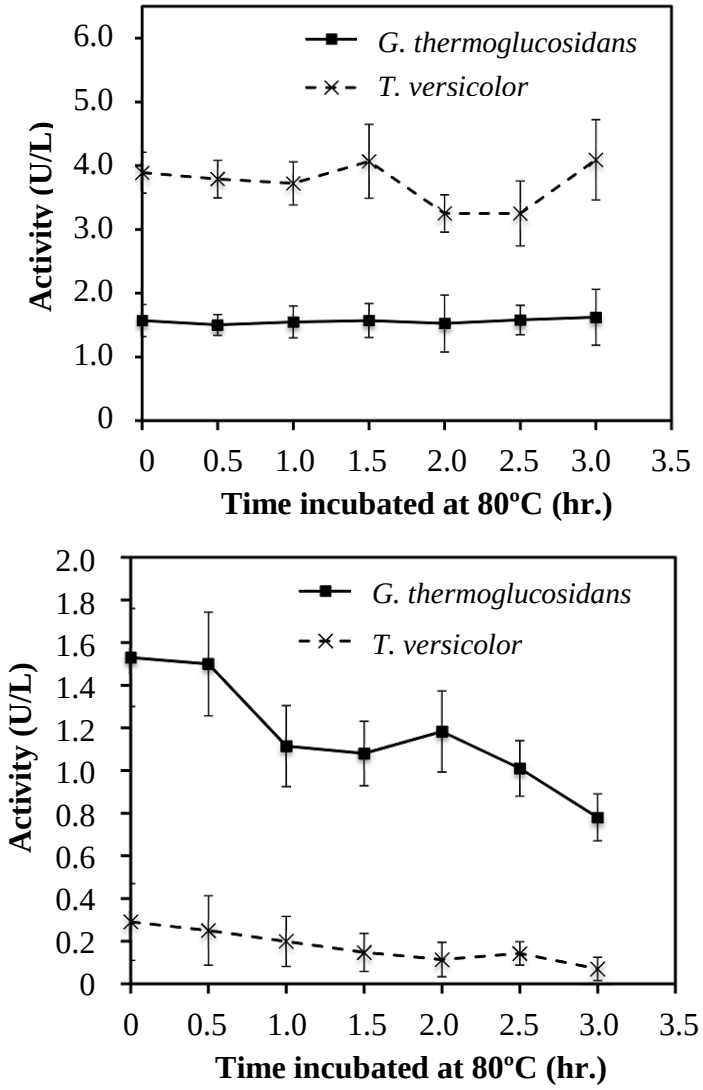

Figure 18. Laccase activity of *G. thermoglucosidans* and *T. versicolor* laccase as a function of incubation time at 35ºC and 80ºC using ABTS as the substrate.

From the figure it is clear that laccase activity was fairly independent of incubation time at 35ºC which verified that both laccases were stable and active at this temperature. On average, the

T. versicolor laccase was approximately 2.5-fold more active than the *G. thermoglucosidans* laccase under the same reaction conditions. This was expected since bacterial laccases are generally not as active as fungal laccases. Margot et al. compared the activity of a fungal laccase from *S. cyaneus* to the same fungal laccase from *T. versicolor* and the fungal laccase was 6.8-fold more active using ABTS as the substrate. From this information it can be concluded that the *G. thermoglucosidans* laccase is more active than the laccase from *S. cyaneus* under ambient conditions. The activities of both laccases fluctuated minimally with incubation time, even for up to 3 hours.

At 80ºC the *G. thermoglucosidans* laccase was far more active than the *T. versicolor* laccase. Initially, the *G. thermoglucosidans* laccase was about 5-fold more active than the *T. versicolor* laccase which was completely inactive after 3 hours of incubation at 80ºC. The *G. thermoglucosidans* laccase, on the other hand, still maintained 50% of its activity after 3 hours, meaning it had a half-life of 3 hours at 80ºC. Additionally, the *G. thermoglucosidans* laccase did not lose any activity with the increase in temperature from 35ºC to 80ºC until about 1 hour of incubation. In contrast, the *T. versicolor* laccase lost about 92% of its activity after increasing the incubation temperature from 35ºC to 80ºC. Using information from a study done by Martins et al., the *G. thermoglucosidans* laccase performed similarly to CotA, the laccase from *B. subtilis*. Martins determined that CotA had a half-life of 2 hours when oxidizing ABTS at 80ºC and maintained significant activity even at 75ºC [110]. The wild-type *B. subtilis* is mesophilic with an optimal growth temperature of 37ºC but CotA is a spore coat protein which accounts for its thermal stability. Thus, the laccase from *G. thermoglucosidans* showed greater thermal stability and activity at higher temperatures than the laccase from *T. versicolor*. It also had similar thermal stability to CotA, a thermally stable spore coat protein from *B. subtilis*.

The results for the enzyme kinetic studies for the laccase purified from *G. thermoglucosidans* C56-YS93 are shown in Figure 19. The inverse of initial reaction rate, or the inverse of the concentration of product generated per second, was plotted against the inverse of eight different initial substrate concentrations to obtain the Lineweaver-Burke plot. From this plot, the Michaelis-Menten parameters were calculated. From the plot V_{max} and K_M were found using Equation 2, $\frac{1}{V} = \frac{1}{Vmax} + \frac{Km}{Vmax}\frac{1}{[S]}$. Using the fact that V_{max} is equal to the inverse of the y-intercept, V_{max} was found to be 0.000103 mM/s. Following this, K_M was was found to be 2.37 mM, or 0.00237 M.

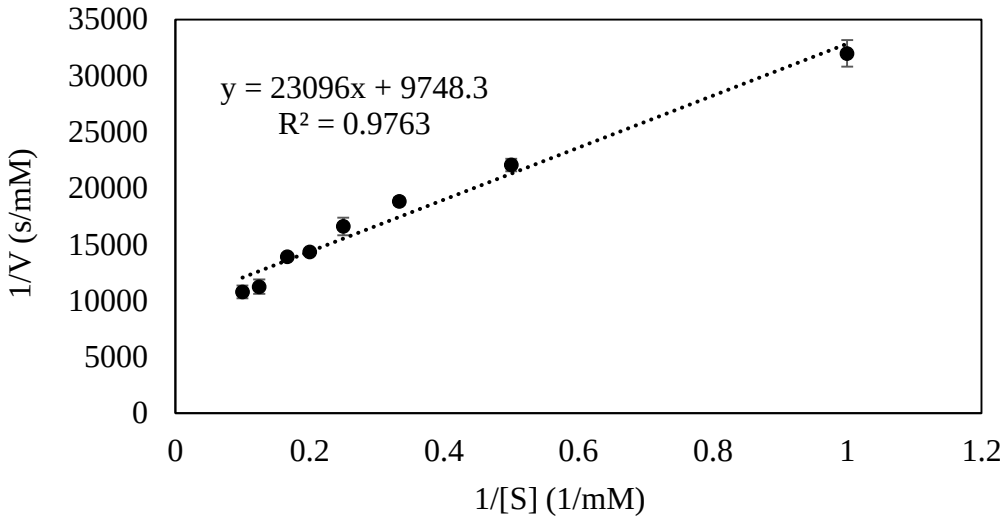

Figure 19. Lineweaver-Burke plot for the enzyme kinetics of purified laccase using 2,6-DMP as the substrate.

Qualitatively, V_{max} is the maximum enzyme reaction rate, K_M is the concentration of substrate at half of the maximum reaction rate which occurs when half of the enzyme's active sites are filled, and k_{cat} is the turnover number, or the number of substrate molecules that one enzyme site converts to product per second. Most enzymes have K_M values ranging from 10^{-7} to 10^{-1} M. The median K_M value for a wide range of enzymes in a study done by Bar-Even et al. was found to be 10^{-4} M and 60% of all enzymes had values ranging from 10^{-5} to 10^{-3} M [153]. The K_M value

for an enzyme depends on environmental factors such as pH, temperature, and ionic strength. It should be noted that before readings were taken the purified enzyme was incubated at 80ºC for 30 minutes to increase the efficiency of the enzyme, but the reaction itself was carried out at room temperature. Performing the reaction in the incubator was not feasible since readings could not be taken every 5 seconds while maintaining a constant reaction temperature. However, the enzyme efficiency probably would have increased if the reaction had been carried out at 60ºC, 70ºC, or even 80ºC. A pH of 8.0 was determined to be optimal for this particular substrate.

Lower values for K_M indicate that less substrate is required to fill the enzyme's active sites while higher values indicate that more substrate is required to fill the enzyme's active sites. Therefore, K_M can also be thought of as an inverse measure of an enzyme's affinity for a substrate. The K_M value for the laccase purified from *G. thermoglucosidans* C56-YS93 was approximately $2x10^{-3}$ M for 2,6-DMP which indicated moderate affinity of laccase for the substrate. According to a study performed by Brander et al. the K_M for the laccase CotA from *B. subtilis* was about 0.000067 M toward 2,6-DMP at pH 8.0 and room temperature [154]. This was between 1 and 2 orders of magnitude lower than the K_M value for the *G. thermoglucosidans* laccase. This CotA had binding affinity for the 2,6-DMP than the *G. thermoglucosidans*.

After immobilization of the *G. thermoglucosidans* C56-YS93 laccase on the *B. subtilis* spore surface, the immobilized laccase was tested to see if it was still active in this state. The results for this are shown in Figure 20. The enyzme reaction was carried out in cuvettes as described previously. Reactions were performed at pH 7.0 and 80ºC for 10 minutes using 2,6-DMP as the substrate. Absorbance readings were taken in the spectrophotometer and converted to activity as described previously. The negative control was *B. subtilis* 1S101 spores with no laccase immobilized on the surface. It is clear from the figure that the spore displayed laccase had activity

using all protein anchor and peptide linker combinations. However, spores displayed using CotC and the long linker generated significantly more product in 10 minutes than spores displayed using the other anchor/linker combinations. These results suggest that laccase can most readily generate product from 2,6-DMP when fused to CotC using the long linker.

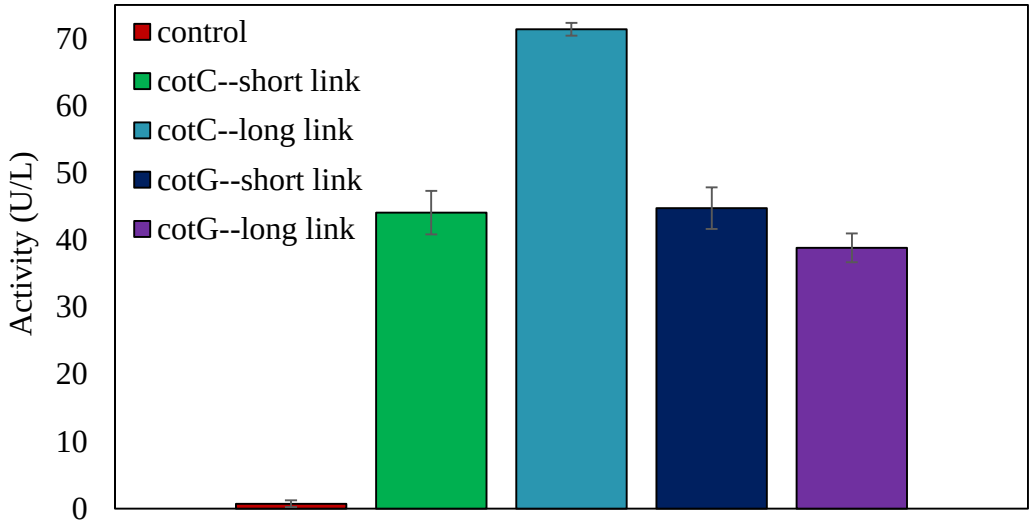

Figure 20. Activity of the spore displayed laccase using 2,6-DMP as the substrate.

Once it was determined that the spore displayed laccase was stable and active, the half-life of the laccase displayed using the different spore coat proteins and linker peptides was determined at 80ºC. This was done to determine the thermostability of the *G. thermoglucosidans* C56-YS93 laccase when displayed on *B. subtilis* spores. ABTS was tested for these experiments to remain consistent with the half-life experiments for the purified laccase. Unfortunately, the mixture of the spores and ABTS created a cloudy mixture which impeded the spectrophotometer from measuring the absorbance of the product generated. For this reason 2,6-DMP was used as the substrate for these experiments. The spore displayed *G. thermoglucosidans* laccase was incubated in 30 minute increments for 8 hours at 80ºC. The laccase was then reacted with the substrate at pH 7.0 and 80ºC and the concentration of product generated after 5 minutes was measured after each incubation period. From the data the half-life of the spore displayed laccase was found at 80ºC.

The thermal stability data for the spore displayed laccase are shown in Figure 21. The first plot shows activity after a 5 minute enzyme reaction at 80ºC verses laccase incubation time at 80ºC. The second plot has all activity values normalized to 1 which serves to show the half-life of the spore displayed laccase more clearly. From the first plot it is clear that laccase displayed with CotC and the long linker was more active than laccase displayed using the other anchor/linker combinations. The activity of the laccase displayed with CotC and the long linker remained higher

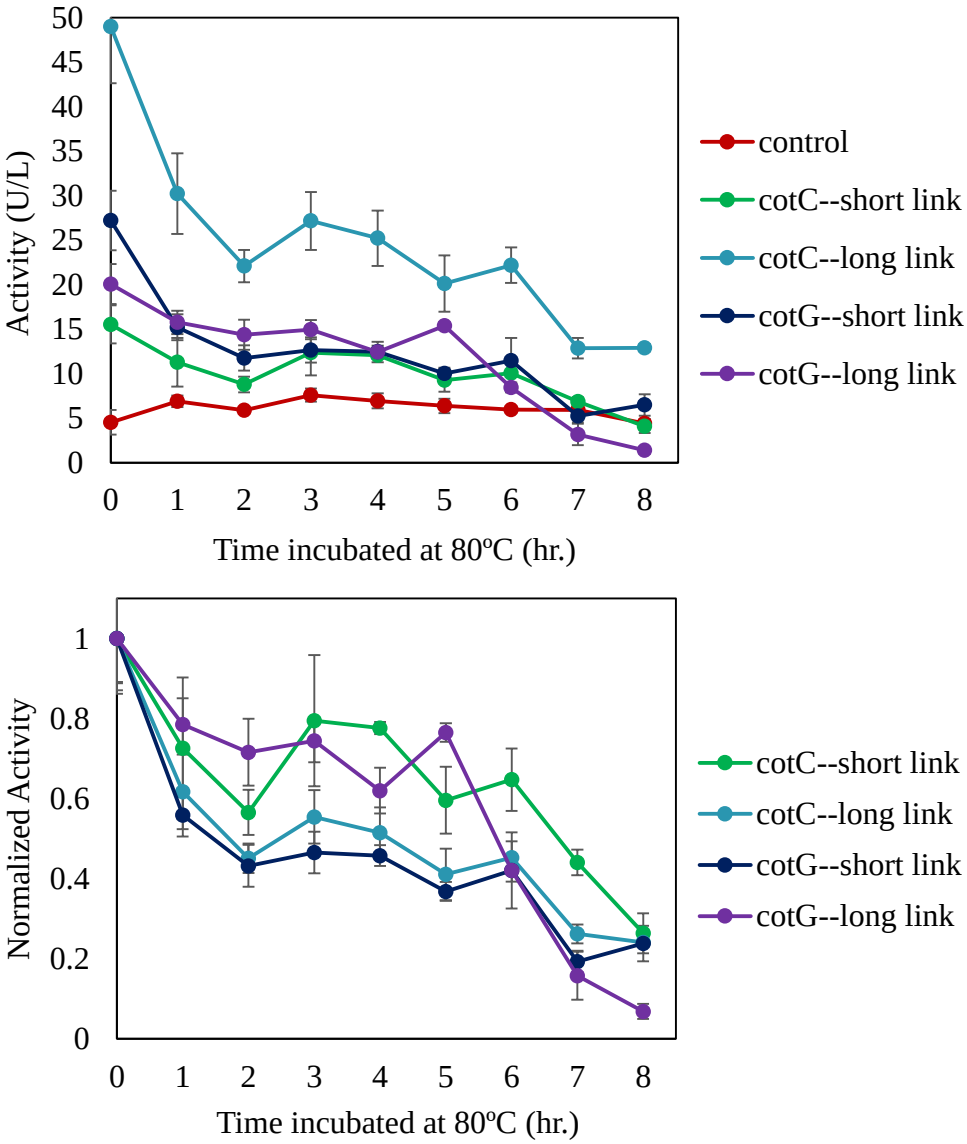

Figure 21. Activity of spore displayed *G. thermoglucosidans* laccase as a function of incubation time at 80ºC using 2,6-DMP as the substrate

than that of laccase displayed with the other anchor/linker combinations even after 8 hours of incubation. However, it was also clear that laccase displayed using CotC and the long linker had one of the shortest half-lives. It lost 50% of its activity after about 2 hours. The other three linker/anchor combinations resulted in similar initial activities, however their trends and half-lives were all very different. From the second figure it is clear that laccase displayed with CotG and the short linker had a very similar trend to laccase displayed with CotC and the long linker. Both had half-lives of about 2 hours after which their activities plateaued for about 4 hours. After 7 hours they both lost 70-80% of their activity. Laccase displayed with CotC and the short linker had the lowest initial activity but also had the longest half-life, about 7 hours. Laccase displayed with CotG and the long linker also had a very long half-life, about 6 hours. Thus, the laccase isolated from *G. thermoglucosidans* 95A1 was quite thermally stable and active when displayed on *B. subtilis* spores. The laccase was the most active when displayed using CotC/long linker and was the most stable when displayed using CotC/short linker and CotG/long linker.

The results for the enzyme kinetic studies for the laccase from *G. thermoglucosidans* C56-YS93 immobilized on the *B. subtilis* spore surface are shown in Figure 22. Spores displaying laccase with CotC and the short linker were used for these experiments since they showed the highest activity. Similar to the kinetic studies for the purified laccase, the inverse of initial reaction rate, or the inverse of the concentration of product generated per second, was plotted against the inverse of 8 different initial 2,6-DMP concentrations to obtain the Lineweaver-Burke plot shown

below. From the plot, the Michaelis-Menten parameters V_{max} and K_m were found to be 0.0000419 mM/s and 0.000417 M respectively.

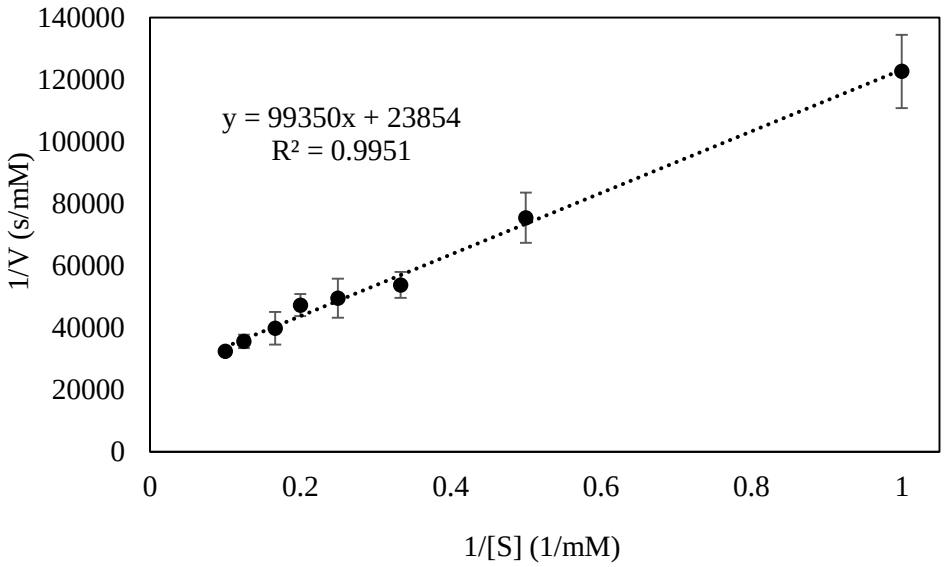

Figure 22. Lineweaver-Burke plot for the enzyme kinetics of spore displayed laccase using 2,6-DMP as the substrate.

Comparing the K_M values of the purified and spore displayed laccase, the value for purified laccase was on the same order of magnitude as the value for the spore displayed laccase. Since K_M represents the inverse of the binding affinity of laccase for the substrate, displaying the laccase on the surface of *B. subtilis* spores did not greatly affect the binding affinity of laccase for 2,6-DMP. The purpose of using the linker peptide when fusing CotC to laccase was to prevent any misfolding of the enzyme, and it can be concluded that the folding conformation of the laccase was not greatly affected by fusion to CotC with the long linker. Therefore, the linker peptide served its purpose and the binding affinity of laccase for 2,6-DMP was virtually unaffected by displaying the laccase on the *B. subtilis* spore surface. Additionally, the V_{max} values for the purified and spore displayed laccase were similar which was to be expected.

In order to determine k_{cat} for the purified laccase, a purer sample of laccase needs to be run on the SDS-PAGE gel. Currently it is difficult to accurately determine the concentration of purified

laccase due to the presence of other histidine rich proteins in the sample. Once a purer sample of laccase is obtained, k_{cat} for the pure laccase will be determined. In order to determine k_{cat} for the spore displayed laccase, dot-blotting experiments need to be performed to determine the amount of CotC—laccase fusion proteins per spore. From there the concentration of laccase in a sample of spores will be calculated using the amount of fusion proteins per spore and the amount of spores in the sample. Using this information, k_{cat} will be calculated in order to compare the k_{cat} values for the purified and spore displayed laccase.

4.4 Discussion

Laccase is an industrially relevant enzyme with a wide variety of applications including paper and pulp bleaching, wastewater decontamination, textile bleaching, removal of phenolic compounds from wine, and second generation biofuel production. Currently, all industrially used laccases are fungal in origin and unstable when exposed to higher temperatures. Since paper and pulp bleaching and biomass pretreatment for biofuel production are both performed at high temperatures, using a thermostable laccase would simplify and lower the cost of both processes by eliminating an extra step. Additionally, purification of laccase and other industrially used proteins is expensive and laborious. *B. subtilis* spores have been used for the display of a variety of proteins for vaccination, bioremediation, and biotechnology applications. Spore surface displayed proteins offer a cheaper, less time-consuming alternative to purified proteins for industrial applications.

In this study, a thermostable laccase was isolated, characterized, and displayed on the surface of *B. subtilis* spores by fusing laccase to the spore coat proteins CotC and CotG using two linker peptides; a short, flexible peptide linker with the amino acid sequence GGGGS and a long, alpha-helical linker with the sequence GGGEAAAKGGG. The laccase isolated from *G. thermoglucosidans* and purified from *E. coli* was found to be active toward the substrates 2,6-DMP

and ABTS and remarkably heat stable with a half-life of 3 hours at 80ºC. The purified laccase was far more heat stable than a commonly used fungal laccase isolated from *T. versicolor* which lost virtually all activity after only a few minutes of incubation at 80ºC. The spore displayed laccase was found to have maintained activity and thermal stability with a half-life of up to 7 hours at 80ºC using CotG and the long linker. Kinetic studies were performed on the purified and spore displayed laccase. The K_M values for the purified and spore displayed laccase were 0.00237 M and 0.00416 M respectively, indicating that the purified and spore displayed laccase had similar binding affinities for 2,6-DMP. This showed that the folding of laccase was virtually unchanged by fusion to CotC via the long linker. The k_{cat} value purified laccase will be determined by obtaining a purer sample of laccase and the k_{cat} value for the spore displayed laccase will be determined via dot-blotting.

The *G. thermoglucosidans* laccase was more heat stable than CotA with a half-life of 3 hours compared to 2 hours at 80ºC. From studies performed on the spore-displayed laccase, CotC, CotG, and both linkers are appropriate for the *B. subtilis* spore surface display of laccase. However, spore display of laccase using CotC and the long linker resulted in the highest activity while display of laccase using CotG and the long linker resulted in the greatest stability at 80ºC. Therefore, spore displayed laccase using CotG and the long linker is the most effective for use in high temperature industrial processes.

The laccase isolated from *G. thermoglucosidans* has great industrial potential due to its high thermostability. Additionally, upon immobilization of the laccase on the surface of *B. subtilis* spores its activity, binding affinity for the substrate 2,6-DMP, and thermostability were all maintained. In order to compare the catalytic efficiencies of the purified and the spore displayed laccase, k_{cat} values need to be determined.

The results of this study show the promise of *B. subtilis* spore surface display as an industial delivery system for proteins. Not only does spore surface display provide a method for increasing the thermal stability of industrially relevant proteins, but it also provides a way to avoid the expensive and laborious process of protein purification. Previously, spore surface display was mainly used as a tool for the creation of novel vaccines, but this work shows that spore surface display using CotC, CotG, and peptide linkers can be expanded to many more industrial sectors including paper production, textile making, food and drink production, and beyond.

4.5 Conclusions and Future Work

A novel laccase from *G. thermoglucosidans* C56-YS93 has been isolated, expressed in *E. coli*, purified, characterized, and displayed on the surface of *B. subtilis* 1S101 spores. The purified laccase was found to be stable and active at high temperatures. In fact, the laccase was found to react more efficiently with certain substrates at higher temperatures. Additionally, the laccase was found to have very high activity toward 2,6-DMP and moderate activity toward ABTS and veratryl alcohol. The thermostability of this laccase is of great use to the pulp and paper industry. Pretreatment of pulp for paper production would greatly benefit from thermostable laccases active at basic conditions since pulping and bleaching are both performed at high temperatures. Furthermore, the thermostability of this laccase proves advantageous for lignin degradation in biomass for second generation biofuel production since the pretreatment of lignocellulosic biomass is performed at high temperatures.

The characterization and kinetic results for the purified laccase are promising, however the process of purification is both expensive and time-consuming, especially on a large scale. Immobilization of the laccase on *B. subtilis* spores offers a more inexpensive alternative. Furthermore, spore surface display of laccase has applications for the food industry, specifically

for the removal of phenol derivatives for the stabilization of fruit juices, wine, and beer. Since laccase has not been approved as a food additive, *B. subtilis* spore surface display allows for easy separation and removal of laccase from the final product. Using *B. subtilis* spores is particularly attractive since they are GRAS by the FDA and some strains have even been used as probiotics. The immobilization of the laccase on the surface of *B. subtilis* 1S101 spores resulted in maintained stability and activity of the enzyme. Display of the laccase using CotC and the long linker resulted in the highest activity while display of the laccase using CotG and the long linker resulted in the longest half-life at 80ºC. Since laccase displayed with CotC and the long linker showed the highest activity, this sample was used for kinetic studies. The experiments revealed that displaying the laccase on the *B. subtilis* spore surface virtually did not alter the binding affinity of laccase for the substrate 2,6-DMP.

Future work will involve determining k_{cat} for the purified laccase and the laccase displayed on the *B. subtilis* spore surface. The k_{cat} value for the purified laccase will be determined by obtaining a purer sample of laccase. This will be done by running the sample of purified laccase through the purification column one or two more times which will remove the other histidine rich proteins from the sample. Additionally, a more concentrated sample of purified laccase should be obtained for better results. This will be done via dialysis of the sample of purified laccase. The k_{cat} value for the spore displayed laccase will be determined by quantification of laccase on the spore surface via dot-blotting. From there the catalytic efficiencies of the purified and spore displayed laccase will be compared. Additionally, more Native PAGE gels will be run to determine if the laccase is monomeric or multimeric. Preliminary results from Native PAGE gels suggest that the laccase is a dimer, however clearer bands need to be obtained before this result can be determined with certainty. Finally, the ability of the purified and the spore displayed laccase to oxidize

additional substrates will be tested. Syringaldazine is of particular interest since it is a very commonly used substrate for laccase. Laccase activity was tested using syringaldazine and a variety of buffers including citrate-phosphate buffer, Sørensen's phosphate buffer, potassium phosphate buffer, and Tris-HCl buffer. All buffers were pH 6.6 or 7.0 as suggested by a variety of sources. Curiously, all of the buffers containing phosphate reacted with syringaldazine even in the absence of laccase. The Tris-HCl buffer did not react with the substrate in the presence or absence of laccase. Therefore, half-life or kinetic data using syringaldazine for the purified or spore displayed laccase have not yet been acquired. Future work will involve testing additional buffers to determine the affinity of the laccase for syringaldazine.

REFERENCES

1. Gurung, Neelam et al. “A Broader View: Microbial Enzymes and Their Relevance in Industries, Medicine, and Beyond.” *BioMed Research International* 2013 (2013): 329121. PMC. Web.

2. Hill, Robert and Needham, Joseph. *The Chemistry of Life: Eight Lectures on the History of Biochemistry*. Cambridge: Cambridge University Press (2008)

3. Dhillon, G. and Kaur, S. *Agro-industrial Wastes as Feedstock for Enzyme Production*. London: Academic Press (2016)

4. Singh, Rajendra et al. “Microbial Enzymes: Industrial Progress in 21st Century.” *3 Biotech* 6.2 (2016): 174. PMC. Web.

5. Volesky, B., Luong, J. and Aunstrup, K. Microbial Enzymes: Production, Purification, and Isolation. *Critical Reviews in Biotechnology*, 2.2 (1984): 119-146.

6. Liu, Long et al. “How to Achieve High-Level Expression of Microbial Enzymes: Strategies and Perspectives.” *Bioengineered* 4.4 (2013): 212–223. PMC. Web.

7. Berlec, A. and Štrukelj, B. “Current state and recent advances in biopharmaceutical production in Escherichia coli, yeasts and mammalian cells.” *Journal of Industrial Microbiology & Biotechnology*, 40.3-4 (2013): 257-274.

8. Fernandez, J. and Hoeffler, J. *Gene Expression Systems: Using Nature for the Art of Expression.* San Diego, Calif., [etc.]: Academic Press. (2008)

9. Rosano, Germán L., and Eduardo A. Ceccarelli. “Recombinant Protein Expression in Escherichia Coli: Advances and Challenges.” *Frontiers in Microbiology* 5 (2014): 172. PMC. Web.

10. Green, Erin R., and Joan Mecsas. “Bacterial Secretion Systems – An Overview.” *Microbiology Spectrum* 4.1 (2016): 10.1128/microbiolspec.VMBF–0012–2015. PMC. Web.

11. Liu, Zihe et al. “Different Expression Systems for Production of Recombinant Proteins in Saccharomyces Cerevisiae.” *Biotechnology and Bioengineering* 109.5 (2012): 1259–1268. PMC. Web.

12. Ahmad, Mudassar et al. “Protein Expression in Pichia Pastoris: Recent Achievements and Perspectives for Heterologous Protein Production.” *Applied Microbiology and Biotechnology* 98.12 (2014): 5301–5317. PMC. Web.

13. Hillebrecht, Jason R, and Shaorong Chong. “A Comparative Study of Protein Synthesis in in Vitro systems: From the Prokaryotic Reconstituted to the Eukaryotic Extract-Based.” *BMC Biotechnology 8* (2008): 58. PMC. Web.

14. Carlson, Erik D. et al. “Cell-Free Protein Synthesis: Applications Come of Age.” *Biotechnology Advances* 30.5 (2012): 1185–1194. PMC. Web.

15. Rosenblum, G. and Cooperman, B. “Engine out of the chassis: Cell-free protein synthesis and its uses.” *FEBS Letters*, 588.2 (2013): 261-268.

16. Smith, G. “Filamentous fusion phage: novel expression vectors that display cloned antigens on the virion surface.” *Science*, 228.4705 (1985): 1315-1317.

17. Paschke, M. “Phage display systems and their applications.” *Applied Microbiology and Biotechnology*, 70.1 (2005): 2-11.

18. Pepper, Lauren R. et al. “A Decade of Yeast Surface Display Technology: Where Are We Now?” *Combinatorial chemistry & high throughput screening* 11.2 (2008): 127–134. Print.

19. Gai, S. and Wittrup, K. “Yeast surface display for protein engineering and characterization.” *Current Opinion in Structural Biology*, 17.4 (2007): 467-473.

20. Boder, Eric T.; Wittrup, K. Dane. "Yeast surface display for screening combinatorial polypeptide libraries". *Nature Biotechnology*. 15.6 (1997): 553–557

21. Getz JA, Schoep TD & Daugherty PS. "Peptide Discovery Using Bacterial Display and Flow Cytometry". *Methods Enzymol*. 503 (2012): 75–97.

22. Kenrick, Sophia A., and Patrick S. Daugherty. “Bacterial Display Enables Efficient and Quantitative Peptide Affinity Maturation.” *Protein Engineering, Design and Selection* 23.1 (2010): 9–17. PMC. Web.

23. Hanes, Jozef, and Andreas Plückthun. “In Vitro Selection and Evolution of Functional Proteins by Using Ribosome Display.” Proceedings of the National Academy of Sciences of the United States of America 94.10 (1997): 4937–4942. Print.

24. Sawata, S., Suyama, E. and Taira, K. “A system based on specific protein-RNA interactions for analysis of target protein-protein interactions in vitro: successful selection of membrane-bound Bak-Bcl-xL proteins in vitro.” *Protein Engineering Design and Selection*, 17.6 (2004): 501-508.

25. Tan, Irene S. and Ramamurthi, Kumaran S. “Spore Formation in *Bacillus Subtilis*.” *Environmental microbiology reports* 6.3 (2014): 212–225. PMC. Web.

26. Isticato R and Ricca E. “Spore surface display.” *Microbiology Spectrum* 2.5 (2014): 351-366. doi:10.1128/microbiolspec.TBS-0011-2012.

27. Leisola, Matti et al. “Industrial Use of Enzymes.” *Physiology and Maintenance* 2 (n.d.): 1-24.

28. Vijayaraghavan, Ponnuswamy et al. “Thermostable Alkaline Phytase from *Alcaligenes sp*. in Improving Bioavailability of Phosphorus in Animal Feed: In Vitro Analysis,” *ISRN Biotechnology* (2013): 1-6. Article ID 394305. doi:10.5402/2013/394305

29. Sundarram, Ajita, and Thirupathihalli Pandurangappa Krishna Murthy. "α-Amylase Production and Applications: A Review." *Journal of Applied & Environmental* Microbiology 2.4 (2014): 166-175.

30. Vieille, Claire, and Gregory J. Zeikus. “Hyperthermophilic Enzymes: Sources, Uses, and Molecular Mechanisms for Thermostability.” *Microbiology and Molecular Biology Reviews* 65.1 (2001): 1–43. PMC. Web.

31. Littlechild, Jennifer A. “Enzymes from Extreme Environments and Their Industrial Applications.” *Frontiers in Bioengineering and Biotechnology* 3 (2015): 161. PMC. Web.

32. Rakotoarivonina, H., Revol, P., Aubry, N. and Rémond, C. “The use of thermostable bacterial hemicellulases improves the conversion of lignocellulosic biomass to valuable molecules.” *Applied Microbiology and Biotechnology*, 100.17 (2016): 7577-7590.

33. "U.S. Energy Information Administration (EIA) - Independent Statistics and Analysis." International Energy Outlook 2017. 12 December 2017. Web.

34. “U.S. Energy Information Administration (EIA). U.S. energy-related carbon dioxide emissions, 2014.” Washington, DC: U.S. Department of Energy. 10 July 2016. Web. http://www.eia.gov/environment/emissions/carbon/

35. Environmental Protection Agency (EPA). “Abandoned mine drainage.” (2015) Washington, DC. 3 May 2016. Web. https://www.epa.gov/polluted-runoff-nonpoint-source-pollution/abandoned-mine-drainage

36. Environmental Protection Agency (EPA). “Memorandum: Improving EPA review of Appalachian surface coal mining operations under the Clean Water Act, National Environmental Policy Act, and the Environmental Justice Executive Order.” (2010) Washington, DC. 3 May 2016. Web.

37. Colborn, T et al. “Natural gas operations from a public health perspective.” *Human and Ecological Risk Assessment: An International Journal,* 17.5 (2011): 1039–1056.

38. Myhre, G., D. et al: Anthropogenic and Natural Radiative Forcing. In: Climate Change 2013: The Physical Science Basis. Contribution of Working Group I to the Fifth Assessment Report of the Intergovernmental Panel on Climate Change [Stocker, T.F., D. Qin, G.-K. Plattner, M. Tignor, S.K. Allen, J. Boschung, A. Nauels, Y. Xia, V. Bex and P.M. Midgley (eds.)]. Cambridge University Press, Cambridge, United Kingdom and New York, NY, USA

39. Global Gas Flaring Reduction Partnership (GGFR): Improving energy efficiency & mitigating impact on climate change. Washington, DC: The World Bank. Web. http://www.worldbank.org/en/programs/gasflaringreduction#1

40. Hall, Jeremy et al. “Managing Technological and Social Uncertainties of Innovation: The Evolution of Brazilian Energy and Agriculture.” *Technological Forecasting and Social Change*. 78 (2011): 1147–1157

41. Hill, J., Nelson, E., Tilman, D., Polasky, S. and Tiffany, D. “Environmental, economic, and energetic costs and benefits of biodiesel and ethanol biofuels.” *Proceedings of the National Academy of Sciences*, 103.30 (2006): 11206-11210.

42. Boot, M. *Biofuels from Lignocellulosic Biomass – Innovations beyond Bioethanol*. Weinheim: Wiley-VCH (2016)

43. Energy Independence and Security Act of 2007. Alternative Fuels Data Center. Washington DC: U.S. Department of Energy, Energy Efficiency & Renewable Energy. Web. https://www.afdc.energy.gov/laws/eisa.html

44. Nguyen, Que et al. Global Production of Second Generation Biofuels: *Trends and Influences*. Dovetail Partners, Inc. January 2017. Web. www.dovetailinc.org/report_pdfs/2017/dovetailbiofuels0117.pdf

45. US Department of Energy. U.S. Billion-Ton Update: Biomass Supply for a Bioenergy and Bioproducts Industry. R.D. Perlack and B.J. Stokes (Leads), ORNL/TM-2011/224. Oak Ridge National Laboratory, Oak Ridge, TN. 2011. Web.

46. Energy Information Administration. Use of Energy in the United States Explained: Energy Use for Transportation. U.S. Department of Energy. 2016. Web.

47. Wang, M. Ethanol: the Complete Energy Lifecycle Picture. U.S. Department of Energy, Energy Efficiency and Renewable Energy. 2007. Web.

48. Bajpai, P. "Structure of Lignocellulosic Biomass." *SpringerBriefs in Molecular Science*, 11.87 (2-16): 7-12.

49. Nanda, S., Mohammad, J., Reddy, S., Kozinski, J. and Dalai, A. "Pathways of lignocellulosic biomass conversion to renewable fuels." *Biomass Conversion and Biorefinery*, 4.2 (2013): 157-191.

50. Huber, G.W., Iborra, S., and Corma, A. "Synthesis of transportation fuels from biomass: chemistry, catalysts, and engineering." *Chem Rev* 106.9 (2006): 4044–4098

51. Moon, J. et al. "Transient behavior of devolatilization and char reaction during steam gasification of biomass." *Bioresour Technol* 133 (2013): 429–436

52. Mohanty, P., Nanda, S., Pant, K., Naik, S., Kozinski, J. and Dalai, A. "Evaluation of the physiochemical development of biochars obtained from pyrolysis of wheat straw, timothy grass and pinewood: Effects of heating rate." *Journal of Analytical and Applied Pyrolysis*, 104 (2013): 485-493.

53. Zhao, L., Zhang, X., Xu, J., Ou, X., Chang, S. and Wu, M. "Techno-Economic Analysis of Bioethanol Production from Lignocellulosic Biomass in China: Dilute-Acid Pretreatment and Enzymatic Hydrolysis of Corn Stover." *Energies* 8.5 (2015): 4096-4117.

54. Lin, Y. and Tanaka, S. "Ethanol fermentation from biomass resources: current state and prospects." *Applied Microbiology and Biotechnology*, 69.6 (2005): 627-642.

55. Biochemical Conversion: Using Enzymes, Microbes, and Catalysts to Make Fuels and Chemicals. Bioenergy Technologies Office. Washington DC: U.S. Department of Energy, Energy Efficiency & Renewable Energy. Web.

56. Wilson, Kate. "Preparation of Genomic DNA from Bacteria." *Current Protocols in Molecular Biology*, (2001)

57. Sambrook, J., Fritsch, E. and Maniatis, T. *Molecular cloning*. Cold Spring Harbor, NY: Cold Spring Harbor Laboratory Press. (2012)

58. Zeigler, Daniel. "Integration Vectors for Gram-Positive Bacteria." Bacillus Genetic Stock Center Catalog of Strains. 7.4 (2002): 17

59. Chambert, R., Cutting, S. and Harwood, C. *Molecular Biological Methods for Bacillus*. Chichester: John Wiley & Sons. (1990).

60. Shafee, T. (2018). *File:Michaelis Menten curve 2.svg - Wikimedia Commons*. [online] Available at: https://commons.wikimedia.org/wiki/File:Michaelis_Menten_curve_2.svg.

61. Michaelis, L. and Menten, M. "Die kinetik der invertinwirkung." *Biochemistry Zeitung* 49 (1913): 333-369.

62. Gordon, R. E., and N. R. Smith. "Aerobic sporeforming bacteria capable of growth at high temperatures." *J. Bacteriol*. 58 (1949): 327-341.

63. White, D., R. J. Sharp, and F. G. Priest. 1993. "A polyphasic taxonomic study of thermophilic bacilli from a wide geographical area." *Antonie Leeuwenhoek* 64 (1993): 357-386.

64. Ash, C., J. A. E. Farrow, S. Wallbanks, and M. D. Collins. "Phylogenetic heterogeneity of the genus *Bacillus* revealed by comparative analysis of small-subunit-ribosomal RNA sequences." *Lett. Appl. Microbiol*. 13 (1991): 202-206.

65. Nazina, T. N., A. E. Ivanova, and A. V. Blagov. "Microbiological characteristics of oil formations of Mangyshlak Peninsula." *Microbiology* 62 (1993): 216-221.

66. Nazina, T. N., A. E. Ivanova, L. L. Mityushina, and S. S. Belyaev. "Thermophilic hydrocarbon-oxidizing bacteria from oil strata." *Microbiology* 62 (1993): 359-365.

67. Nazina, T. N et al. "Physiological and Phylogenetic Diversity of Thermophilic Spore-forming Hydrocarbonoxidizing Bacteria from Oil Fields." *Microbiology* 69 (2000): 96-102.

68. Nazina, T. N. et al. "Taxonomic study of aerobic thermophilic bacilli: descriptions of *Geobacillus subterraneus* gen. nov., sp. nov. and *Geobacillus uzenensis* sp. nov. from petroleum reservoirs and transfer of *Bacillus stearothermophilus*, *Bacillus thermo-catenulatus*, *Bacillus thermoleovorans*, *Bacillus kaustophilus*, *Bacillus thermoglucosidasius* and *Bacillus thermodenitrificans* to *Geobacillus* as the new combinations *G. stearothermophilus, G. thermocatenulatus, G. thermoleovorans, G. kaustophilus, G. thermoglucosidasius and G. thermodenitrificans*." *Int. J. Syst. Evol. Microbiol*. 51 (2001): 433-446.

69. Al-Qodah, Z. "Production and characterization of thermostable α-amylase by thermophilic *Geobacillus stearothermophilus*." *Biotechnology Journal*, 1.7-8 (2006) 850-857.

70. Bhalla, Aditya, Kenneth M. Bischoff, and Rajesh Kumar Sani. "Highly Thermostable Xylanase Production from A Thermophilic *Geobacillus* Sp. Strain WSUCF1 Utilizing

Lignocellulosic Biomass." *Frontiers in Bioengineering and Biotechnology* 3 (2015): 84. PMC. Web.

71. Jia, Xianbo et al. "Cloning, Expression, and Characterization of a Novel Thermophilic Monofunctional Catalase From *Geobacillus* Sp. CHB1." *BioMed Research International* 2016 (2016): 7535604. PMC. Web.

72. Zeigler, Daniel. "The Genus *Geobacillus*." Bacillus Genetic Stock Center Catalog of Strains. 7.3 (2001): 5-13

73. Zhou, J., Wu, K. and Rao, C. "Evolutionary engineering of *Geobacillus thermoglucosidasius* for improved ethanol production." *Biotechnology and Bioengineering*, 113.10 (2016): 2156-2167.

74. Perfumo, A., Banat, I., Marchant, R. and Vezzulli, L. "Thermally enhanced approaches for bioremediation of hydrocarbon-contaminated soils." *Chemosphere*, 66.1 (2007): 179-184.

75. P.K. Singh and R.L. Singh. "Bio-removal of Azo Dyes: A Review." *Int. J. Appl. Sci. Biotechnol.* 5.2 (2017): 108-126.

76. Brumm, Phillip J., Miriam L. Land, and David A. Mead. "Complete Genome Sequence of *Geobacillus Thermoglucosidasius* C56-YS93, a Novel Biomass Degrader Isolated from Obsidian Hot Spring in Yellowstone National Park." Standards in Genomic Sciences 10 (2015): 73. PMC. Web. 4 Jan. 2018.

77. Cripps, R., Eley, K., Leak, D., Rudd, B., Taylor, M., Todd, M., Boakes, S., Martin, S. and Atkinson, T. "Metabolic engineering of *Geobacillus thermoglucosidasius* for high yield ethanol production." *Metabolic Engineering*, 11.6 (2009): 398-408.

78. Lin, P., Rabe, K., Takasumi, J., Kadisch, M., Arnold, F. and Liao, J. "Isobutanol production at elevated temperatures in thermophilic *Geobacillus thermoglucosidasius*." *Metabolic Engineering*, 24 (2014): 1-8.

79. Olson, D., Sparling, R. and Lynd, L. "Ethanol production by engineered thermophiles." *Current Opinion in Biotechnology*, 33 (2015): 130-141.

80. Murai, R. and Yoshida, N. "*Geobacillus thermoglucosidasius* Endospores Function as Nuclei for the Formation of Single Calcite Crystals." *Applied and Environmental Microbiology*, 79.9 (2013): 3085-3090.

81. Studholme, David J. "Some (bacilli) like It Hot: Genomics of *Geobacillus* Species." *Microbial Biotechnology* 8.1 (2015): 40–48. PMC. Web.

82. Pogrebnyakov, I., Jendresen, C. and Nielsen, A. "Genetic toolbox for controlled expression of functional proteins in *Geobacillus* spp." *PLOS ONE*, 12.2 (2017).

83. Reeve, B., Martinez-Klimova, E., de Jonghe, J., Leak, D. and Ellis, T. "The *Geobacillus* Plasmid Set: A Modular Toolkit for Thermophile Engineering." *ACS Synthetic Biology*, 5.12 (2016): 1342-1347.

84. Koo, J., Kim, Y., Kim, J., Yeom, M., Lee, I. and Nam, H. “A GUS/Luciferase Fusion Reporter for Plant Gene Trapping and for Assay of Promoter Activity with Luciferin-Dependent Control of the Reporter Protein Stability.” *Plant and Cell Physiology*, 48.8 (2007): 1121-1131.

85. Gohar, Ali Vaziri et al. “Subcellular Localization-Dependent Changes in EGFP Fluorescence Lifetime Measured by Time-Resolved Flow Cytometry.” *Biomedical Optics Express* 4.8 (2013): 1390–1400. PMC. Web.

86. Shimomura O, Johnson FH, Saiga Y. “Extraction, purification and properties of aequorin, a bioluminescent protein from the luminous hydromedusan, Aequorea.” *Journal of Cellular and Comparative Physiology*. 59.3 (1962): 223–239

87. Chalfie M, Tu Y, Euskirchen G, Ward WW, Prasher DC. “Green fluorescent protein as a marker for gene expression.” *Science*. 263.5148 (1994): 802–805.

88. Cormack BP, Valdivia RH, Falkow S. “FACS-optimized mutants of the green fluorescent protein (GFP).” *Gene*. 173 (1996): 33–38.

89. Baffour-Awuah, N., Fedeles, F. and Zimmer, M. “Structural features responsible for GFPuv and S147P-GFP’s improved fluorescence.” *Chemical Physics*, 310.1-3 (2005) 25-31.

90. Pe´delacq, J., Cabantous, S., Tran, T., Terwilliger, T. and Waldo, G. “Erratum: Corrigendum: Engineering and characterization of a superfolder green fluorescent protein.” *Nature Biotechnology*, 24.9 (2006): 1170-1170.

91. Overkamp, W., Beilharz, K., Detert Oude Weme, R., Solopova, A., Karsens, H., Kovács, Á., Kok, J., Kuipers, O. and Veening, J. “Benchmarking Various Green Fluorescent Protein Variants in *Bacillus subtilis*, Streptococcus pneumoniae, and Lactococcus lactis for Live Cell Imaging.” *Applied and Environmental Microbiology*, 79.20 (2013): 6481-6490.

92. Anderson, Jens Bo et al. “New Unstable Variants of Green Fluorescent Protein for Studies of Transient Gene Expression in Bacteria.” *Appl. Environ. Microbiol.* 64.6 (1998): 2240-2246

93. Scholz, O., Thiel, A., Hillen, W. and Niederweis, M. “Quantitative analysis of gene expression with an improved green fluorescent protein.” *European Journal of Biochemistry*, 267.6 (2000): 1565-1570.

94. Lelimousin M, Noirclerc-Savoye M, Lazareno-Saez C, Paetzold B, Le Vot S, Chazal R, Macheboeuf P, Field MJ, Bourgeois D, Royant A. “Intrinsic dynamics in ECFP and Cerulean control fluorescence quantum yield.” Biochemistry. 48.42 (2009): 10038–10046.

95. Nagai, T., Ibata, K., Park, E., Kubota, M., Mikoshiba, K. and Miyawaki, A. (2002). A variant of yellow fluorescent protein with fast and efficient maturation for cell-biological applications. *Nature Biotechnology*, 20(1), pp.87-90.

96. Campbell, Robert E. et al. “A Monomeric Red Fluorescent Protein.” Proceedings of the National Academy of Sciences of the United States of America 99.12 (2002): 7877–7882. PMC. Web.

97. Shaner, N., Campbell, R., Steinbach, P., Giepmans, B., Palmer, A. and Tsien, R. “Improved monomeric red, orange and yellow fluorescent proteins derived from Discosoma sp. red fluorescent protein.” *Nature Biotechnology*, 22.12 (2004): 1567-1572.

98. Trassaert, M., Vandermies, M., Carly, F., Denies, O., Thomas, S., Fickers, P. and Nicaud, J. “New inducible promoter for gene expression and synthetic biology in Yarrowia lipolytica.” *Microbial Cell Factories*, 16.1 (2017)

99. Bartosiak-Jentys, J., A. H. Hussein, C. J. Lewis, and D. J. Leak. "Modular System for Assessment of Glycosyl Hydrolase Secretion in *Geobacillus Thermoglucosidasius*." *Microbiology Society* 159.7 (2013): 1267-275. Print

100. Daber, R; Stayrook, S; Rosenberg, A; Lewis, M. “Structural analysis of lac repressor bound to allosteric effectors.” *J. Mol. Biol*. 370 (2007): 609–19

101. Gerk, L., Leven, O. and Müller-Hill, B. “Strengthening the dimerisation interface of lac repressor increases its thermostability by 40 deg. C.” *Journal of Molecular Biology*, 299.3 (2000): 805-812.

102. Thurston, C. “The structure and function of fungal laccases.” *Microbiology*, 140.1 (1994): 19-26.

103. Wang, Jinhui et al. “Lignin Engineering through Laccase Modification: A Promising Field for Energy Plant Improvement.” *Biotechnology for Biofuels 8* (2015): 145. PMC. Web.

104. Maestre-Reyna, M., Liu, W., Jeng, W., Lee, C., Hsu, C., Wen, T., Wang, A. and Shyur, L. “Structural and Functional Roles of Glycosylation in Fungal Laccase from Lentinus sp.” *PLOS ONE*, 10.4 (2015): 0120601.

105. Ausec, L., Zakrzewski, M., Goesmann, A., Schlüter, A. and Mandic-Mulec, I. “Bioinformatic Analysis Reveals High Diversity of Bacterial Genes for Laccase-Like Enzymes.” *PLoS ONE*, 6.10 (2011): 25724.

106. Martins LO, Soares CM, Pereira MM, Teixeira M, Costa T, et al. “Molecular and biochemical characterization of a highly stable bacterial laccase that occurs as a structural component of the *Bacillus subtilis* endospore coat.” J *Biol Chem* 277 (2002): 18849–18859

107. Givaudan A, Effosse A, Faure D, Potier P, Bouillant ML, et al. “Polyphenol oxidase in *Azospirillum lipoferum* isolated from rice rhizosphere: Evidence for laccase activity in non-motile strains of *Azospirillum lipoferum*.” *FEMS Microbiol Lett* 108 (1993): 205–210.

108. Suzuki T, Endo K, Ito M, Tsujibo H, Miyamoto K, et al. “A thermostable laccase from *Streptomyces lavendulae* REN-7: purification, characterization, nucleotide sequence, and expression.” *Biosci Biotechnol Biochem* 67(2003): 2167–2175.

109. Enguita, F., Martins, L., Henriques, A. and Carrondo, M. “Crystal Structure of a Bacterial Endospore Coat Component.” *Journal of Biological Chemistry*, 278.21 (2003): 19416-19425.

110. Martins, L., Soares, C., Pereira, M., Teixeira, M., Costa, T., Jones, G. and Henriques, A.

"Molecular and Biochemical Characterization of a Highly Stable Bacterial Laccase That Occurs as a Structural Component of the *Bacillus subtilis* Endospore Coat." *Journal of Biological Chemistry,* 277.21 (2002): 18849-18859.

111. Madhavi, V. and Lele, S. "Laccase: Properties and Applications." *BioResources,* 4.4 (2009): 1694-1717.

112. Sirim, Demet et al. "The Laccase Engineering Database: A Classification and Analysis System for Laccases and Related Multicopper Oxidases." *Database: The Journal of Biological Databases and Curation 2011* (2011): bar006. PMC. Web.

113. Claus, H. "Laccases: structure, reactions, distribution." *Micron,* 35.1-2 (2004): 93-96.

114. Sharma, P., Goel, R., and Capalash, N. "Bacterial Laccases." *World J Microbiol Biotechnol* 23.6 (2007): 823-832.

115. Piontek, K., Antorini, M. and Choinowski, T. "Crystal Structure of a Laccase from the FungusTrametes versicolorat 1.90-Å Resolution Containing a Full Complement of Coppers." *Journal of Biological Chemistry*, 277.40 (2002): 37663-37669.

116. Galhaup, C., Goller, S., Peterbauer, C., Strauss, J. and Haltrich, D. (2002). Characterization of the major laccase isoenzyme from *Trametes pubescens* and regulation of its synthesis by metal ions a. *Microbiology,* 148(7), pp.2159-2169.

117. Sitarz, A., Mikkelsen, J. and Meyer, A. "Structure, functionality and tuning up of laccases for lignocellulose and other industrial applications." *Critical Reviews in Biotechnology,* 36.1 (2015): 70-86.

118. Upadhyay, Pooja, Rahul Shrivastava, and Pavan Kumar Agrawal. "Bioprospecting and Biotechnological Applications of Fungal Laccase." *3 Biotech* 6.1 (2016): 15. PMC. Web.

119. Gianfreda, L., Xu, F. and Bollag, J. "Laccases: A Useful Group of Oxidoreductive Enzymes." *Bioremediation Journal*, 3.1 (1999): 1-26.

120. Montazer, M., Dadashian, F., Hemmatinejad, N. and Farhoudi, K. "Treatment of Wool with Laccase and Dyeing with Madder." *Applied Biochemistry and Biotechnology,* 158.3 (2008): 685-693.

121. Swamy, J. and Ramsay, J. A. "The evaluation of white rot fungi in the decoloration of textile dyes." *Enzyme and Microbiol Tech.* 24 (1999): 321-323.

122. Stutz, C. "The use of enzymes in ultrafiltration." *Fruit Processing,* 3 (1993): 248-252.

123. Mate, Diana M., and Miguel Alcalde. "Laccase: A Multi-purpose Biocatalyst at the Forefront of Biotechnology." *Microbial Biotechnology* 10.6 (2017): 1457–1467. PMC. Web.

124. Minussi, R. C., Pastore, G. M., and Duran, N. "Potential applications of laccase in the food industry." *Trends in Food Science and Technology,* 3 (2002): 205-216.

125. Kudanga, T. and Le Roes-Hill, M. “Laccase applications in biofuels production: current status and future prospects.” *Applied Microbiology and Biotechnology*, 98.15 (2014): 6525-6542.

126. Kudanga, T. and Le Roes-Hill, M. “Laccase applications in biofuels production: current status and future prospects.” *Applied Microbiology and Biotechnology*, 98.15 (2014): 6525-6542.

127. Margot, J., Bennati-Granier, C., Maillard, J., Blánquez, P., Barry, D. and Holliger, C. “Bacterial versus fungal laccase: potential for micropollutant degradation.” *AMB Express*, 3.1 (2013): 63.

128. Maté, Diana et al. “Directed Evolution of Fungal Laccases.” *Current Genomics* 12.2 (2011): 113–122. PMC. Web.

129. “*Geobacillus Thermoglucosidasius* C56-YS93, Complete Genome.” *National Center for Biotechnology Information*. U.S. National Library of Medicine, n.d. Web.

130. “Basic Local Alignment Search Tool.” BLAST: National Center for Biotechnology Information, n.d. Web.

131. Wu lab, unpublished data

132. Beloqui, Ana et al. “Novel Polyphenol Oxidase Mined from a Metagenome Expression Library of Bovine Rumen.” *Journal of Biological Chemistry*, 281.32 (2006): 22933-22942.

133. Chen, Cheng-Yu et al. “Properties of the Newly Isolated Extracellular Thermo-Alkali-Stable Laccase from Thermophilic Actinomycetes, Thermobifida Fusca and Its Application in Dye Intermediates Oxidation.” AMB Express 3 (2013): 49. PMC. Web.

134. Kim, H. W. et al. “Expression, refolding, and characterization of a small laccase from *Thermus thermophilus* HJ6.” *Protein Expression and Purification*, 114 (2015): 37-43.

135. “Study of the optimum growth conditions of *Bacillus subtilis* (strain WT 168), and *Pseudomonas fluorens* (strain SBW25).” iGEM Toulouse (2016).

136. Tindall, B. and Garrity, G. “Should we alter the way that authorship of a subspecies name that is automatically created under Rule 40d of the Bacteriological Code is cited?” *INTERNATIONAL JOURNAL OF SYSTEMATIC AND EVOLUTIONARY MICROBIOLOGY*, 58.8 (2008): 1991-1992.

137. Nakano, M. and Zuber, P. “ANAEROBIC GROWTH OF A ‘STRICT AEROBE’ (*BACILLUS SUBTILIS*).” *Annual Review of Microbiology*, 52.1 (1998): 165-190.

138. Hong, H., Duc, L. and Cutting, S. “The use of bacterial spore formers as probiotics.” *FEMS Microbiology Reviews*, 29.4 (2005): 813-835.

139. Ciprandi G, Scordamaglia A, Venuti D, Caria M, and Canonica GW. “In vitro effects of *Bacillus subtilis* on the immune response.” *Chemioterapia.* 5.6 (1986): 404–407.

140. Horneck G, Klaus DM, and Mancinelli RL. “Space microbiology.” *Microbiology and*

Molecular Biology Reviews. 74.1 (2010): 121–56.

141. Van Dijl JM and Hecker M. "*Bacillus subtilis*: from soil bacterium to super-secreting cell factory." *Microbial Cell Factories*. 12.3 (2013): 3.

142. Vojcic, L., Pitzler, C., Körfer, G., Jakob, F., Ronny Martinez, Maurer, K. and Schwaneberg, U. "Advances in protease engineering for laundry detergents." *New Biotechnology*, 32.6 (2015): 629-634.

143. "Effect of flower-applied Serenade biofungicide (*Bacillus subtilis*) on pollination-related variables in rabbiteye blueberry." Biological Control. 33.1 (2005): 32–38.

144. "The International Pharmacopoeia Fourth Edition - Pharmacopoea Internationalis Editio Quarta - Fourth Supplement: Methods of Analysis: 5. Pharmaceutical technical procedures: 5.8 Methods of sterilization."

145. Eberle, H. and Lark, K. "Chromosome segregation in *Bacillus subtilis*." *Journal of Molecular Biology*, 22.1 (1966): 183-186.

146. Zandomeni, Ruben et al. "Spore Size Comparison between Several *Bacillus* Species." *GeoCenters, Inc.* Edgewood Biological Center, US Army, Aberdeen Proving Ground, MD. (2005)

147. Istacato, R. and Ricca, E. "Spore Surface Display." *Microbiology Spectrum* 2.5 (2014): 351-366.

148. "Bacterial Endospores." Department of Microbiology, Cornell University. Web. https://micro.cornell.edu/research/epulopiscium/bacterial-endospores

149. McKenney, Peter T., and Patrick Eichenberger. "Dynamics of Spore Coat Morphogenesis in *Bacillus Subtilis*." Molecular Microbiology 83.2 (2012): 245–260. PMC. Web.

150. Isticato R, Cangiano G, De Felice M, Ricca E. "Display of molecules on the spore surface." *Bacterial Spore Formers: Probiotics and Emerging Applications*. (2004): 193–200.

151. Knecht LD, Pasini P, Daunert S. "Bacterial spores as platforms for bioanalytical and biomedical applications." *Anal Bioanal Chem* 400 (2011): 977–989.

152. Knecht LD, Pasini P, Daunert S. "Bacterial spores as platforms for bioanalytical and biomedical applications." *Anal Bioanal Chem* 400 (2011): 977–989.

153. Isticato R, Sirec T, Treppiccione L, Maurano F, De Felice M, Rossi M, Ricca E. "Non-recombinant display of the B subunit of the heat labile toxin of *Escherichia coli* on wild type and mutant spores of *Bacillus subtilis*. *Microb Cell Fact* 12 (2013): 98.

154. Bar-Even, A., Noor, E., Savir, Y., Liebermeister, W., Davidi, D., Tawfik, D. and Milo, R. "The Moderately Efficient Enzyme: Evolutionary and Physicochemical Trends Shaping Enzyme Parameters." *Biochemistry*, 50.21 (2011) 4402-4410.

155. Brander, S. et al. "Characterization of an Alkali- and Halide-Resistant Laccase Expressed in E. coli: CotA from *Bacillus clausii*." *PLoS ONE*, 9.6 (2014).

156. Thompson, Richard et al. “Our plastic age.” *Phil. Trans. R. Soc. B* (2009): 364.

157. Yoshida, Shosuke et al. “A bacterium that degrades and assimilates poly(ethylene terephthalate).” *Science* (2016): 351.
158. Jaroslawiecka, A. and Piotrowska-Seget, Z. "Lead Resistance in Micro-Organisms". *Microbiology* 160.Pt_1 (2013): 12-25. Web.

159. Taghavi, S. et al. "Lead(II) Resistance In *Cupriavidus Metallidurans* CH34: Interplay Between Plasmid And Chromosomally-Located Functions". *Antonie van Leeuwenhoek* 96.2 (2008): 171-182. Web.
160. Chen, Peng R and He, Chuan. "Selective Recognition of Metal Ions by Metalloregulatory Proteins". *Current Opinion in Chemical Biology* 12.2 (2008): 214-221. Web.
161. Wei, W. et al. “Simple whole-cell biodetection and bioremediation of heavy metals based on an engineered lead-specific operon.” *Environ Sci Technol*, 48.6 (2014): 3363-3371. Web.
162. Kumar, A; Bisht, B S; Joshi, V D; Dhewa, T. “Review on Bioremediation of Polluted Environments: A Management Tool. *International Journal of Environmental Sciences; Kangayam* 1.6 (2011): 1079-1093. Web.